Namensnennung-Keine kommerzielle Nutzung-Keine Bearbeitung 3.0 Schweiz
(CC BY-NC-ND 3.0 CH)

Sie dürfen: **Teilen** — den Inhalt kopieren, verbreiten und zugänglich machen

Unter den folgenden Bedingungen:

Namensnennung — Sie müssen den Namen des Autors/Rechteinhabers in der von ihm festgelegten Weise nennen.

Keine kommerzielle Nutzung — Sie dürfen diesen Inhalt nicht für kommerzielle Zwecke nutzen.

Keine Bearbeitung erlaubt — Sie dürfen diesen Inhalt nicht bearbeiten, abwandeln oder in anderer Weise verändern.

Wobei gilt:

- **Verzichtserklärung —** Jede der vorgenannten Bedingungen kann **aufgehoben** werden, sofern Sie die ausdrückliche Einwilligung des Rechteinhabers dazu erhalten.
- **Public Domain (gemeinfreie oder nicht-schützbare Inhalte) —** Soweit das Werk, der Inhalt oder irgendein Teil davon zur Public Domain der jeweiligen Rechtsordnung gehört, wird dieser Status von der Lizenz in keiner Weise berührt.
- **Sonstige Rechte —** Die Lizenz hat keinerlei Einfluss auf die folgenden Rechte:
    - Die Rechte, die jedermann wegen der Schranken des Urheberrechts oder aufgrund gesetzlicher Erlaubnisse zustehen (in einigen Ländern als grundsätzliche Doktrin des **fair use** bekannt);
    - Die **Persönlichkeitsrechte** des Urhebers;
    - Rechte anderer Personen, entweder am Lizenzgegenstand selber oder bezüglich seiner Verwendung, zum Beispiel für **Werbung** oder Privatsphärenschutz.
- **Hinweis —** Bei jeder Nutzung oder Verbreitung müssen Sie anderen alle Lizenzbedingungen mitteilen, die für diesen Inhalt gelten. Am einfachsten ist es, an entsprechender Stelle einen Link auf diese Seite einzubinden.

Quelle: http://creativecommons.org/licenses/by-nc-nd/3.0/ch/ Datum: 12.11.2013

Mouse embryonic stem cells as a discovery tool in skeletal muscle biology

Inauguraldissertation

zur

Erlangung der Würde eines Doktors der Philosophie

vorgelegt der

Philosophisch-Naturwissenschaftlichen Fakultät

der Universität Basel

von

Hyunwoo Lee

aus Seongnam, Republik Korea

Basel, 2015

Genehmigt von der Philosophisch-Naturwissenschaftlichen Fakultät

auf Antrag von

Prof. Dr. Susan Gasser, Dr. Matthias Müller, und Prof. Dr. Patrick Matthias

Basel, den 11 November 2014

Prof. Dr. Jörg Schibler (Dekan)

Contents

Abstract

Skeletal muscle and its progenitor cells are formed during the development. In adulthood the progenitor cells remain inactive until a differentiation signal is sensed, such as an exercise or tissue damages. Under certain conditions like aging, chemotherapy and genetic disorder, the capacity of skeletal muscle regeneration declines and progenitors can't differentiate properly, resulting in immobilizing problems. Embryonic stem (ES) cells have been highlighted as a great source which can provide amplifiable skeletal muscle progenitors. ES cells have the capacity of self-renewal and the potential of differentiation into every cell type in the human body, including skeletal muscle. Although amplifiable skeletal muscle can be differentiated from ES cells by ectopic over-expression of key transcription factors, genetic integration of cDNA into host is a prerequisite. Therefore, efforts have increasingly focused on the identification of small molecules which can induce skeletal muscle differentiation from ES cells in the field. Using small molecules for cellular differentiation provides invaluable advantages compared to other methods such as genetic modifications. Modulation of signaling by small molecules is rather straight forward and the effect can be controlled with a fine-tuning manner by applying various concentration and time points. In spite of the prominent advantages, there has been no single molecule known to drive ES cells at high efficiency to skeletal muscle thus far.

My thesis work was focused on the identification of small molecules which can drive differentiation of mouse embryonic stem cells toward skeletal muscle. I also investigated the biological process during embryonic skeletal muscle differentiation that manipulates the development process taking place *in vivo*. Embryonic stem cells have been a popular tool for studying development processes as well as a great source for cell therapy *via* manipulations of physiological events. In this study a small molecule was identified from a mouse embryoid body (EB) screening and used as a tool compound for skeletal muscle differentiation. The small molecule was named as SMI (Skeletal Muscle Inducer). Its chemistry is N-[4-(trifluoromethyl)-6-methoxymethyl-2-pyrimidinyl]-N-(2-methyl-6-nitrophenyl)-urea. In the screening Pax3 mRNA induction was one of the major readouts since Pax3 has been known as a key transcription factor for early skeletal muscle development. SMI1 showed a high efficiency for skeletal muscle differentiation without any extra effort such as fluorescent cell sorting step. Even

though the effect of the compound driving mouse ES cells from 129 mice to skeletal muscle was very clear, it did not have the same effect in ES cells of other mouse strains, BalbC and Bl6. By discovering the mechanism of action of this small molecule, I expect that it could be applied and transferred to other cell lines as well as human pluripotent stem cells. These insights can pave way to determining the complexity of embryonic skeletal muscle differentiation.

Comprehensive gene expression level analysis with SMI incubation resulted in the discovery of three pathways which are involved and play critical roles in skeletal muscle differentiation by the molecule. Wnt pathway and Nodal pathway were identified from EB day 4, and Shh signaling was found at EB day 4+4. All the three pathways are closely related to the development process of the mouse embryo. The action of SMI1 was reproduced independently using other small molecules which are known to modulate the Wnt, Nodal and Shh pathways in all mouse ES cells from different strains tested. Taken together, these results demonstrate that the differentiation of mouse embryonic stem cells into skeletal muscle by SMI1 occurs through Wnt, Nodal and Shh pathways' modulation. Therefore, SMI1 can be used as a tool to study the skeletal muscle biology and to establish a cellular skeletal muscle disease model for therapeutic research.

Chapter1: Introduction

1.1 Skeletal muscle disease

1.1.1 Skeletal muscle

The human body consists of around 600 individual skeletal muscles which covers about 40% of an adult's body mass (Reviewed in Jung and Williams, 2012). Skeletal muscle is composed of thousands of muscle fibers that are multinucleated and are formed during development by the fusion of mononucleated myoblasts. They are surrounded by a specialized plasma membrane, the sarcolemma, which transduces signals from motor neurons to muscle fibers. Skeletal muscle can adapt muscle fiber size, functional capacity and metabolism in response to physiological stimuli. Severe muscle damage activates satellite cells, which are resident population of stem cells to proliferate and differentiate in order to rebuild the new muscle. Satellite cells were identified on the basis of their distinct anatomical position between the sarcolemma and the basal lamina of muscle fibers (Mauro, 1961). The basal lamina is composed of layers of extracellular matrix known as the basement membrane of muscle fibers (Sanes, 2003).

The regenerative potential of adult muscle depends on the endogenous source of muscle progenitor cells, satellite cells (Goldring et al., 2002). Satellite cells stay mitotically and metabolically quiescent through most of life. Quiescent satellite cells are triggered to proliferate by growth factors and cytokines which are released after damage to skeletal muscle. They include insulin-like growth factor, epidermal growth factor and platelet-derived growth factor (Ciemerych et al., 2011).

Molecular mechanism of the skeletal muscle mass regulation in adulthood can be explained as the balance between relative rate of protein synthesis and degradation (Reviewed in Schiaffino et al., 2013). Growth of muscle occurs through increases in myofiber size by protein synthesis exceeding protein degradation, which is a process of hypertrophy. Conversely, loss of muscle mass is mediated by loss of proteins, organelles and cytoplasm, which is a process of atrophy. FoxO3, which is negatively regulated by Akt, controls well known muscle-specific atrophy-related ubiquitin ligases such as Atrogin1 (MAFbx). Atrogin1 is an E3 ubiquitin ligase, regulated by FoxO (Forkhead box O) transcription factors, which catalyzes the rate-limit step in the

ubiquitination process (Sandri et al., 2004). Recent studies suggest that other potential key cellular processes may also be involved in causing skeletal muscle related diseases. For example, the TGFbeta superfamily may cause skeletal muscle waste by coordinating the balance between protein degradation and synthesis, according to the physiological state of the muscle fibers (Reviewed in Sartori et al., 2014). It is well known that Myostatin, a member of TGFbeta family, is a negative regulator of muscle growth (McPherron and Lee, 1997). Recent findings suggest that Myostatin's effect on muscle mass may also be involved with the activation of Atrogin1 and inhibition of IGF1/Akt/mTOR pathway (Trendelenburg et al., 2009). The exact mechanism of the TGFbeta family on protein degradation still remains unclear. Further investigations are needed to reveal the mechanisms and pathways downstream of Smad2/3 by the TGFbeta family during protein synthesis and degradation.

1.1.2 Skeletal muscle diseases

Skeletal muscle wasting and diseases are caused by the loss or absence of ability of skeletal muscle to control muscle mass. Muscle atrophy can also occur because of muscle inactivity from immobilization, casting and age-related loss of skeletal muscle. The skeletal muscle diseases caused by genetic disorder or ageing are described in detail below.

1.1.2.1 Genetic diseases of skeletal muscle

Genetic disorder can cause muscle degenerative diseases too. For example, mutations in the dystrophin gene results in Duchenne muscular dystrophy (DMD), the most common X-linked genetic disorder in humans (Burghes et al., 1987). Point mutations in dystrophin are responsible for 40% of DMD cases and the remaining 60% are caused by large deletions or duplications in this gene (Chaturvedi et al., 2001). Most boys with DMD show symptoms within the first years of life. The symptom is progressive muscle weakening resulting in walking delay and repeated falls. Dystrophin is a structural protein which is a component of the DGC (dystrophin glycoprotein complex) (Ervasti and Campbell, 1991). Dystrophin links the muscle fiber cytoskeleton to the extracellular matrix and stabilizes the sarcolemma (Straub et al., 1992). Absence of functional dystrophin protein destabilizes DGC and increases the susceptibility of dystrophic muscle fibers to contraction induced injury (Campbell and Kahl, 1989).

Myotonic dystrophy type 1 is also a well-studied genetic skeletal muscle disease. It is known as dystrophia myotonica type 1 (DM1), an autosomal dominant disease caused by a trinucleotide repeat, cytosine-thymine-guanine (CTG), expansion in the 3' UTR of DMPK (Dystrophia Myotonica Protein Kinase) on chromosome 19 (Brook et al., 1992). Normal individual have less than 30 repeats, and expansions more than this range can initiate DM symptoms. CTG repeat expansions of the DMPK 3'UTR are transcribed into mRNA and form intranuclear foci, resulting in nuclear retention of DMPK mRNA. Age of onset and disease severity appear to correlate with repeat expansion length. The symptom of DM is myotonia or the inability to relax skeletal muscles after contraction. Additional DM symptoms include skeletal muscle wasting and weakening, smooth and cardiac muscle malfunction.

1.1.2.2 Progressive loss of skeletal muscle by ageing

In a society where the increasing aged population is becoming more prevalent, age-related decline in muscle mass and strength are present and growing health concerns. Progressive muscle wasting, known as sarcopenia, is a decrease in skeletal muscle mass associated with aging which compromises the ability to live independently at advanced age. The underlying molecular mechanisms which contribute to the progression of sarcopenia are not clearly known yet (Reviewed in Lang et al., 2010). Current potential causes of sarcopenia include an increase in chronic inflammation, metabolic processes that lead to increased insulin resistance, activated catabolic pathways, accumulation of genotoxic DNA damage and insufficiency in satellite cells that impair the normal muscle regenerative response.

1.1.3 Therapeutic possibilities for skeletal muscle diseases

Current therapeutic options for skeletal muscle disease are very limited and focus on managing symptoms and suppressing the inflammatory response (Muir and Chamberlain, 2009). Some investigators have focused on development of direct gene therapy in affected muscle fibers by exogenous delivery of a normal copy of the mutated gene for example dystrophy genes using viral vectors (Partridge, 2011). However, viral vectors are susceptible to antiviral host immune responses which can prevent repeated gene-delivery attempts.

Cell therapy is another attractive option to treat the skeletal muscle disease through the delivery of cells which can regenerate new skeletal muscle tissues (Darabi et al., 2012). Cell therapy

involving transplantation of multi-potent hematopoietic stem cells derived from bone marrow has already been demonstrated as a successful option (Thomas et al., 1957), however it did not give rise to skeletal muscle diseases. Early clinical trials tested the efficacy of transplanted myoblasts from explants of donor muscle and injected directly into the muscle. Unfortunately the trials were not successful (Miller et al., 1997). Perhaps it was because of significant cell loss after transplantation caused by the death of injected cells.

Due to the challenges in studies using satellite cells which cannot be amplified *in vitro* easily, researchers in this area have tried to establish skeletal muscle differentiation from pluripotent stem cells (Chang et al., 2009; Sakurai et al., 2008). By taking advantage of pluripotent stem cell differentiation potential, amplifiable skeletal muscle stem cells might be obtainable. Current methods for skeletal muscle differentiation from pluripotent stem cells involve either treating cells biochemically or through genetic modification resulting in over-expression of master genes (Darabi et al., 2008; Kennedy et al., 2009). Progress in the ability to isolate and expand satellite state cells from pluripotent cells will also be an essential step for cell therapy approaches. Considering the embryonic stem cells' potentially unlimited capacity for self-renewal and ability to differentiate into the muscle, embryonic stem cells may be a great source for cell therapy and useful in creating cellular models for biomedical research.

1.2Skeletal muscle development

1.2.1 Early Skeletal Muscle Development

1.2.1.1. Primitive streak formation at embryonic day 6.5

Vertebrate skeletal muscle differentiation is controlled tightly by morphogens secreted from neighbor tissues in a spatiotemporal manner (Reviewed in Gurdon et al., 1998). Morphogens control the genetic networks and the pattern of tissues in developing embryos. During mouse development skeletal muscle is differentiated from mesoderm which arises around embryonic day 6.5 with the primitive streak formation (Reviewed in Tam and Behringer, 1997). Gastrulation after primitive streak formation is a pivotal step in setting the vertebrate body plan. In gastrulation stage, primary germ layers appear that are ectoderm, mesoderm and definitive endoderm. Ectoderm develops further to neurons mainly and endoderm makes lung, liver and pancreas for instance. Nodal is a key effector together with BMP4 and Wnt family for the initial mesoderm formation (Conlon et al., 1994; Hogan, 1996; Yamaguchi, 2001).

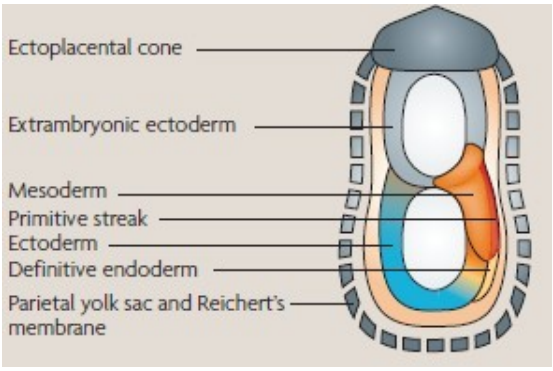

Figure 1.1: E6.5 Primitive-streak formation Primitive streak is a structure that forms in the posterior region of the embryo and is the first visible sign of gastrulation at E6.5 (Adapted from Tam and Loebel, 2007).

Anatomically mesoderm is subdivided to four main tissues which are paraxial, intermediate, chorda and lateral plate mesoderm depending on the position from the midline (Reviewed in Tam and Loebel, 2007). In the primitive streak of the late gastrula, the paraxial mesoderm, also called somatic dorsal mesoderm, comes from the anterior segment of the streak. It is forming the somite which is a block of mesodermal cells on both sides of the neural tube. The lateral mesoderm comes from the mid-segment of the streak and forms the circulatory systems

including heart, blood vessels and blood cells as well as the lining of the body cavities and all the mesodermal components of the limbs except the muscles. Intermediate mesoderm forms the urogenital system, kidney and gonads. Chordamesoderm forms the notochord which is a transient organ. The major function of notochord is the induction of the formation of the neural tube.

1.2.1.2. Somitogenesis at embryonic day 9

Paraxial mesoderm experiences presomitic mesoderm stage which is still unsegmented, moving along from the posterior tail bud region to the anterior. As the cells in the presomitic mesoderm (PSM) differentiate further, they move to the anterior region. Receiving the differentiation signal of morphogen gradients, condensed paraxial mesoderm makes somites which will be further differentiated into connective tissues of the back such as bone, muscle, cartilage and dermis. It is known that the formation of somites is mediated by Wnt pathway and the gradient of FGF and retinoic acid (Aulehla and Pourquie, 2006). Wnt1 and Wnt3 are secreted from the dorsal neural tube and are positively involve in somite patterning. Sonic Hedgehog (Shh) which is released from the notochord mediates muscle progenitors' specification in somite. Unlike Wnt and Shh, bone morphogenetic protein (BMP) works negatively in skeletal muscle development, delaying induction of Myf5 and MyoD and keeping the muscle progenitors in an undifferentiated state (Pourquie et al., 1996). Wnt and Shh antagonize BMP signals in the dermomyotome through increased levels of Noggin, which inhibits Bmp4 signal (Marcelle et al., 1997). Pathways which are involved in this process will be mentioned in detail below.

At the genetic level, it was reported that the differentiation and movement of PSM progenitor cells are regulated by the transcription factor Mesogenin1 (Fior et al., 2012). Mesogenin1 controls the genesis of the paraxial mesoderm and maintains the differentiation to its derivatives.

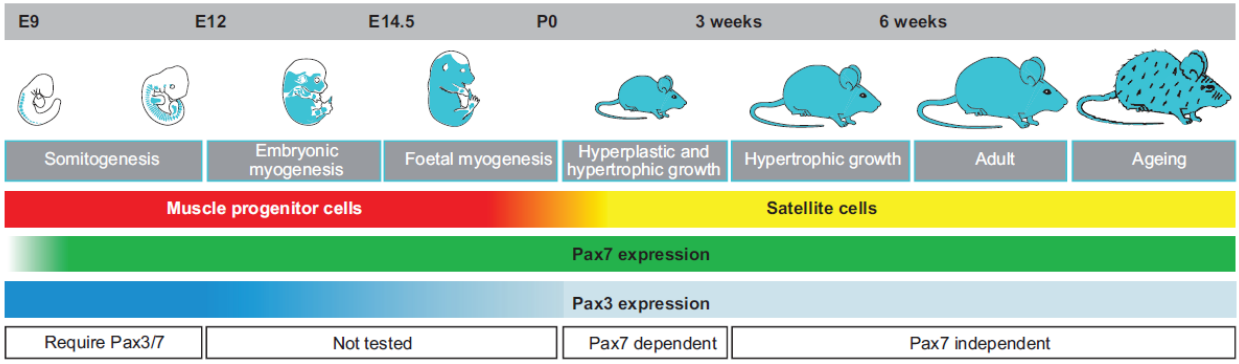

Figure 1.2: Pax genes and myogenic stem cell populations

The timing of muscle development in the embryo and postnatal periods in mouse is indicated. Skeletal muscle is marked in blue in the embryo. Embryonic and foetal muscle progenitors cells are in red and the period of satellite cells is marked in yellow color. The function of Pax3 and Pax7 genes are indicated (Adapted from Relaix and Zammit, 2012).

1.2.1.3. Embryonic skeletal myogenesis in dermomyotome

All the skeletal muscles, except some head muscles, are differentiated from dermomyotome. Cells in dermomyotome express the paired box transcription factors Pax3 and Pax7 (Goulding et al., 1991; Jostes et al., 1990). And they are also marked by low level of Myf5, a basic helix-loop-helix transcription factor (Kiefer and Hauschka, 2001). In muscle progenitors, MyoD is downstream of Pax3 and Pax7 in the genetic hierarchy of myogenic regulators (Bismuth and Relaix, 2010). The dermomyotome matures into the myotome, which consists of muscle cells expressing MyoD and Myf5 considered to be markers of terminal specification of the muscle lineage (Pownall et al., 2002).

The myogenic regulatory factors (MRFs) are MyoD, Myf5, Mrf4 (also known as Myf6) and Myogenin. MRFs are basic helix-loop-helix structured transcription factors which can convert fibroblast to myoblast (Braun et al., 1990; Davis et al., 1987; Rhodes and Konieczny, 1989). They are highly conserved and expressed in the skeletal muscle lineage. The basic domain of the basic helix-loop-helix transcription factor mediates DNA binding to the CACCTG sequence while the helix-loop-helix motif is required for heterodimeriation with E-proteins that mediate the recognition of genomic E-boxes (CANNTG sequence) in the promoters of many muscle-

specific genes(Massari and Murre, 2000). In the mouse embryo myotome, Myogenin is downstream of Myf5 and Mrf4. The promoter regions of Myogenin contain two E-Boxes directly bound by Myf5, MyoD and Mrf4 (Bismuth and Relaix, 2010).

1.2.2. Mouse model studies in development

Expression of Pax3 is found in various tissues during development such as the dorsal neural tube, neural crest cells and muscle progenitors (Goulding et al., 1991). The absence of Pax3 causes impaired muscle development as well as neural crest cell loss and dorsal neural tube closure defects (Bajard et al., 2006). In contrast Pax7 is not mandatory for muscle development because the phenotype of Pax7 absence is pronounced at the post-natal stage (Seale et al., 2000). Pax7-deficient mice show a loss of satellite cells after birth suggesting that Pax3 can't compensate the loss of Pax7 in satellite cells' post-natal survival. Muscle precursor cells can't enter the myogenic program in Pax3/Pax7-double mutant mice (Relaix et al., 2005).

Inactivation of MyoD in mice leads to upregulation of Myf5 which compensates the function of MyoD and results in apparently normal muscle development (Rudnicki et al., 1992). Also normal skeletal muscle phenotype was reported in Myf5 knockout mice (Braun et al., 1992). Myf5 is dispensable for the development of skeletal muscle, because other members of the myogenic regulatory factors such as MyoD, Myogenin and Mrf4 substitute for its activity. In Myf5 and MyoD double-null mice, complete lack of skeletal muscle and Myogenin expression appeared (Rudnicki et al., 1993). Myogenin knockout mice showed reduced levels of Myosin heavy chain and Mrf4 expression but normal MyoD level (Hasty et al., 1993). Myogenin-mutant mice have no muscle defect showing normal development but malfunctioning skeletal muscle after birth. It suggests that Myogenin is critical for the progression of functional skeletal muscle. These results suggest a model in which MyoD and Myf5 act genetically upstream of Myogenin to specify muscle precursors for terminal differentiation (Bentzinger et al., 2012).

1.2.3 Pathways involved in early skeletal muscle formation

Here I introduce the biological background of pathways involved in early skeletal muscle development in detail.

1.2.3.1 TGF (Transforming growth factor)-beta family

TGF-beta and its family, such as Nodal, Activin, Bone Morphogenetic Proteins (BMPs), Myostatins, have been studied extensively and their mechanism of action is very well known. The biological actions of TGF-beta signaling are dependent on the combination of ligands and receptors. They have profound effects on many events from cell propagation, differentiation, migration to death (Reviewed in Massague, 1998). Nodal signals are essential for the induction and patterning of mesoderm and endoderm (Conlon et al., 1994). BMPs were originally identified because of their role in early bone formation. Their functions in skeletal muscle development are to expand the pool of myogenic progenitor cells before further differentiation is initiated (Pourquie et al., 1996).

Ligand binding to a TGF-beta type II receptor completes a receptor complex together with a TGF-beta type I receptor. The constitutively active type II receptor kinase phosphorylates and activates the type I receptor. Activins, TGF-betas and Nodal bind to type I receptors, Activin Receptor-like Kinase ALK4, ALK5 (TGF-beta receptor I) and ALK7, respectively. Activation of the type I receptor in turn phosphorylates a Smad protein which is one of receptor-regulated Smad (R-Smad) proteins. Phosphorylated R-Smad proteins make a complex with Co-Smad, Smad4, and move to the nucleus. In the nucleus, the Smad complex plays a role as a transcription factor activating the transcription of target genes. For example, $p15^{Ink4b}$ and $p21^{Cip21}$ are cyclin-dependent kinase inhibitors responding to TGF-beta mediated cell cycle arrest.

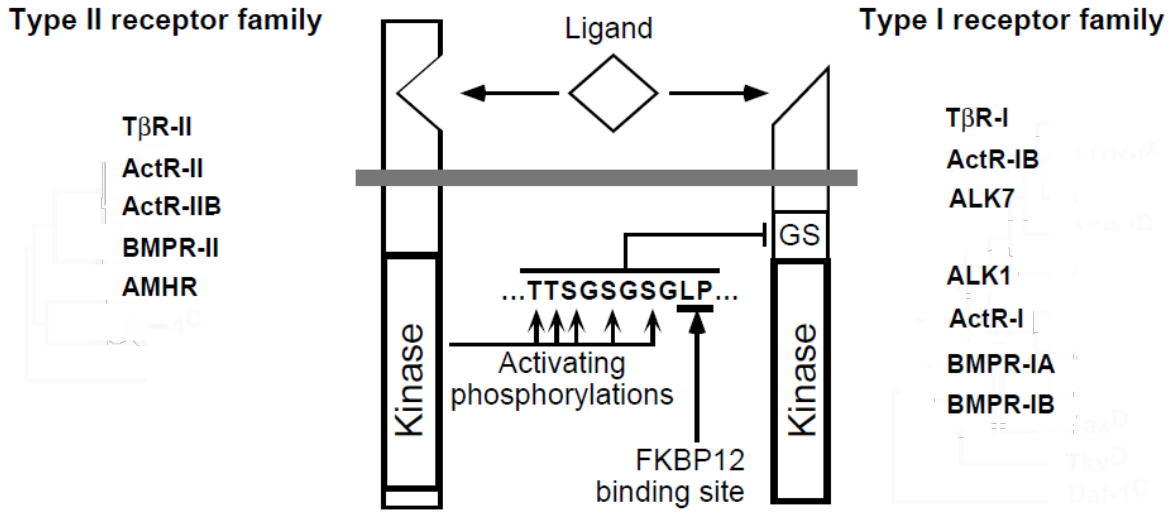

Figure 1.3: Type I and II TGF-beta receptor families.

In type I TGF-beta receptors the protein kinase domain is preceded by the GS domain which is a unique feature of type I receptors containing SGSGSG sequence. Ligand-induced phosphorylation of the serines and threonines in the TTSGSGSG sequence is required for activation of signaling. Arrows indicate the phosphorylation sites. (Adapted from Massague, 1998)

The evolutionary conserved Smad proteins are direct mediators of TGF-beta and its family members' signaling. There are eight Smad proteins identified, Smad1 to Smad8/9 in the human and mouse genomes (Reviewed in Massague et al., 2005). R (regulatory)-Smads are Smad1, Smad2, Smad3, Smad5 and Smad8. Smad1, 5, and 8 act as substrates for the BMP receptors. Smad2 and 3 are substrates for the TGF-bata, Activin and Nodal receptors. Smad4 which is a Co-Smad acts as a common effector for all R-Smads. Smad6 inhibits BMP signaling and Smad7 inhibits TGF-beta and BMP signaling.

1.2.3.2 Wnt Pathway

19 Wnt genes have been identified in the murine and human genome so far. (Wnt homepage http://web.stanford.edu/group/nusselab/cgi-bin/wnt/) The Wnt pathway consists of two different main streams, the canonical (beta-catenin dependent, prototype canonical Wnt3a) pathway and

the non-canonical (independent of beta-catenin, prototype Wnt5a) pathway (Reviewed in Grumolato et al., 2010; Seifert and Mlodzik, 2007).

- **Canonical Wnt Pathway**

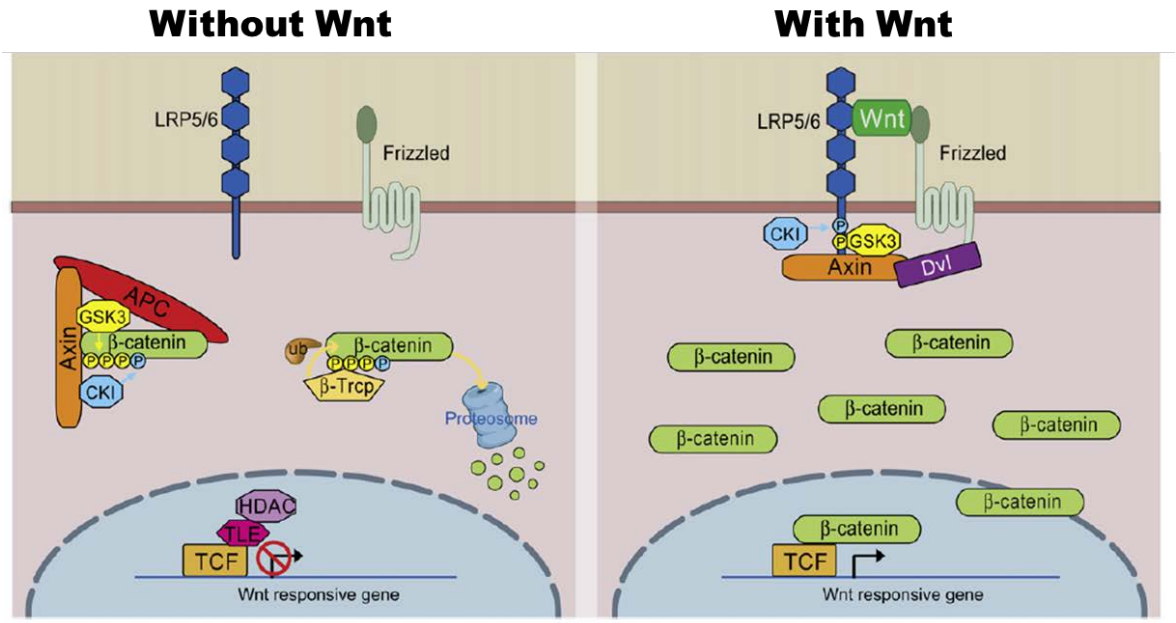

Figure 1.4: Activation Scheme of Canonical Wnt Pathway

In the presence of Wnt ligand, the receptor complex forms between Lrp5/6 and Frz leading to beta-catenin stabilization and localization to nucleus. Beta-catenin in the nucleus acts as a coactivator for TCF activating Wnt-responsive genes (Adapted from MacDonald et al., 2009).

The canonical Wnt Pathway is involved in various biological processes in embryonic development, cell fate determination and adult tissue homeostasis. One key effector of Wnt Pathway is β-catenin. β-catenin is phosphorylated by the complex of Glycogen synthase kinase 3 (GSK3), Axin and Adenomatous polyposis coli (APC) constitutively and degraded through the ubiquitin proteasome pathway (Reviewed in MacDonald et al., 2009). Binding of Wnt to its receptor, LRP5/6 leads to disconnection of β-catenin from its degradation complex and stabilizes β-catenin which translocates to nucleus. β-catenin in nucleus binds to Wnt response gene and induces transcriptional activation. Irregular activation of Wnt pathway due to mutations in APC

is linked not only to colorectal cancer but also to some other cancers such as those of liver (Reviewed in Aoki and Taketo, 2007).

During mouse embryo development, the Wnt pathway is related closely to neurogenesis and anterior-posterior patterning (Reviewed in Yamaguchi, 2001). Wnt3a mutant mice do not show a proper anterior-posterior body axis (Ikeya and Takada, 2001). It has been also reported that Wnt signal is indispensable for neuronal induction and skeletal muscle differentiation. Wnt3a mutant embryos lack somites, have a disrupted notochord and fail to form a tailbud (Takada et al., 1994). Mutant embryos also show brain dysmorphology. At the molecular level Wnt targets Brachyury, Mesogenin1, Tbx6 and Axin2 which are important to maintain cells in a posterior PSM fate (Aulehla and Pourquie, 2010).

1.2.3.3 Sonic Hedgehog Pathway

Hedgehog protein families are secreted glycoproteins that control the multiple developmental processes of many organs and cell groups in metazoans (Reviewed in Ingham et al., 2011). In mammals, there are 3 Hh ligands identified, Sonic (Shh), Indian (Ihh) and Desert (Dhh). Shh is involved in neural development in vertebrates and Ihh participates in bone growth and endoderm differentiation. Dhh is known to mediate spermatogenesis (Clark et al., 2000). In the normal central nervous system of mammals and birds, only Shh is reported to be expressed (Echelard et al., 1993). The Hh proteins bind to the cell surface receptor Patched1 (Ptch1) resulting in release of inhibition on G protein-coupled receptor like protein Smoothened (Smo). Smo translocates to the plasma membrane from intracellular vesicles. Active Smo regulates gene expression through nuclear translocation of the zinc-finger Gli transcription factors. 3 Gli proteins are identified and they mediate the responses to Hh signals. Gli2 is a transcription activator mediating the Hh pathway primarily. Gli1 whose expression is regulated by Gli2 and Gli3 also activates transcription of target genes such as Gli1, Ptch1, Ptch2 and Bcl2. In contrast, Gli3 is a transcription repressor.

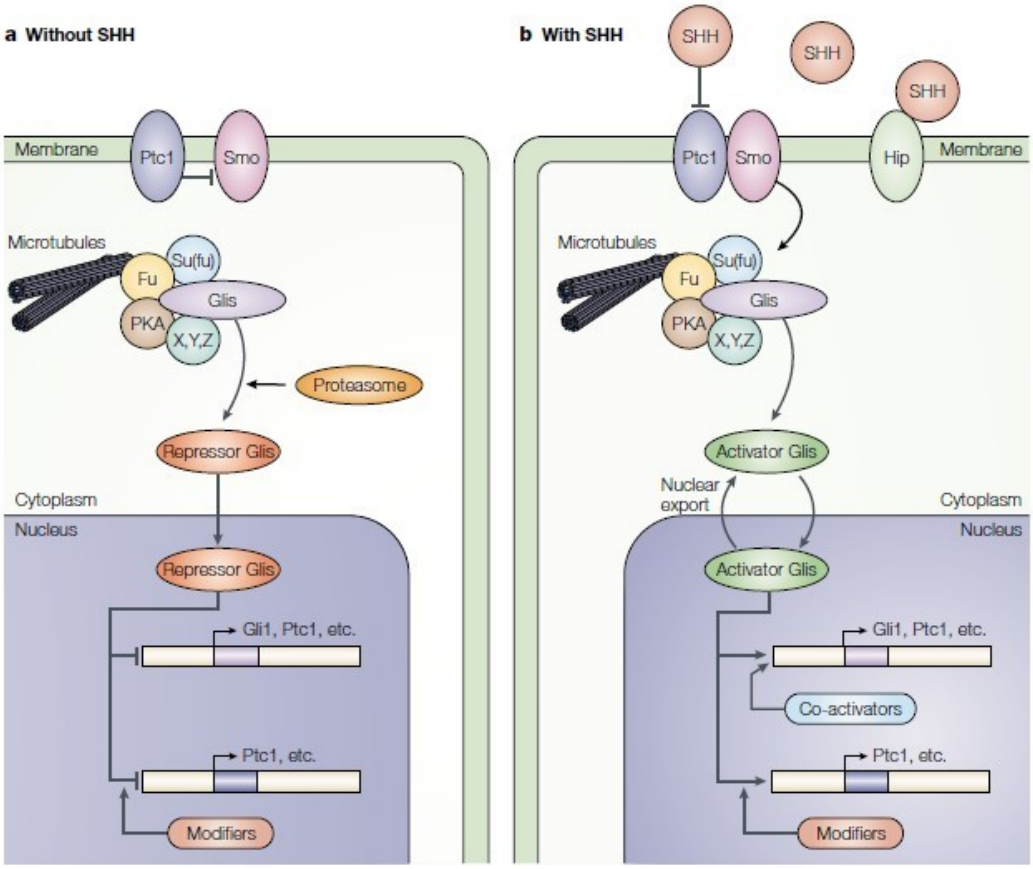

Figure 1.5: Shh-triggered intracellular events resulting in Gli function.

Upon Shh binding to the Ptch1-Smo receptor, a macromolecular complex produces Gli activators. The Macromolecular complex is associated with Su(fu) (Suppressor of fused), Fu (Fused), PKA, the Gli proteins and other possible components represented as X, Y, Z (Adopted from Ruiz i Altaba et al., 2002).

During development, the neural tube and notochord secret Shh. Together with Wnt proteins, Shh also mediates the specification of muscle progenitors in the somite. A genetic study in mice where Shh was deleted showed significant reduction of Myf5 mRNA and similar level of MyoD protein compared to wild type mice (Chiang et al., 1996). However, in a laterstage of Shh mutant embryos, the appearance of skeletal muscle indicates that differentiation of myotomal derivatives does not require Shh function. Shh is essential for the maturation of skeletal muscle progenitors into Myf5 expressing committed cells (Borycki et al., 1999; Borycki et al., 1998). In chicken embryos, ectopic overexpression of Shh upregulates the level of Pax1, sclerotomal marker but inhibites the expression of Pax3 in the dermomytome (Johnson et al., 1994).

1.3Embryonic stem (ES) cells

1.3.1 What are ES cells

ES cells are originated from the inner cell mass of a blastocyst. They can proliferate unlimitedly and can be maintained *in vitro* without any loss of differentiation potential (Ying et al., 2008). In 1981, Evans and Kaufman succeeded to cultivate pluripotent stem cell lines from mouse blastocysts, taking a feeder layer of mouse embryonic fibroblasts (Evans and Kaufman, 1981). Martin also established embryonic pluripotent cells in the same year using embryonic carcinoma cell-conditioned medium (Martin, 1981). Pluripotency of these cell lines was demonstrated *in vivo* by injecting ES cells back into blastocysts. The successful generation of chimeric mice demonstrate that ES cells keep the full developmental potency to contribute to all cell lineages including the germ line (Bradley et al., 1984). Later, Leukemia inhibitory factor (LIF) was identified as the trophic factor in the culture medium which suppresses differentiation of the ES cells, (Williams et al., 1988). LIF is a soluble glycoprotein of the interleukin-6 family of cytokines. It acts through a membrane-bound gp130 signaling complex to regulate a variety of cell functions (Burdon et al., 1999). The signal cascade of the receptor involves the JAK kinase mediated activation and STAT3 transcription factor recruitment. An external signal, LIF, keeps ES cells undifferentiated by regulating the pluripotent genes such as Oct4, Nanog and Sox2 (Chen et al., 2008). Oct4 is a POU domain transcription factor which plays a critical role in maintaining ES cell pluripotency. Oct4 deficient mouse embryos fail to develop beyond the blastocyst stage because of the lack of pluripotent inner cell mass (Nichols et al., 1998). Nanog also maintain the undifferentiated state of pluripotent epiblast. Nanog was described as a regulator for cell fate decision of the pluripotent stem cells during embryonic development. It prevents the differentiation of ES cells to primitive endoderm (Chambers et al., 2003).

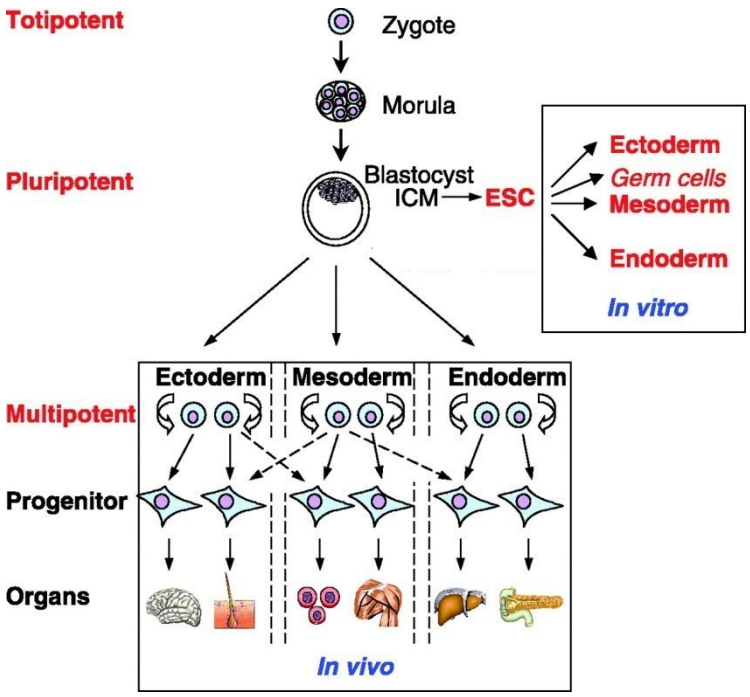

Figure Stem cell hierarchy. ICM stands for the inner cell mass. ESC represents embryonic stem cells.

Zygote and Morula stage are defined as totipotent. At blastocyst stage only the cells of inner cell mass retain the capacity to differentiate to all three primary germ layers. In adult tissues, multipotent stem and progenitors exist in tissues and organs to replace lost or injured cells. (Adapted from Wobus and Boheler, 2005)

1.3.2 *In vitro* differentiation of ES cells

During mouse development, three germ layers interact to form all tissues and organs of the embryo. The *in vitro* differentiation potential of mouse ES cells has been tested in comparison with these *in vivo* developmental processes. Differentiation of mouse ES cells can be initiated by making 3D aggregations of dissociated cells in the absence of LIF or feeder cells. This process is called embryoid body (EB) formation (Reviewed in Boheler et al., 2002). In EBs it was shown that ES cells can be differentiated into all three primary germ layers by showing the temporal expression of tissue specific marker genes and proteins (Leahy et al., 1999). By providing the proper differentiation environment, in principle ES cells can be pushed to almost all the somatic cells.

Thanks to the feature and potency of ES cells to differentiate to somatic cells, we can take advantage of them for several purposes in the area of biomedical research. First, differentiated somatic cells from ES cells are helpful for disease model generation at cellular level for the development of therapeutics (Chen et al., 2009a). Also ES cells can be a useful tool to establish the cellular disease model in order to study the pathological background of disease, where animal model is not available due to embryonic lethality. For instance, since homozygous disruption of mouse SMN (survival motor neuron) is lethal, it was not possible to isolate tissue from adult animals. However by using spinal muscular atrophy motor neurons derived from homozygous mouse ES cells *in vitro*, it was possible to do a transcriptome profiling study (Maeda et al., 2014). In this study, the gene expression levels in motor neurons derived from cell lines with or without SMN were compared. By this comparison it was discovered that pluripotency and cell proliferation transcripts were significantly increased in SMA motor neurons, while transcripts related to neuronal development and activity were reduced.

In a similar way ES cells differentiation system can be applied for uncovering unknown genes' function via genetic manipulation. In the case of functional study on lysine methyltransferase (KMT1E previously known as ESET or Setdb1) which mediates histone H3-K9 methylation, no ES cell lines could be obtained from the inner cell mass of Setdb1 (KMT1E)-null embryos (Dodge et al., 2004). The reason was the homozygous mutations of Eset resulted in peri-implantation lethality between E3.5 and E5.5. It was possible to investigate the function of KMT1E in ES cells with generation of ES cells in which the Setdb1 gene is conditionally ablated

by tamoxifen treatment using the Cre/loxP recombination system (Lohmann et al., 2010). In this report, KMT1E deficiency in ES cells resulted in derepression of genes controlling trophectoderm including as Cdx2 and Hand1 wherease pluripotency genes such as Nanog, Sox2 and Oct4 and ES cell self-renewal were downregulated.

Lastly, *in vitro* ES cells differentiation systems can be used for pharmacological or toxicological screening, as somatic cells differentiated from ES cells can react like the organs *in vivo*. For instance, cardiomyocytes derived from ES cells can be used to test cardiotoxicity of substances (Reviewed in Davila et al., 2004).

Even though ES cells have the capacity to differentiate to somatic cells, often the final populations of the differentiated cells are not pure and uniform. In addition differentiation protocols are often time consuming and complicated. Often sorting protocols for precursor cells are included. These are major limitations of *in vitro* ES cells differentiation to standardized high-throughput studies. The elucidation of a direct differentiation driver can solve some of these problems. In this thesis small molecules were taken as a tool to drive ES cells differentiation to defined skeletal muscle cells.

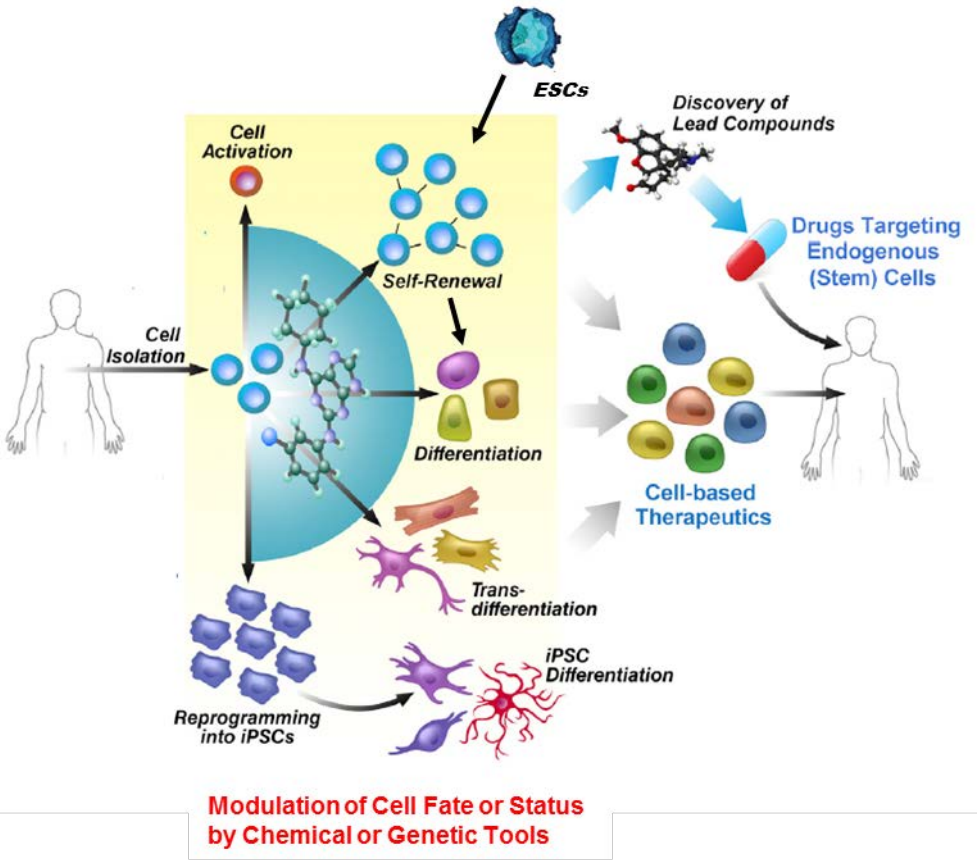

Figure Stem Cell Biology and Therapeutics.

Chemical approaches are applied *in vitro* and *in vivo* to manipulate cell fate toward desired therapeutic applications including cell expansion, differentiation (Adapted fom Li et al., 2013).

1.3.3 Small molecule screening system in EB

Small molecules are chemicals which are less than 1000 Da. They have the possibility of free diffusion to the cell membrane. And they possess unique advantages compared to growth factors as a therapy and research tools (Reviewed in Lo et al., 2014). As a biomedical research tool, taking small molecules is useful due to its easy temporal control. The effects of small molecules are mostly rapid and reversible and can be fine-tuned by controlling concentrations and combinations (Reviewed in Li et al., 2013). Compared to protein agents, small molecules have relatively simple storage and quality control requirements. They are cheaper to buy or to produce. These distinct advantages of small molecules allow flexible regulation of complicated signaling networks. However, small molecule methodologies are not flawless. For instance, off target effects of small molecules can be problematic because they can affect proteins with a similar conformation.

Small molecules based methodologies are facilitating the development of regenerative medicines. Therefore they are getting more and more important as a cell fate regulator. A molecule that was found from a screening can also provide fundamental information about uncovered biology. For example, (-)-indolactam V (ILV) was identified as an inducer of pancreatic progenitors from human ES cells. In that screening, around 5000 compounds that are already known signaling pathway regulators and kinase inhibitors were tested (Chen et al., 2009b). Studying the mechanism of ILV's action provided information that activating protein kinase C (PKC) induces beta-cell differentiation from human ES cells which was not known before. Small molecules which direct the differentiation of pluripotent stem cells to a defined somatic lineage will be described below in detail.

1.3.4 Example of small molecules as differentiation inducers identified from screening

- **Wnt pathway inhibitors for cardiomyocyte induction**

The extensive effort to obtain cardiac muscle from ES cells reported several molecules inhibiting Wnt pathway. From a screening in human ES cells with around 500 pathway modulators, IWP-1 was discovered as a hit for cardiac muscle differentiation (Willems et al., 2011). A small molecule XAV939 which inhibits Wnt signaling also induced cardiac muscle from mouse ES

cells (Wang et al., 2011). The time window for Wnt inhibition leading to cardiomyocytes induction is critical, suggesting temporal control is very important for differentiation. For example, Wnt pathway inhibition between at EB day 3 and 5 pronounced 95.2% EB beating. However, Wnt pathway inhibition between at day 3 and 4 showed only 8.3% beating mouse EBs. (Wang et al., 2011). From human ES cells, the addition of Wnt pathway inhibitors at day 4 showed the maximal cardiac induction (Willems et al., 2011).

Crescent, a member of the sFRP (Secreted Frizzled-related protein, Wnt antagonists) family, was also identified from a screen for heart inducers (Marvin et al., 2001). Crescent is expressed in anterior endoderm during development of chick embryo. The expression of Crescent is restricted to anterior endoderm and complementary to Wnt3a and Wnt8c, the homolog of human and mouse Wnt8. When Wnt3a or Wnt8c was overexpressed in anterior mesoderm which is normally differentiated to heart, the formation of heart was blocked and the promotion to blood cell fates was shown. The transgenic mouse which overexpresses Wnt8c had the phenotype of absent or reduced in size of heart (Popperl et al., 1997). These reports suggest that Wnt activity is involved in determination of the fate between blood cells and heart formation in posterior and anterior region, respectively. The Wnt pathway inhibitors' activity inducing cardiac muscle from ES cells is in line with developmental background.

- **Inducer of type II TGF-beta receptor degration-1 (ITD-1) for cardiomyocyte induction**

A TGF-beta receptor degrading molecule was identified as a driver of ES cells to cardiac muscle lineage (Willems et al., 2011). The direct target of ITD-1 is not identified but it was found to inhibit the TGF-beta pathway specifically. It induces degradation of TGF-beta receptors *via* proteasome's action. When ITD-1 was treated at an early stage of differentiation before mesoderm was formed, mesoderm formation was inhibited. As a result the effect driving to cardiac muscle was blocked. Instead it enhanced differentiation of ES cells to neuro-ectodermal fate. This molecule, ITD-1 is effective only when it was treated after mesoderm formation. It suggests that TGF-beta signaling inhibits the specification step from progenitors to cardiac muscle.

- **Stauprimide for the augmentation of directed differentiation**

Stauprimide is reported to enhance and prime the directed differentiation of ES cells to multiple lineages with synergy manner to the cue provided in culture (Zhu et al., 2009). Initially this compound was screened by a high-content imaging screening for definitive endoderm differentiation. Approximately 20,000 compounds from a kinase-oriented library were tested by a fluorescent Sox17 antibody staining. Sox17 is a transcription factor expressed specifically in the endoderm (Qu et al., 2008). By using streptavidin immobilized on agarose beads, they tried pull-down analysis in order to identify the binding targets of active analogue with linker. Mass spectroscopy identified the protein, NME2 (Nonmetastatic cells, protein expressed in-2) which is also known as PUF (a c-Myc transcription factor). Indeed Stauprimide repressed c-Myc expression in ES cells by inhibiting the nuclear localization of NME2. Repression of c-Myc expression by Stauprimide promotes ES cells differentiation.

1.3.5 Skeletal muscle differentiation from ES cells up to date

1) Genetic tools

It was reported that ectopic overexpression of Pax3 in mouse ES cells was sufficient to obtain skeletal muscle (Darabi et al., 2008). Similarly, in human ES cells overexpression of Pax7, a homolog of Pax3, showed induction of skeletal muscle (Darabi et al., 2012). Both Pax3 and Pax7 can grant and guide the skeletal muscle lineage in paraxial mesoderm. They also proved that induced skeletal muscle by Pax3 and Pax7 overexpression could ameliorate symptoms in muscular disease model such as CTX (Cardiotoxin) injected mice and dystrophic mice by transplantation.

Recently the group which published skeletal muscle differentiation from embryonic stem cells by Pax3 overexpression identified the function of Pax3 in paraxial mesoderm development and myogenesis (Magli et al., 2013). By sorting with surface markers for paraxial mesoderm, PDGFRalpha+FLK-1-, they concluded that Pax3 induces the myogenic program in the cell population which is already differentiated to the mesodermal lineage. They also identified the domain which is essential for function of Pax3. Pax3 protein consists of paired domain, homeodomain and transactivation domain. Deletion mutant analysis of Pax3 protein revealed that carboxy-terminal part of the paired domain is essential for Pax3 activity.

2) Biochemicals

- **Retinoic Acid**

Incubation with low concentration of RA (retinoic acid, 25nM) during mouse EB differentiation enhances the skeletal muscle differentiation (Kennedy et al., 2009). It was shown that RA receptors bind to the regulatory region of Meox1, Pax3 and Wnt3a genes. At the same time, RA abrogates the inhibitory activity of BMP4 on skeletal myogenesis by downregulating BMP4 expression and upregulating Tob1, which is an inhibitor of BMP4. Induction of Pax3 by RA turns on the myogenic program and upregulates myogenic regulatory factors. A genetically modified cell line which contains a dominant negative beta-catenin/engrailed repressor fusion protein did not react to RA addition. It suggests that RA acts through Wnt signaling in this differentiation protocol.

Likewise, RA incubation increases the percentage of skeletal muscle from human ES cells (Ryan et al., 2012). By treating RA in human ES differentiation, the duration of differentiation to skeletal muscle was shortened. Considering the difference in gestation time between mouse and human, this group compared and established the timeline of myogenic differentiation from mouse and human ES cells by RA. The duration until mesoderm and premyogenic mesoderm is similar in mouse and human ES cells but it takes longer time in human ES cells differentiation for myoblast and muscle formation. But the efficiency of myogenesis by RA is low. It requires further effort and improvement to obtain a better protocol for skeletal muscle differentiation from ES cells.

- **Wnt pathway activators for skeletal muscle**

In ES cells differentiation, Wnt signaling has a different action on cardiac and skeletal muscle differentiations. For cardiac muscle induction from human and mouse ES cells, inhibition of Wnt is positively effective. In contrast, Wnt activation is enhancing the skeletal muscle differentiation from ES cells. Wnt pathway activation by GSK3beta inhibitor induces paraxial mesoderm and activates the myogenic program in human ES culture system (Borchin et al., 2013). Recently another publication which was carried out with zebrafish embryos also showed that Wnt activation drives them to skeletal muscle lineage (Xu et al., 2013). This group conducted a screening using dissociated zebrafish embryo in order to identify molecules inducing skeletal muscle. A combination of chemicals (basic FGF, BIO and Forskolin) enhances the skeletal muscle differentiation in zebrafish embryos. And this combination also works in mouse and human iPS cells for skeletal muscle differentiation showing conserved activities across species. They also found a set of compounds which block the differentiation of muscle progenitors into mature muscle cells, for example, p38 pathway inhibitors. Previously it was reported that p38 pathway is required for muscle formation (Wu et al., 2000). Those studies imitated the knowledge from embryo development. For skeletal muscle progenitors during development, dorsal neuroepithelial and neural crest cells send the differentiation cues like Wnt signal for patterning of paraxial mesoderm.

Objective of the Thesis

To identify small molecules which drive embryonic stem cell differentiation to skeletal muscle with a high efficiency

Up to date the protocols known for skeletal muscle differentiation from embryonic stem cells are labor intensive, not very efficient and slow. In my Ph.D. thesis, I aimed to identify low molecular weight compounds which can enhance the efficiency and speed up the differentiation to skeletal muscle differentiation from mouse embryonic stem cells. The rational of the small molecule screening was set up based on the literature and known findings about mouse embryo development and embryonic stem cell differentiation. Pax3 transcription factor was known as the first markers of skeletal muscle during embryonic stem cell differentiation. Therefore I aimed to find small molecules which induce the level of Pax3 during mouse embryonic stem cells differentiation.

To elucidate the mechanism of action of a small molecule and provide pathways involved in embryonic skeletal muscle differentiation

Dissecting molecular pathways that are involved in ES cell derived skeletal muscle differentiation can provide critical information about the developmental process toward skeletal muscle. Since embryonic stem cell differentiation often recapitulates the development process, taking this cellular system can help to understand the complex system of embryo development. It will also help to transfer the protocol which modulates pathways from mouse ES cells to human ES cells once we know the mechanism of actions of a highly active small molecule. In this thesis I focused on identifying the mechanisms involved in skeletal muscle differentiation from mouse embryonic stem cells. The approach was based on a comparison at the mRNA and microRNA level during embryonic skeletal muscle differentiation with and without a small molecule.

Chapter 2: Result

2.1 Submitted Manuscript

Running head: A Small Molecule Drives Skeletal Muscle in ES Cells

Title: A Small Molecule Drives Skeletal Muscle Differentiation in Embryonic Stem Cells *via* Reciprocal Activation of the Wnt Pathway and Inhibition of Smad2/3 and Sonic Hedgehog Pathways.

Authors: Hyunwoo Lee,[a,d] Corinne Haller,[a] Thierry Doll,[a] Isabelle Fruh,[a] Caroline Gubser-Keller,[a] Shola M. Richards,[a] Yvonne Ibig-Rehm,[b] Maude Patoor,[c] Marjo Goette,[b] Laure C. Bouchez,[c] Matthias Mueller [a]

Address: [a]Developmental and Molecular Pathways, [b]Center for Proteomic Chemistry, [c]Global Discovery Chemistry, Novartis Institute for Biomedical Research, CH-4056 Basel, Switzerland, [d]Faculty of Sciences, University of Basel, CH-4056 Basel, Switzerland

Author contribution summary: H. L.: conception and design, collection and assembly of data, data analysis and interpretation, manuscript writing; C. H.: collection and/or assembly of data, data analysis and interpretation; T. D.: collection and/or assembly of data, data analysis and interpretation; I. F.: collection and/or assembly of data, data analysis and interpretation; C. G.-K.: collection and/or assembly of data, data analysis and interpretation, manuscript writing ; S. M. R.: collection and/or assembly of data, data analysis and interpretation, manuscript writing; Y. I.-R.: collection and/or assembly of data, data analysis and interpretation; M. P.: provision of study material; M. G.: conception and design, manuscript writing; L. C. B.: conception and design, manuscript writing; M. M.: conception and design, data analysis and interpretation, manuscript writing, final approval of manuscript

***Correspondence: Matthias Mueller**, Ph.D.; Novartis Institute for Biomedical Research, Fabrikstrasse 22, Basel, Switzerland. Phone: + 41 79 863 45 66; Fax: +41 61 324 29 90, E-Mail: matthias.mueller@novartis.com

Keywords: Embryonic stem cells, Pax3, skeletal muscle, gene expression

Disclosure of Potential Conflicts of Interest: All authors were employees of Novartis Institutes for BioMedical Research at the time of work completion.

Abstract:

The multi-lineage differentiation capacity of mouse and human embryonic stem (ES) cells offers a testing platform for small molecules that mediate mammalian lineage determination and cellular specialization. Here we report the identification of a small molecule which drives mouse ES cell differentiation to skeletal muscle with high efficiency without any genetic modification. Mouse embryoid bodies (EBs) were used to screen a library of 1,000 small molecules to identify compounds capable of inducing high levels of Pax3 mRNA. Stimulation of EBs with SMIs (Skeletal Muscle Inducer, SMI1 and SMI2) from the screen resulted in a high percentage of intensively twitching skeletal muscle fibers three weeks after induction. Gene expression profiling studies that were carried out for Mode of Actions (MoA) analysis showed that SMIs activated genes regulated by the Wnt pathway, and inhibited expression of Smad2/3 and Sonic Hedgehog target genes. A combination of three small molecules known to modulate these three pathways acted similarly to the SMIs found here, driving ES cells to skeletal muscle. Taken together, these data demonstrate that the SMI drives ES cells to skeletal muscle *via* concerted activation of the Wnt pathway, and inhibition of Smad2/3 signaling and Sonic Hedgehog (Shh) pathways. This provides important developmental biological information about skeletal muscle differentiation from embryonic stem cells and may lead to the development of new therapeutics for muscle disease.

Introduction:

Many drug discovery programs use cell-based assays for hit identification based on disease specific phenotypes. Embryonic stem (ES) cells or induced pluripotent stem (iPS) cells which can be differentiated into almost all cell types of the body may help to generate cells that are primarily affected by the disease and often can only be isolated from live animals or humans. Characterization of these cells may yield information about the signals and mechanisms of these diseases and could lead to new targets and drugs for therapy. Thus, there are considerable efforts in adopting stem cell assays for drug discovery (Tabar and Studer, 2014). However, in the case of ES cells this approach is still limited by the availability of effective differentiation protocols for specific cell types.

In embryogenesis, all skeletal muscles except for those of the head are derived from the somites. Somites are located adjacent to the neural tube and notochord and are transient, segmentally organized structures which contain the paraxial mesoderm. Signals from these structures trigger the somite to form the sclerotome, and the dermomyotome, thus giving rise to the generation of the dermis and muscle (Bentzinger et al., 2012). Cells expressing the transcription factor Pax3 in the dermomyotome migrate medially through the dorsomedial lip of the dermomyotome to form an epithelial sheet, known as the myotome (Goulding et al., 1991). Myogenesis occurs at this site upon activation of myogenic regulatory factor (MRF) genes, including; Myod1, Myf5, Mrf4 and Myog (Pownall et al., 2002). While Myf5 and MyoD activate muscle-specific gene expression and commit the progenitor cells into skeletal muscle lineage, myogenin and Mrf4 largely regulates late stage myogenic differentiation, such as the fusion of myoblasts into myotubes (Darabi and Perlingeiro, 2008). Wnt and Shh signaling, from the dorsal neural tube and notochord respectively, act as the positive regulators of Myf5 gene expression; whereas MyoD gene expression depends on Pax3 and Myf5 (Bryson-Richardson and Currie, 2008). Several groups have demonstrated the role of Pax3 in myogenesis where it activates upstream of MRFs (Magli et al., 2013). Pax7, a homologue of Pax3, also marks cells of the dermomyotome as well as satellite - the stem cells of the muscle (Jostes et al., 1990). Current methods for the generation of skeletal muscle cells from pluripotent stem cells include treating the cell with small molecules or over-expression of master regulatory genes such as MyoD or Pax3. Differentiation of the skeletal muscle by retinoic acid that upregulates Pax3 and MyoD is

substantially low in mouse and human ES cells (Kennedy et al., 2009; Ryan et al., 2012), whereas directed differentiation with Pax3 or Myf5 is more efficient but requires each desired line to be engineered for transgene expression which is slow, labor intensive and may interfere with other genes (Darabi et al., 2008; Iacovino et al., 2011).

However, protocols to proficiently produce specific cell types from ES cells with either small molecules identified by screening or by guided differentiation using multistep cell culture procedures do not currently exist for muscle (Chambers et al., 2009; Kattman et al., 2011; Shan et al., 2013). Therefore we designed a screen to identify small molecules that could induce skeletal muscle differentiation from ES cells. Based on the finding that Pax3 overexpression is sufficient to induce skeletal muscle from mouse ES cells (Darabi et al., 2008), we aimed to identify small molecules which induced Pax3 mRNA during mouse EB differentiation leading to subsequent skeletal muscle differentiation. In this study we describe, a small molecule potent inducer for skeletal muscle differentiation from mouse embryonic stem cells. Further, we could mimic its action by adding small molecules modulating well known development pathways.

Materials and Methods:

Cell Culture and Reagents

Mouse embryonic stem cells were cultured in Knock-Out Dulbecco's modified Eagle's medium (DMEM) (Ambion/ Life Technologies/ Gibco/ Invitrogen, Carlsbad, CA, http://www.invitrogen.com/site/us/en/home.html) supplemented with 15% of FBS (Biowest, Nuaillé, France http://www.biowest.net/), 1% penicillin/streptomycin (Gibco), 2 mM Glutamine (Gibco), 0.1 mM β-mercaptoethanol (Gibco), 1,000 U/ml leukemia inhibitory factor (LIF) (1000 U/ml ''ESGRO'', Millipore, Billerica, MA, http://www.millipore.com) and 3i compounds (3 μM CHIR99021, 0.8 μM PD184352, and 0.1 μM PD173074) (Sigma, St. Louis, MO, http://www.sigmaaldrich.com/sigma-aldrich/home.html) on gelatin-coated plate. Embryoid body (EB) was formed in differentiation medium containing Iscove's Modified Dulbecco's Medium (Sigma) supplemented with 10% FBS, 1% penicillin/streptomycin (Gibco), 2mM Glutamine (Gibco), 1% Insulin-Transferrin-Selenium (Invitrogen) in ultra-low-attachment (ULA) plate (Corning Costar, Corning, NY, http://www.corning.com). The number of cells for EB formation was controlled as 1,000cells/ml for 96-well format and 200,000cells/ml for 6-well format. SMI's were added at EB day 1 as well as at day 4 when EBs were transferred on 0.1% gelatin-coated plates. If not other indicated the concentration used for SMI1 and 2 was 10μM. From day 4, EB was maintained in differentiation medium which was changed every other day. Activin A (R&D, Minneapolis, MN, http://www.rndsystems.com,) was used at 50ng/ml, IWP3 (Stemgent, Cambridge, MA, https://www.stemgent.com/) at 10μM and Hh-Ag1.5 was added at 1μM. Differentiation to skeletal muscle with pathway inhibitors was carried out with 2.5μM SB431542 (Stemgent), 0.5μM BIO (Calbiochem/ Merck Millipore, Darmstadt, Germany, https://www.emdmillipore.com/index.do) and 10μM NVP-LDE225. All the three compounds were added at EB day 4. SB431542 was incubated for 2 days. Both BIO and NVP-LDE225 were incubated until EB day4+6.

Embryoid body screen

500 ES cells were dispensed in 0.1ml of DM medium into a well of a 96-well ULA plate and incubated at 37°C and 5% CO2. Next day, EB formation was controlled by imaging with Cellavista. 80μl of fresh medium was added to the well, then 20μl compound was added to have

a final compound concentration of 10μM. All samples were in duplicate. At day 4 EBs were transferred by a Hamilton robot to normal tissue culture 96-well plates (Nunc/ Thermo Fisher Scientific, Waltham, MA, http://www.thermofisher.com/en/home.html, 167008) coated for one hour with 50μl of 0.1% gelatin (Sigma, G1890). Three days later one replica was washed with PBS and frozen at -80°C for RNA analysis. For the second replica medium (0.2 ml) was changed every other day. At day 4+12 visual examination for skeletal muscle was performed. For mRNA quantification the frozen plate was slowly thawed on ice and then washed with 60μl of FCW buffer from FastLane kit (Qiagen, Hilden, Germany, http://www.qiagen.com/default.aspx). Before lysis the FCW buffer was completely removed and then 25 μl of cell processing mix (23.5 μl FCPL + 1.5 μl Wipeout Buffer 2 from FastLane kit) was added. The plate was incubated for 10 min at room temperature with gentle shaking on a plate shaker. Afterwards the lysate was transferred to a PCR (Polymerase Chain Reaction) plate containing 25 μl RNase-free water and heated up for 5 min at 75°C and before it was briefly centrifuged. Immediately thereafter the reverse transcription (RT) and PCR reactions were initiated or the plate was stored at -80°C. For RT-PCR 2μl of lysate was mixed with 5μl of mastermix from Fast Lane kit, 0.25μl TaqMan assays-on-demand Pax3 (Applied biosystems, Foster City, CA, http://www.appliedbiosystems.com/absite/us/en/home.html), 0.25μl TaqMan assays-on-demand 20x GAPDH (Applied Biosystems), 0.1 μl RT mix from FastLane kit and 2.4 μl H2O. For the RT-PCR a 7900HT AB instrument (Applied Biosystems) was used with the following program 1x20min at 50°C; 1x15min at 95°C ; 40x (45sec at 94°C, 45sec at 60°C).

Generation of Pax7 ES cells

The mouse Pax7 11.9kb sequence containing exon 8 and exon 9 until STOP codon was amplified by PCR from C57Bl/6 mouse genomic DNA together with a 3.8kb 3' arm containing the 3' end of exon 9 from STOP codon. Both arms were cloned into pRAY neomycin vector resulting in the targeting vector. Ires luciferase cassette was then integrated within exon 9 exactly downstream of the STOP codon. Sequences were compared to sequences available from the Ensembl database (Ensembl Gene ID ENSMUSG00000028736). Homologous recombination was done in 129S4 ES cell culture by electroporation of 20 μg of the linearized targeting plasmid. Transfected ES cells were selected for neomycin resistance (0.2 mg/ml G418

(Gibco#10131-019) the day after transfection. 300 neo-resistant ES cell clones were isolated and analyzed by PCR for homologous recombination as well as southern blot for the correct integration.

Luciferase Assay

Envision plate reader (Perkin Elmer, Waltham, MA, http://www.perkinelmer.com/default.xhtml) was used to measure luminescence levels of Luciferase *via* Steady-Glo kit (Promega, Madison,WI, http://www.promega.com) from differentiated EBs according to the manufacturer's recommendations. FireFly luciferase activities were normalized to the cell viability measured at the beginning with Resazurin.

Flow Cytometry Analysis

EBs were dissociated by TrypLE Express (Life Technologies) for 30 min at 37°C and fixed by 4% paraformaldehyde for 10 min. Single cells were incubated for 1 hour with Pax3-PE (R&D Systems, IC2457P, 1:50 dilution) after permeabilization with 0.1% Tween-20 in PBS. Flow cytometry analysis was done with CyAn ADP Analyzer (Beckman Coulter, High Wycombe, UK, https://www.beckmancoulter.com).

Reverse Transcription quantitative PCR

Total RNA was extracted from differentiated EBs at indicated time points with Trizol (Invitrogen) according to the manufacturer's instructions. RNA concentration was determined by Nanodrop and reverse transcription was done with 500ng of total RNA by Reverse Transcription kit (Applied Biosystems). qPCR reactions were carried out on a 9600 (Applied Biosystems) with TaqMan mastermix (Applied Biosystems). mRNA levels were normalized to levels of GAPDH mRNA in each sample. TaqMan Probes for PCR were purchased from Applied Biosystems (See Supporting Information Table S1).

Immunocytochemistry

For Pax3 staining from EB, paraffin section staining was carried out after embedding EBs to agarose and paraffin. Differentiated EBs were fixated with 4% paraformaldehyde and

permeabilized with 0.2% Triton X-100 in PBS followed by citrate buffer antigen retrieval using the Citrate Buffer Concentrate pH 6.0 (Quartett Immunodiagnostika, Berlin, Germany, http://www.quartett.com/). Pax3 antibody supernatant (DSHB, Iowa City, IA, http://dshb.biology.uiowa.edu/, 1:50 dilution) was incubated overnight at 4℃. Prior to incubation with primary Myogenin (DAKO, Glostrup, Denmark, www.dako.com, M3559, 1:200 dilution) and MHC (Merck Millipore, 05-716, 1:500 dilution) antibodies, EBs were incubated with blocking solution containing normal goat serum. Incubation with detection antibodies labeled with Alexa 594(Invitrogen) or Texas Red (Invitrogen) was followed by DAPI (Promokine, Heidelberg, Germany, http://www.promokine.info/) staining.

Immunoblot Antibodies

For immunoblot assay for phosphorylation of Smad proteins, EBs were differentiated in 6 well ULA plate (Corning) with 200,000 cells/ml concentration. 10μM SB431542 was treated at EB day 1 to inhibit the phosphorylation of Smad proteins. Protein lysate at the indicated time point was prepared with RIPA buffer (Rockland, Gilbertsville, PA, http://www.rockland-inc.com/Default.aspx). Antibodies used include phospho-Smad2 (Merck Millipore, AB3849), phospho-Smad3 (Merck Millipore, 04-1042), Pax3 (DSHB, Univeristy of Iowa) and GAPDH (Ambion, AM4300).

Microarray processing and data analysis

RNA samples were subjected to microarray analysis on Affymetrix GeneChip Mouse Genome 430 2.0 chips (Affymetrix) according to the manufacturer's recommendations. All statistical analyses were performed using R/Bioconductor (www.bioconductor.org). Quality control was performed using both AffyQCreport and arrayQCmetrics packages. Data was Robust Multichip Average (RMA) normalized using RMA and scaled to a 2% trimmed mean of 150. Probes with normalized expression values below 50 in 75% of samples were filtered out. Differential gene expression was performed using a linear model approach (Limma). Genes with a fold change higher than 2 and a P-value below 0.01 (Benjamini and Hochberg multiple testing correction) were considered regulated. Gene set enrichment analysis (GSEA) (Subramanian et al., 2005), was performed on fold change ranked list of all non-filtered probesets collapsed to

gene symbols using Panther Pathway Library and Metacore gene sets databases. GSEA results were further analyzed using the enrichment map tool (Merico et al., 2010). GSEA results were visualized using Tibco Spotfire.

Results:

EB screening identified skeletal muscle inducers (SMIs)

To identify factors that permit skeletal muscle formation from mouse ES cells, we designed a screen based on embryoid body differentiation. Because EB spontaneously differentiates into the three germlayers, they may represent an efficient system to identify specific compounds which can influence this differentiation process. The readouts in our screen for skeletal muscle induction were; Pax3 mRNA upregulation at an early time point (d4+3) and the occurrence of skeletal morphology by visual examination at a later time point (d4+12). As a consequence the screen was performed in duplicate to have both readouts. EB formation was carried out using ULA (Ultra Low Attachment) culture plates with 500 dissociated ES cells per well in suspension culture. Compounds, as a 10 μM solution in DMSO, were added at day 1. EB size measurement demonstrated a very low 'well-to-well' variation during the first 4 days (Fig. S1). As EB size became more variable from day 4, we transferred the EB at day 4 to gelatin-coated culture plates for further differentiation. Three days later from transfer (d4+3) Pax3 and GAPDH (for normalization) mRNA levels were measured in the first replica by Real-Time RT-multiplex PCR. In the second replica, skeletal muscle formation was evaluated by visual inspection followed by MHC (Myosin Heavy Chain) staining at day 4+12. Out of 968 small molecules tested, 18 compounds increased Pax3 RNA more than 6 fold (Fig. 1A). Six compounds induced both Pax3 mRNA and skeletal muscle morphology. However, only one compound showed a dose dependent induction of Pax3 mRNA. Further validation showed that *N*-[4-(trifluoromethyl)-6-methoxymethyl-2-pyrimidinyl]-*N*-(2-methyl-6-nitrophenyl)-urea (→ called Skeletal Muscle Inducer 1 (SMI1)) was also the most potent inducer of skeletal muscle (Fig. 1B) with an EC50 of 8 μM (Fig. 1C). Structure-activity relation experiments for SMI1 identified SMI2, a N-methyl-pyrimidinyl analogue, that exhibited 30% higher induction of skeletal mRNA markers compared to its parent compound (Fig. 1B). Interestingly, the EC50 of SMI2 was not significantly increased (Fig. 1C).

The increase of Pax3 was also further confirmed by Immunofluorescence staining for Pax3 of 8 day old EBs (Fig. 1D) and by FACS analyses (Fig. 1E). Cells treated with SMI1 showed about 15 to 20% Pax3 positive cells whereas untreated control showed around 1%. To confirm skeletal muscle lineage commitment additional muscle markers were analyzed. First

induction of the satellite cell marker, Pax7, was examined using an ES Cell line containing a Luciferase coding region inserted into the endogenous Pax7 gene's 3'-UTR. SMI1 induced a time dependent increase of Pax7-luciferase expression starting at day 4+2 with a peak at day 4+7 (Fig. 2A). At day 4+4 MyoD, Myf5 and Myogenin demonstrates the presence of fully developed skeletal muscle. SMI1 induced significant increase in MyoD, Myogenin and Myf5 mRNAs (Fig 2B and S2). Induction of a muscle phenotype was confirmed by immunofluorescence staining staining for Myogenin and skeletal MHC (Fig 2C) and by the spontaneous contraction at later time points, which demonstrates the presence of a functional contraction apparatus (Movie 1). The kinetics of mRNA expression shows the expected order of the different markers. Pax3 and Pax7 were first detected at day 4+1 followed by MyoD, Myogenin and Myf5 at day 4+5 (Fig. S2). To quantify the percentage of skeletal muscle at the end of differentiation we used an indirect measurement based on the area which stains positive in immunofluorescence staining for MHC three weeks after the initiation. The percentage varied between EB, although often up to 100% of the cell area stained positive for MHC when treated with SMIs whereas in DMSO treated controls only in very rare cases positive cells were found (Fig. 2D; Fig.S7). Interestingly, we found very often beside skeletal muscle fibers also adipocytes (Fig. S3).

Comprehensive gene expression level study

In order to better understand the mechanism of action of SMI, we performed gene expression analysis with mRNA samples of three independent experiments from undifferentiated mouse ES cells and differentiated mouse EBs at day 4 and day 4+4, either in presence or absence of SMI1. Using Affymetrix expression arrays, 68 genes (d4) and 569 genes (d4+4) were expressed differentially by SMI1 treatment at a threshold of fold change more than 4 and a p-value less than 0.05 (Supporting Information Table S2). As expected, pluripotency genes, such as Nanog, Oct4, Sox2, Rex1 and Klf4 (Takahashi and Yamanaka, 2006), were downregulated as ES cells progressed towards differentiation in both groups (Fig. S4). However, the pluripotency genes were not differentially regulated by SMI1 treatment compared to control. Among the most upregulated genes after day 4+4 from SMI1 treatment we found Pax3 and Pax7 as well as the myogenic regulatory factor MyoD and Myogenin (Supporting Information Table S2).

In order to explain and understand the MoA induced by SMI1, we performed a Gene Set Enrichment Analysis (GSEA) for day 4 and day 4+4 time points (Supporting Information Table S3). Using the Panther Pathway Library and Metacore gene sets databases a number of pathways linked to development process like ectoderm development (Bessarabova et al., 2012; Thomas et al., 2003) were differentially expressed in SMI1 treated samples compared to the control group. Interestingly at day 4 the Wnt pathway was clearly upregulated. Therefore we looked at Wnt pathway and its target genes more carefully. From 82 genes categorized as part of the Wnt pathway, 9 genes were upregulated more than 2 fold and only 2 genes were negatively regulated more than 2 fold in EBs at day 4 after SMI1 treatment (Supporting Information Table S4). Out of 13 Wnt target genes, 5 genes were significantly induced more than 2-fold compared to the untreated control group (Fig. 3A). The strong regulation of sets of genes related to Wnt pathway is consistent with the critical role of Wnt activation during embryonic skeletal muscle differentiation (Aulehla and Pourquie, 2010). It has been shown that canonical Wnt activation is an initial step to induce skeletal muscle developed from paraxial mesoderm. Other well-known developmental pathways were negatively regulated by SMI1, including the Nodal Pathway at day 4 and the Sonic Hedgehog pathway at day 4+4. At EB day 4, GSEA analysis revealed that many gene sets involved in Nodal signaling in early mesendoderm formation were downregulated in the SMI1 treated group. At day 4+4, the number of gene sets involved in hedgehog signaling in medulloblastoma stem cells was reduced. Strikingly, Shh itself was one of the most down regulated genes (Supporting Information Table S2). Based on these findings we hypothesized that Wnt pathway, Nodal pathway and Sonic hedgehog signaling play a significant part in the skeletal formation out of mouse EB formation induced by the SMI.

Dependency of Wnt activation during SMI's action

To validate if the Wnt pathway plays a major role in SMI's action, we measured the mRNA level *via* Real-time RT-PCR analyses of Brachyury T (BraT), Mesogenin1 and Axin2, that are known as important Wnt signaling outputs during development (Aulehla and Pourquie, 2010). SMI stimulation was indeed increasing the level of BraT and Axin 2 as well as Mesogenin1, which is a key player for genesis of the paraxial mesoderm at either EB day 3 or 4 (Fig. 3B) (Fior et al., 2012). To further validate if SMI's action is dependent on Wnt pathway

activation, EBs were differentiated together with an inhibitor of the Wnt pathway, IWP3 (Chen et al., 2009a; Willems et al., 2011). As expected, EB differentiation toward skeletal muscle lineage was effectively inhibited. After co-treatment with IWB3 none of the skeletal myogenic genes, Pax3, MyoD, Myf5 and Myogenin were upregulated in EB day 4+4 (Fig. 3C) cultures, whereas Nkx2-5 which is a key transcription factor for the cardiac differentiation was not affected (Fig. S5A). To further confirm the effect of Wnt pathway inhibition during SMI1's action, we examined the activity on a Pax7 Luciferase knock-in ES cell line. Intriguingly the level of Pax7 Luciferase was completely downregulated by Wnt pathway inhibition when added together with SMI2 (Fig. 3D). Based on these findings we conclude that Wnt activation was a key event of SMI's action for skeletal formation of ES cells. However, addition of BIO, a Wnt pathway activator, did not stimulate skeletal muscle differentiation (Fig. S5B). Thus, we speculate that additional pathways must also be necessary for the action of SMI.

Nodal pathway is involved in SMI's action

GSEA at day 4 indicated that SMI1 affected the Nodal pathway in EBs at day 4. Indeed 4 genes (Cer1, Gsc, Eomes1 and Otx2) which are described as members of the Nodal pathway were among the top 12 downregulated genes in SMI1 treated EBs at day 4 (Fig. 4A, 4B, Supporting Information Table S2) (Liu et al., 2011). Smad signaling led by Nodal/Activin has been known to be involved in ES cell propagation (Ogawa et al., 2007). In addition, the signal gradient of Nodal/Activin pathway is an important factor for cell fate decisions between mesendoderm and trophectoderm lineages (Lee et al., 2011). These data suggested that Smad signaling might be affected by SMI1 addition. Indeed, phosphorylation level on Smad2/3 proteins in EBs at day 4 was moderately decreased 3 days after SMI1 addition (Fig. 4C). To elucidate if the decrease of Smad signaling is critical for SMI1 action, we tested EB differentiation in presence of both SMI1 and Activin A. When Smad signaling was activated by Activin A together with SMI1, the differentiation to skeletal muscle lineage was inhibited. mRNA levels of Myogenin at EB day 4+4 was dramatically reduced by Activin A treatment (Fig. 4D). These observations are consistent with inhibition of Nodal/Activin signaling being part of skeletal muscle differentiation by SMI.

Sonic Hedgehog activation inhibits SMI's action

GSEA analysis of the microarray data at day 4+4 revealed that the majority of genes belonging to Sonic Hedgehog transcriptional signatures were significantly downregulated during differentiation induced by SMI1 (Fig. 5A). Confirmation experiments by Real-time RT-PCR for key components of the Shh pathway (Shh, Gli and Ptch) showed that expression of all tested genes was dramatically decreased by SMI1 (Fig. 5B). In order to further validate the function of Shh pathway during SMI action, we differentiated EBs with SMI2 and the well characterized Smo agonist Hh-Ag1.5 (Frank-Kamenetsky et al., 2002). As expected the inducing effect on mRNA of Pax3, MyoD, Myf5 and Myogenin by SMI2 was dramatically decreased when the Smo agonist was added to EBs at day 4 together with SMI2 (Fig. 5C). Likewise, increase of Pax7 reporter Luciferase activity by SMI2 was blocked by adding Smo agonist Hh-Ag1.5 (Fig. 5D). Based on these data, we conclude that inhibition of the Shh pathway as well as Wnt and Nodal pathway modulation is part of SMI's induction of skeletal muscle formation. As a consequence of this finding we speculated that it should be possible to induce skeletal muscle formation by adding compounds which modulate these three pathways.

Mimic of SMI1's action by small molecule cocktails modifying identified signalings

The data obtained so far suggest that differentiation of skeletal muscle from ES cells by SMI is initiated by Wnt pathway stimulation and Nodal pathway inhibition at an early time point followed by Shh signaling inhibition at a later time point. To test this hypothesis the following compounds were used: as a stimulator of the Wnt pathway the glycogen synthase kinase-3 inhibitor (BIO) was selected because of its low toxicity and as inhibitors of Nodal and Shh the Alk4/5/7 inhibitor (SB431542) and the Smo antagonist (NVP-LDE225 also known as Erismodegib) were added, respectively (Inman et al., 2002; Pan et al., 2010; Sato et al., 2004; Xu et al., 2013). First we tested modulation of each single pathway on skeletal muscle differentiation. However, single molecules showed no positive effect on skeletal muscle differentiation (Fig. S5B, data not shown). Next we tested the combination of the inhibitors of Smad and Hedghog signaling at different time points. Because Nodal inhibition was found earlier than Shh inhibition we kept the time point of the addition of NVP-LDE225 constant and varied the time point of Nodal inhibition. Indeed, when SB431542 was added to EBs at day 1, where mesoderm was not

yet formed (Fig. S6), EB differentiation to skeletal muscle based on mRNA induction was not induced whereas addition of SB at day4 showed dramatic Pax7 induction (Fig. 6A; Fig. S6). This induction could be further enhanced by adding BIO on top of SB431542 and NVP-LDE225 at day 4. Again addition of BIO at day 4 showed the highest synergistic effect with SB431542 and NVP-LDE225 (Fig. 6B). Real-time RT-PCR analyses for muscle specific markers as well as immunofluorescence staining demonstrate that BIO/SB/LDE (BSL) treatment alone was enough for induction of skeletal muscle. Pax3, Pax7 and Myf5 mRNA were significantly induced at EB day 4+4 as well as MyoD and MyoG at day 4+8 (Fig. 6C, 6D). Again immunofluorescence staining of Myogenin and MHC at day 4+8 and day 4+20 confirmed the skeletal muscle induction at later time points (Fig. 6E, S7). Similar to EBs treated with SMIs, intensive twitching was observed (Movie 2). Finally, combining SMI1 to the BSL protocol was not an additive process (Fig. S8). All these data indicate that SMI1 acts indeed through Wnt, Smad signaling and Hedgehog pathway and that BSL treatment could be an alternative way for inducing skeletal muscle from mouse ES cells.

Discussion:

Currently available differentiation protocols for the generation of skeletal muscle from ES cells are still very labor intensive and often not very efficient. The aim of this study was to identify small molecules which can push ES cell differentiation towards skeletal muscle cells. In an initial screen we identified SMI1 as a potent inducer of skeletal muscle differentiation. Although the direct target of SMI1 has not yet been identified, the work presented here suggests that the SMI acts directly or indirectly by activating Wnt and inhibiting Nodal and Shh pathways. Indeed a cocktail of molecules that able to interact directly with these pathways induced differentiation of mouse EBs similarly to the SMIs. The method described herein, offers a robust and simple methodology for the induction of highly functional skeletal muscle from mouse EBs.

EBs represent complex, ordered, 3-dimensional structures with the capacity to reproduce a number of developmental processes and produce a remarkable number of cell lineages present in mature organs. EB differentiation protocols are thought to allow many of the same inductive processes that accompany the development of embryonic organs. It is also assumed that many of these processes will be similar in adult organ regeneration (Rohwedel et al., 1994). Thus EBs may provide a platform to identify genes that can enhance or inhibit lineage commitment and expansion in the context of diverse cell-cell interactions that occur *in vivo*. Our finding that activating Wnt and inhibiting Smad2/3 and Shh pathways can push ES cell into the muscle lineage is consistent with several *in vivo* studies. In vertebrate skeletal muscle originates from somites where paraxial mesoderm receives the cue for further differentiation to dermomyotome from the dorsal neural tube and notochord by many different factors (Bailey et al., 2001). In this complex and well-coordinated interplay of various pathways, members of the Wnt family play an important role for the formation of the somites and the dermomyotome (Bentzinger et al., 2012). Other studies have also found that Wnt activation is indeed a key step for skeletal muscle induction in ES cells differentiation (Borchin et al., 2013; Xu et al., 2013). The finding the number of Pax3 positive cells is increased in Shh deficient embryos from mouse and zebrafish is also consistant with our findings that Shh inhibition increases Pax3 levels in EBs (Borycki et al., 1999; Feng et al., 2006). In contrast, the finding that the Nodal/Activin A pathway is involved in skeletal muscle formation is at present novel. One explanation for this activity is that Nodal/Activin A inhibition acts indirectly by suppression of endoderm formation. Activin A

stimulation is normally used to push ES cell into the definitive endoderm. Inhibition of this prominent differentiation pathway in EBs could lead to the enhancement of mesoderm formation and thereby to an increase of skeletal muscle formation. This explanation is supported by the analysis of genes regulated at day 4+4 after SMI induction. These studies demonstrated that Nodal signaling associated with early mesendoderm formation as well as Activin A signaling was downregulated whereas early embryonal epaxial and hypaxial myogenesis were enhanced by SMI treatment (Supporting Information Table S3).

The similarity of the EB differentiation to the *in vivo* development is further supported by two observations. During the experiments we realized that SMI as well as BSL were not only inducing skeletal muscle but often also adipocytes (Fig. S3). Pathway analysis indeed indicated that the brown fat differentiation was induced (Supporting Information Table S3). These data imply that the protocol we identified induced a common precursor cell population. Skeletal muscle and brown adipocytes have the same differentiation history coming from mesoderm and are separated later in development at the stage of mesenchymal stem cells (Gesta et al., 2007). In addition we realized that SMI is not only inducing skeletal muscle and adipocytes formation but also inhibiting the formation of cardiomyocytes. Normally no beating cardiomyocyte clusters were found in the SMI-treated EBs, which was in strong contrast to untreated samples (data not shown). This finding was supported by an external finding that Wnt inhibition as well as Alk 2/3 inhibition by Dorsomorphin or Noggin can enhance the formation of cardiomyocytes (Hao et al., 2008; Wang et al., 2011). It appears that these differences in signaling are important for switching between skeletal and cardiac differentiation.

Finally, there is considerable interest in creating myogenic precursors for cell based therapy in muscle disease such as muscular dystrophy. Darabi and Iacovino et al. have demonstrated that expression of Pax3, Pax7 or Myf5 in ES and iPS cells can drive differentiation to myogenic precursors that can be transplanted in mice (Darabi et al., 2012; Darabi et al., 2008; Iacovino et al., 2011). However, the use of genetically modified ES cells for gene therapy creates potential safety issues for ultimate use in patients, which could be eliminated by efficient transgene-free differentiation procedures. Although the SMI and BSL procedures described here are highly efficient, similar procedures still need to be optimized for human ES and iPS cell cultures. Also the ability of chemically induced myogenic cells described here to engraft into

adult muscle needs to be determined. If successful this method could provide an efficient, scalable transgene free platform for production of myogenic cells for human therapy.

Conclusion

In this study, we identified two molecules, SMI1+2, which were able to direct the fate of differentiating ES cells to skeletal muscle and elucidated their mode of action. It may provide a new platform to produce functional skeletal muscle derived from ES cells.

Acknowledgments

We thank Bettina Leonhard, Carole Manneville and Annick Werner for helpful discussion and for their help on week-ends. Susan Gasser, Patrick Matthias, Mark Labow and Tewis Bouwmeester we thank for critical reading of the manuscript and enthusiastic support.

Figure legends:

Figure 1: EB-Screen identified SMI1 as a modifier of skeletal muscle development

(A) Delta Ct mRNA levels of Pax3 normalized to GAPDH of each compound used in the screen. Each row represents a 96 well plate. Threshold was set 2.5 Ct values over the average Ct of DMSO treated EBs which are marked with black color. Arrow indicates data for SMI1.

(B) Structure of SMI1 and its more potent analogue, SMI2.

(C) Dose-dependent induction of Pax3 mRNA levels by SMI1 and SMI2, normalized to GAPDH in mouse EBs measured by Real-time RT-PCR. The bars indicate standard deviation for 3 independent EBs from a representative experiment.

(D) Immunofluorescence staining for Pax3 expression on a section of an eight day old EB treated with SMI1 compared to untreated control. Scale bar indicates 80 μm.

(E) Representative flow cytometry analysis with an antibody against Pax3 of dissociated EBs at day 4+4 either treated with SMI1 (red) or untreated (blue).

Figure 2: Characterization of skeletal muscle induction by SMI treatment

(A) Kinetics of Pax7 luciferase activity in Pax7 luciferase knock-in ES cells after treatment with SMI1 or DMSO. The bars indicate standard deviation for 3 independent EBs from a representative experiment.

(B) The relative transcript levels at day 4+4 of MyoD, Myf5 and Myogenin were determined by real-time RT-PCR analysis and plotted as fold change of untreated controls after being normalized to GAPDH. Both compounds were added at 10 μM at day 1 and day 4. The bars indicate standard deviation for 3 independent pools of 10 EBs from a representative experiment.

(C) Immunofluorescence staining for Myogenin (red) of a mouse EB at day 4+8 (upper panel, scale bar indicates 20 μm) and at day 4+20 for MHC (lower panel, scale bar indicates 160 μm). DAPI was used to stain the nucleus. The white square indicates the region with higher magnification demonstrating the striation of the muscle cells.

(D) Immunofluorescence staining for MHC (red) of a whole single EB in a 24 well plate at day 4+20 either untreated or SMI2 treated. The image is a composition of many individual pictures in order to visualize the entire EB. DAPI was used to stain the nucleus. Scale bar indicates 2mm.

Figure 3: The Wnt pathway is critical for SMI action for skeletal muscle formation.

(A) Microarray analysis of SMI1 treated mouse EBs revealed that Wnt pathway downstream genes are mostly upregulated ($p<0.05$).

(B) The relative transcript levels of mesodermal markers (T and Mesogenin1) and Wnt pathway downstream genes (T, Mesogenin1, Axin2) in SMI2 treated EBs compared to untreated controls. Data is normalized to GAPDH. RNA was isolated at day 3 and 4 after treatment with SMI2 (10μM) at day 1. The bars indicate standard error of the mean for at least 3 independent pools of 10 EBs from a representative experiment. (* ; $p < 0.05$ and *** ; $p < 0.001$ by student's t test, significance vs control)

(C) Relative transcript levels at day 4+4 of Pax3, Pax7, MyoD, Myf5 and Myogenin were determined by real-time RT-PCR analysis and plotted as fold variance of controls after being normalized to GAPDH. All compounds were added at 10μM at day 1 and day 4. The bars indicate standard error of the mean for 3 independent pools of 10 EBs from a representative experiment. (* ; $p < 0.05$ and ** ; $p < 0.01$ by student's t test, significance vs SMI2 treated)

(D) Pax7 luciferase activity of a Pax7 luciferase knock-in ES cell line after treatment at day 1 and day 4 with SMI2 (10μM) and/or IWP3 (10μM). The bars indicate standard error of the mean for 4 independent EBs from a representative experiment. (** ; $p < 0.01$ by student's t test)

Figure 4: Inhibition of Smad2/3 signaling pathway is a key event in SMI action toward skeletal muscle differentiation.

(A) Microarray analysis of mouse EBs at day4 shows that Nodal pathway related genes are differentially regulated at day 4 in presence of SMI1. ($p<0.05$)

(B) The relative transcript levels at day 4 of FoxaA2, Gsc and Otx2 were determined by real-time RT-PCR analysis and plotted as fold variance of SMI treated EBs to controls after being normalized to GAPDH. SMI1 was added at 10uM at day 1. The bars indicate standard error of the mean for 3 independent pools of 10 EBs from a representative experiment. (* ; $p < 0.05$, (** ; $p < 0.01$ and *** ; $p < 0.001$ by student's t test, significance vs control)

(C) Western blot for p-SMAD2 and p-SMAD3 indicates decreased phosphorylation on Smad2/3 proteins in EBs which were treated at day 1 with 10μM SMI1 or 10μM SB431542, respectively. Protein was isolated at day4.

(D) The relative transcript levels at day 4+4 of Myogenin was determined by real-time RT-PCR analysis and plotted as fold variance of DMSO treated controls after being normalized to GAPDH. SMI1 was added at 10μM at day 1 and day 4. At the same time points Activin A was added at concentration of 50ng/ml. The bars indicate standard error of the mean for 5 independent EBs from a representative experiment. (* ; $p < 0.05$ by student's t test)

Figure 5: Sonic Hedgehog pathway signaling is inhibited by SMI.

(A) Microarray analysis of mouse EBs at day 4+4 in presence of SMI1 revealed that some of Sonic Hedgehog pathway related genes were downregulated. ($p<0.05$)

(B) The relative transcript levels at day 4+4 of Shh, Gli1, and Ptch1 were determined by real-time RT-PCR analysis and plotted as fold variance of untreated controls after being normalized to GAPDH. SMI2 was added at 10μM at day 1 and day 4. The bars indicate standard error of the mean for 3 independent pools of 10 EBs from a representative experiment. (* ; $p < 0.05$ by student's t test, significance vs control)

(C) Relative transcript levels at day 4+4 of Pax3, Pax7, MyoD, Myf5 and Myogenin were determined by real-time RT-PCR analysis and plotted as fold variance of untreated controls after being normalized to GAPDH. SMI2 was added at 10μM at day 1 and day 4. The Smo Agonist Hh-Ag1.5 was added from day 4 until day 4+4 at a concentration of 1μM. The bars indicate standard error of the mean for 3 independent pools of 10 EBs from a representative experiment. (* ; $p < 0.05$ and ** ; $p < 0.01$ by student's t test, significance vs SMI2 treated)

(D) Pax7 luciferase activity of a Pax7 luciferase knock-in ES cell line at day 4+8 in mouse EB treated with 10μM SMI2 (day1 and day4) and 1μM Smo Agonist Hh-Ag1.5 (from day4 until day 8). The bars indicate standard error of the mean for 4 independent EBs from a representative experiment. (** ; $p < 0.01$ by student's t test)

Figure 6: A Cocktail of small molecules can mimic the action of SMI.

(A), (B) Graphs represent Pax7 luciferase activity in a Pax7 luciferase knock-in ES cell line at day 4+8 in mouse EBs treated with the indicated combination of small molecules. The concentration used were for NVP-LDE225 (10μM), SB431542 (2.5μM) and BIO (0.5μM). In (A)

LDE 225 was added at day 4 and time point of SB addition was varied and the bars indicate standard error of the mean for 3 independent EBs from a representative experiment. In (B), addition of SB431542 +NVP-LDE225 was kept constant at day 4 and the time point of addition of BIO was varied. The bars indicate standard error of the mean for 3 independent experiments. (* ; $p < 0.05$, ** ; $p < 0.01$ and *** ; $p < 0.001$ by ANOVA test, significance vs control)

(C), (D) Relative transcript levels at day 4+4 (C) and day 4+8 (D) of Pax3, Pax7, MyoD, Myf5 and Myogenin were determined by real-time RT-PCR analysis and plotted as fold variance of DMSO treated controls after being normalized to GAPDH. EB were treated with the combination of small molecules, BIO, SB431542 and NVP-LDE225 at day 4. SB431542 was incubated for 2 days and BIO and NVP-LDE225 were kept until day 4+6. The bars indicate standard error of the mean for 3 independent pools of 10 EBs from a representative experiment. (* ; $p < 0.05$, ** ; $p < 0.01$ and *** ; $p < 0.001$ by student's t test, significance vs DMSO treated)

(E) Immunofluorescence staining staining of Myogenin (red) and MHC (red) in mouse EB with combination of BIO, SB431542 and NVP-LDE225 at EB day 4+8. DAPI was used to stain the nucleus. Scale bar indicates 20μm.

Supporting Information:

Supplementary Figure 1: Kinetic change in EB size in a 96 well ULA plate after plating of 500 ES cells in DM medium. Each well was measured automatically with a Cellavista instrument and the area was calculated automatically.

Supplementary Figure2: Kinetics of myogenic factor expression after addition of SMI1. The relative transcript levels of Pax3, Pax7, MyoD, Myf5 and Myogenin were determined by real-time RT-PCR analysis and plotted as fold variance of DMSO treated controls at day 4 after being normalized to GAPDH. SMI1 was added at 10μM at day 1 and day 4.

Supplementary Figure 3: **SMI1 as well as BSL induced adipocyte as well as skeletal muscle differentation.**

(A) Bright-field microscopy images showing adipocytes on top of skeletal muscle fibres. On the left a culture stimulated with 10μM SMI1 and on the right in higher magnifaction a BSL stimulated culture.

(B) Adipocytes were stained with Sudan Red.

Supplementary Figure 4: Microarray analysis of expression levels of pluripotency genes in mouse ES cells and EBs treated with SMI1 at 10μM.

Supplementary Figure 5:

(A) Relative transcript levels at day 4+4 of Nkx2-5 was determined by real-time RT-PCR analysis and plotted as fold variance of DMSO treated controls after being normalized to GAPDH. SMI2 was added at 10μM at day 1 and day 4. 10μM IWP3 was added at day1.

(B) Pax7 luciferase activity in a Pax7 luciferase knock-in ES cell line after treatment with 10μM SMI at day1 and day 4 or with 0.5 μM BIO at indicated time point. The bars indicate standard deviation. (* ; $p < 0.01$ by student's t test)

Supplementary Figure 6:

When mesoderm formation was inhibited by 10μM SB431542 treatment, induction of skeletal muscle by SMI was also inhibited. Graph shows relative transcript levels at day 4 (BraT), d4+4 (Pax3) and d4+8 (Myogenin). Values were determined by real-time RT-PCR analysis and plotted as fold variance of untreated controls after being normalized to GAPDH.

Supplementary Figure 7: IHC for MHC of a whole single EB in a 24 well plate at day 4+20. Each image is a composition of many individual pictures. Scale bar indicates 2mm. Upper row EBs are DMSO treated control, middle row EB treated with 10μM SMI 1 and lower row EB' stimulated with BSL.

Supplementary Figure 8: Graph shows relative transcript levels of Pax7, Myf5, MyoD and MyoG at day 4+8. SMI2 did not enhance the induction of myogenic genes mRNA level in combination with BSL. Values were determined by real-time RT-PCR analysis and plotted as fold variance of DMSO treated controls after being normalized to GAPDH. Error bars indicate the standard deviations.

Supplementary Table 1: Applied Biosystems TaqMan Gene Expression Assays used in Real-Time RT-PCR analysis

Supplementary Table 2: Differentially expressed genes at day 4 and day4+4

Supplementary Table 3: GSEA at EB day4 and day4+4

Supplementary Table 4: Wnt signaling genes

References

1. Tabar V, Studer L. Pluripotent stem cells in regenerative medicine: challenges and recent progress. Nature reviews Genetics. 2014;15:82-92.
2. Bentzinger CF, Wang YX, Rudnicki MA. Building muscle: molecular regulation of myogenesis. Cold Spring Harbor perspectives in biology. 2012;4.
3. Goulding MD, Chalepakis G, Deutsch U et al. Pax-3, a novel murine DNA binding protein expressed during early neurogenesis. The EMBO journal. 1991;10:1135-1147.
4. Pownall ME, Gustafsson MK, Emerson CP, Jr. Myogenic regulatory factors and the specification of muscle progenitors in vertebrate embryos. Annual review of cell and developmental biology. 2002;18:747-783.
5. Darabi R, Perlingeiro RC. Lineage-specific reprogramming as a strategy for cell therapy. Cell cycle. 2008;7:1732-1737.
6. Bryson-Richardson RJ, Currie PD. The genetics of vertebrate myogenesis. Nature reviews Genetics. 2008;9:632-646.
7. Magli A, Schnettler E, Rinaldi F et al. Functional dissection of Pax3 in paraxial mesoderm development and myogenesis. Stem cells. 2013;31:59-70.
8. Jostes B, Walther C, Gruss P. The murine paired box gene, Pax7, is expressed specifically during the development of the nervous and muscular system. Mechanisms of development. 1990;33:27-37.
9. Kennedy KA, Porter T, Mehta V et al. Retinoic acid enhances skeletal muscle progenitor formation and bypasses inhibition by bone morphogenetic protein 4 but not dominant negative beta-catenin. BMC biology. 2009;7:67.
10. Ryan T, Liu J, Chu A et al. Retinoic acid enhances skeletal myogenesis in human embryonic stem cells by expanding the premyogenic progenitor population. Stem cell reviews. 2012;8:482-493.
11. Darabi R, Gehlbach K, Bachoo RM et al. Functional skeletal muscle regeneration from differentiating embryonic stem cells. Nature medicine. 2008;14:134-143.

12. Iacovino M, Bosnakovski D, Fey H et al. Inducible cassette exchange: a rapid and efficient system enabling conditional gene expression in embryonic stem and primary cells. Stem cells. 2011;29:1580-1588.
13. Shan J, Schwartz RE, Ross NT et al. Identification of small molecules for human hepatocyte expansion and iPS differentiation. Nature chemical biology. 2013;9:514-520.
14. Chambers SM, Fasano CA, Papapetrou EP et al. Highly efficient neural conversion of human ES and iPS cells by dual inhibition of SMAD signaling. Nature biotechnology. 2009;27:275-280.
15. Kattman SJ, Witty AD, Gagliardi M et al. Stage-specific optimization of activin/nodal and BMP signaling promotes cardiac differentiation of mouse and human pluripotent stem cell lines. Cell stem cell. 2011;8:228-240.
16. Subramanian A, Tamayo P, Mootha VK et al. Gene set enrichment analysis: a knowledge-based approach for interpreting genome-wide expression profiles. Proceedings of the National Academy of Sciences of the United States of America. 2005;102:15545-15550.
17. Merico D, Isserlin R, Stueker O et al. Enrichment map: a network-based method for gene-set enrichment visualization and interpretation. PloS one. 2010;5:e13984.
18. Takahashi K, Yamanaka S. Induction of pluripotent stem cells from mouse embryonic and adult fibroblast cultures by defined factors. Cell. 2006;126:663-676.
19. Thomas PD, Campbell MJ, Kejariwal A et al. PANTHER: a library of protein families and subfamilies indexed by function. Genome research. 2003;13:2129-2141.
20. Bessarabova M, Ishkin A, JeBailey L et al. Knowledge-based analysis of proteomics data. BMC bioinformatics. 2012;13 Suppl 16:S13.
21. Aulehla A, Pourquie O. Signaling gradients during paraxial mesoderm development. Cold Spring Harbor perspectives in biology. 2010;2:a000869.
22. Fior R, Maxwell AA, Ma TP et al. The differentiation and movement of presomitic mesoderm progenitor cells are controlled by Mesogenin 1. Development. 2012;139:4656-4665.

23. Chen B, Dodge ME, Tang W et al. Small molecule-mediated disruption of Wnt-dependent signaling in tissue regeneration and cancer. Nature chemical biology. 2009;5:100-107.
24. Willems E, Spiering S, Davidovics H et al. Small-molecule inhibitors of the Wnt pathway potently promote cardiomyocytes from human embryonic stem cell-derived mesoderm. Circulation research. 2011;109:360-364.
25. Liu Z, Scannell DR, Eisen MB et al. Control of embryonic stem cell lineage commitment by core promoter factor, TAF3. Cell. 2011;146:720-731.
26. Ogawa K, Saito A, Matsui H et al. Activin-Nodal signaling is involved in propagation of mouse embryonic stem cells. Journal of cell science. 2007;120:55-65.
27. Lee KL, Lim SK, Orlov YL et al. Graded Nodal/Activin signaling titrates conversion of quantitative phospho-Smad2 levels into qualitative embryonic stem cell fate decisions. PLoS genetics. 2011;7:e1002130.
28. Frank-Kamenetsky M, Zhang XM, Bottega S et al. Small-molecule modulators of Hedgehog signaling: identification and characterization of Smoothened agonists and antagonists. Journal of biology. 2002;1:10.
29. Xu C, Tabebordbar M, Iovino S et al. A zebrafish embryo culture system defines factors that promote vertebrate myogenesis across species. Cell. 2013;155:909-921.
30. Sato N, Meijer L, Skaltsounis L et al. Maintenance of pluripotency in human and mouse embryonic stem cells through activation of Wnt signaling by a pharmacological GSK-3-specific inhibitor. Nature medicine. 2004;10:55-63.
31. Pan S, Wu X, Jiang J et al. Discovery of NVP-LDE225, a Potent and Selective Smoothened Antagonist. ACS medicinal chemistry letters. 2010;1:130-134.
32. Inman GJ, Nicolas FJ, Callahan JF et al. SB-431542 is a potent and specific inhibitor of transforming growth factor-beta superfamily type I activin receptor-like kinase (ALK) receptors ALK4, ALK5, and ALK7. Molecular pharmacology. 2002;62:65-74.
33. Rohwedel J, Maltsev V, Bober E et al. Muscle cell differentiation of embryonic stem cells reflects myogenesis in vivo: developmentally regulated expression of myogenic determination genes and functional expression of ionic currents. Developmental biology. 1994;164:87-101.

34. Bailey P, Holowacz T, Lassar AB. The origin of skeletal muscle stem cells in the embryo and the adult. Current opinion in cell biology. 2001;13:679-689.
35. Borchin B, Chen J, Barberi T. Derivation and FACS-Mediated Purification of PAX3+/PAX7+ Skeletal Muscle Precursors from Human Pluripotent Stem Cells. Stem cell reports. 2013;1:620-631.
36. Feng X, Adiarte EG, Devoto SH. Hedgehog acts directly on the zebrafish dermomyotome to promote myogenic differentiation. Developmental biology. 2006;300:736-746.
37. Borycki AG, Brunk B, Tajbakhsh S et al. Sonic hedgehog controls epaxial muscle determination through Myf5 activation. Development. 1999;126:4053-4063.
38. Gesta S, Tseng YH, Kahn CR. Developmental origin of fat: tracking obesity to its source. Cell. 2007;131:242-256.
39. Wang H, Hao J, Hong CC. Cardiac induction of embryonic stem cells by a small molecule inhibitor of Wnt/beta-catenin signaling. ACS chemical biology. 2011;6:192-197.
40. Hao J, Daleo MA, Murphy CK et al. Dorsomorphin, a selective small molecule inhibitor of BMP signaling, promotes cardiomyogenesis in embryonic stem cells. PloS one. 2008;3:e2904.
41. Darabi R, Arpke RW, Irion S et al. Human ES- and iPS-derived myogenic progenitors restore DYSTROPHIN and improve contractility upon transplantation in dystrophic mice. Cell stem cell. 2012;10:610-619.

MM_Figure 1

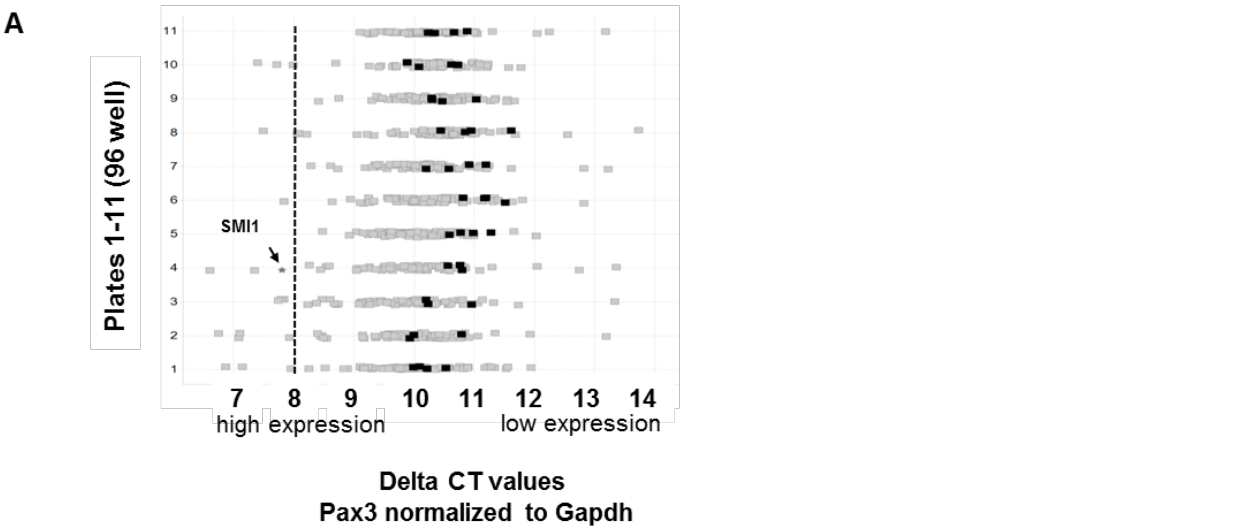
A
Plates 1-11 (96 well)
SMI1
7 8 9 10 11 12 13 14
high expression
low expression
Delta CT values
Pax3 normalized to Gapdh

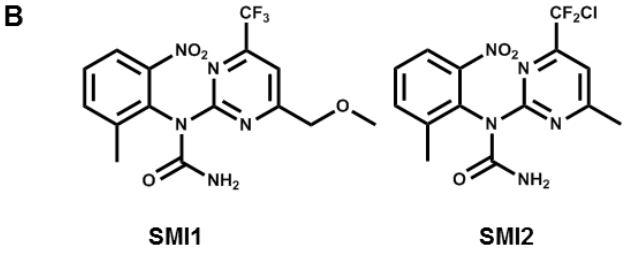
B
SMI1
SMI2

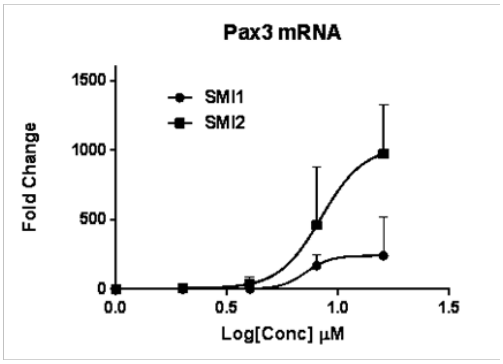
C
Pax3 mRNA
SMI1
SMI2
Fold Change
Log[Conc] µM

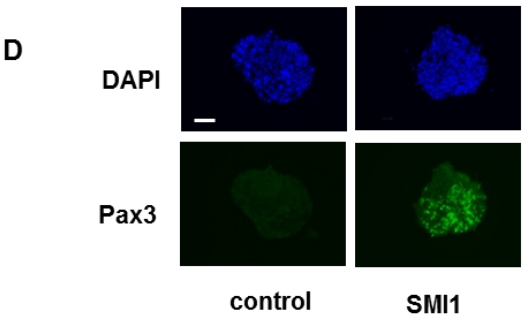
D
DAPI
Pax3
control
SMI1

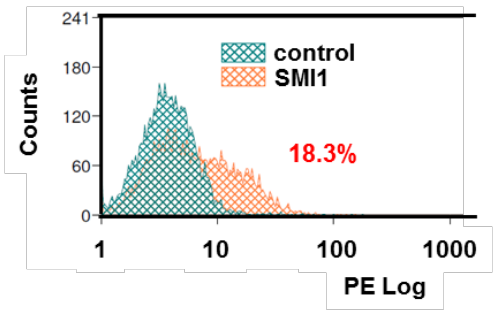
E
Counts
control
SMI1
18.3%
PE Log

MM_Figure 2

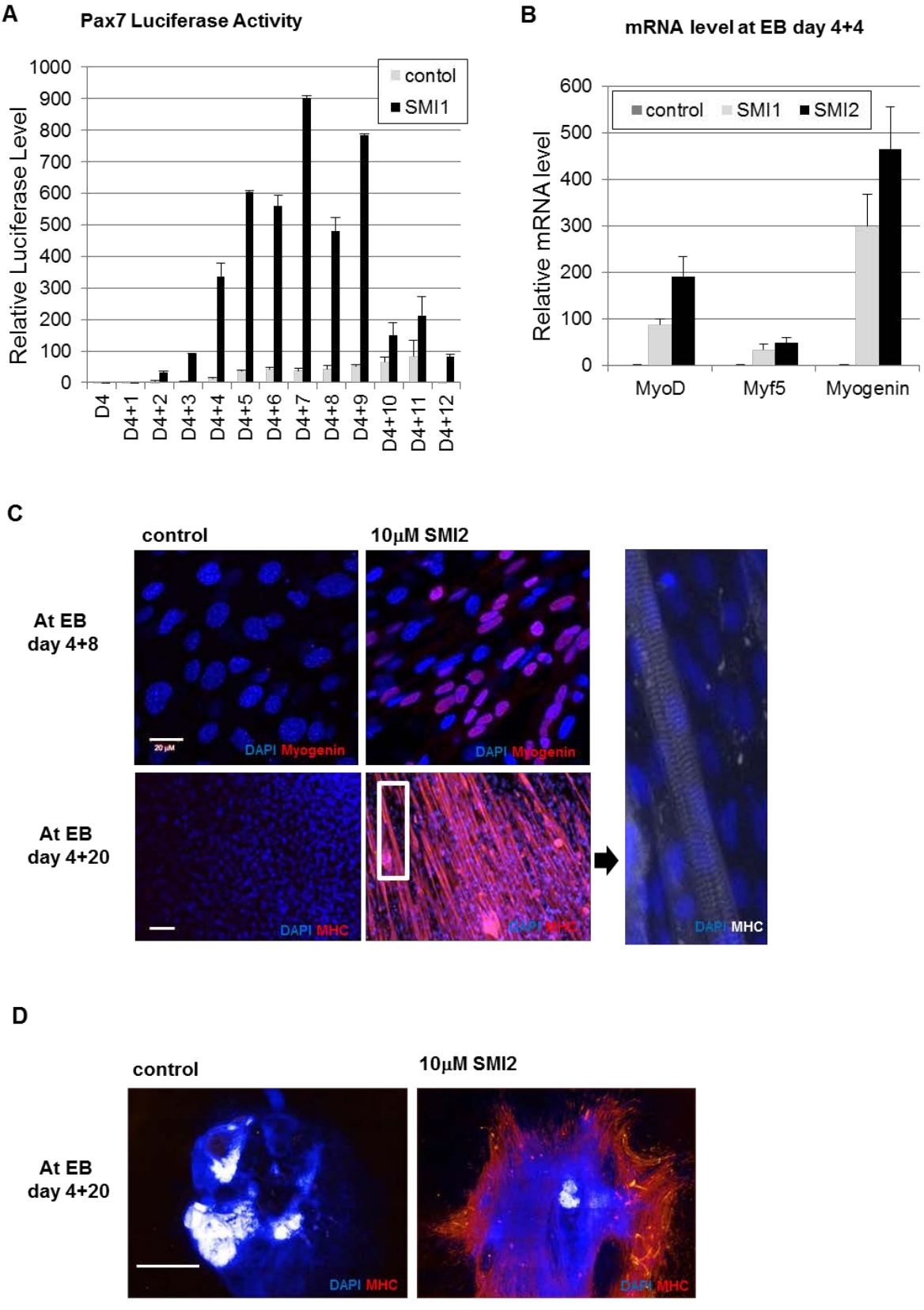
A
Pax7 Luciferase Activity
Relative Luciferase Level
contol
SMI1
D4
D4+1
D4+2
D4+3
D4+4
D4+5
D4+6
D4+7
D4+8
D4+9
D4+10
D4+11
D4+12
B
mRNA level at EB day 4+4
Relative mRNA level
control
SMI1
SMI2
MyoD
Myf5
Myogenin
C
control
10μM SMI2
At EB day 4+8
At EB day 4+20
DAPI Myogenin
DAPI MHC
D
control
10μM SMI2
At EB day 4+20
DAPI MHC

MM_Figure 3

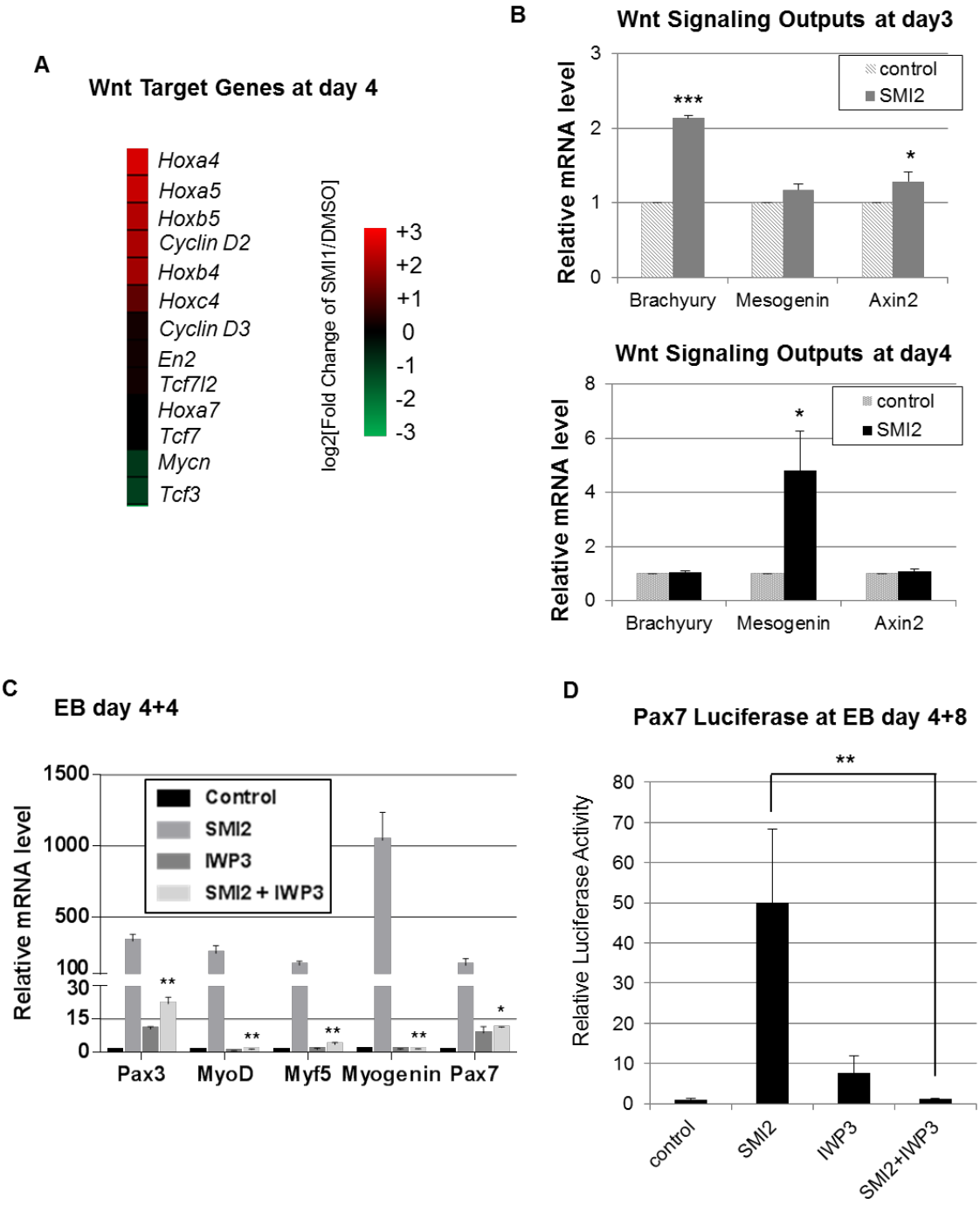
A
Wnt Target Genes at day 4
Hoxa4
Hoxa5
Hoxb5
Cyclin D2
Hoxb4
Hoxc4
Cyclin D3
En2
Tcf7l2
Hoxa7
Tcf7
Mycn
Tcf3
log2[Fold Change of SMI1/DMSO]
+3
+2
+1
0
-1
-2
-3
B
Wnt Signaling Outputs at day3
Relative mRNA level
control
SMI2
***
*
Brachyury
Mesogenin
Axin2
Wnt Signaling Outputs at day4
Relative mRNA level
control
SMI2
*
Brachyury
Mesogenin
Axin2
C
EB day 4+4
Relative mRNA level
Control
SMI2
IWP3
SMI2 + IWP3
Pax3
MyoD
Myf5
Myogenin
Pax7
D
Pax7 Luciferase at EB day 4+8
Relative Luciferase Activity
**
control
SMI2
IWP3
SMI2+IWP3

MM_Figure 4

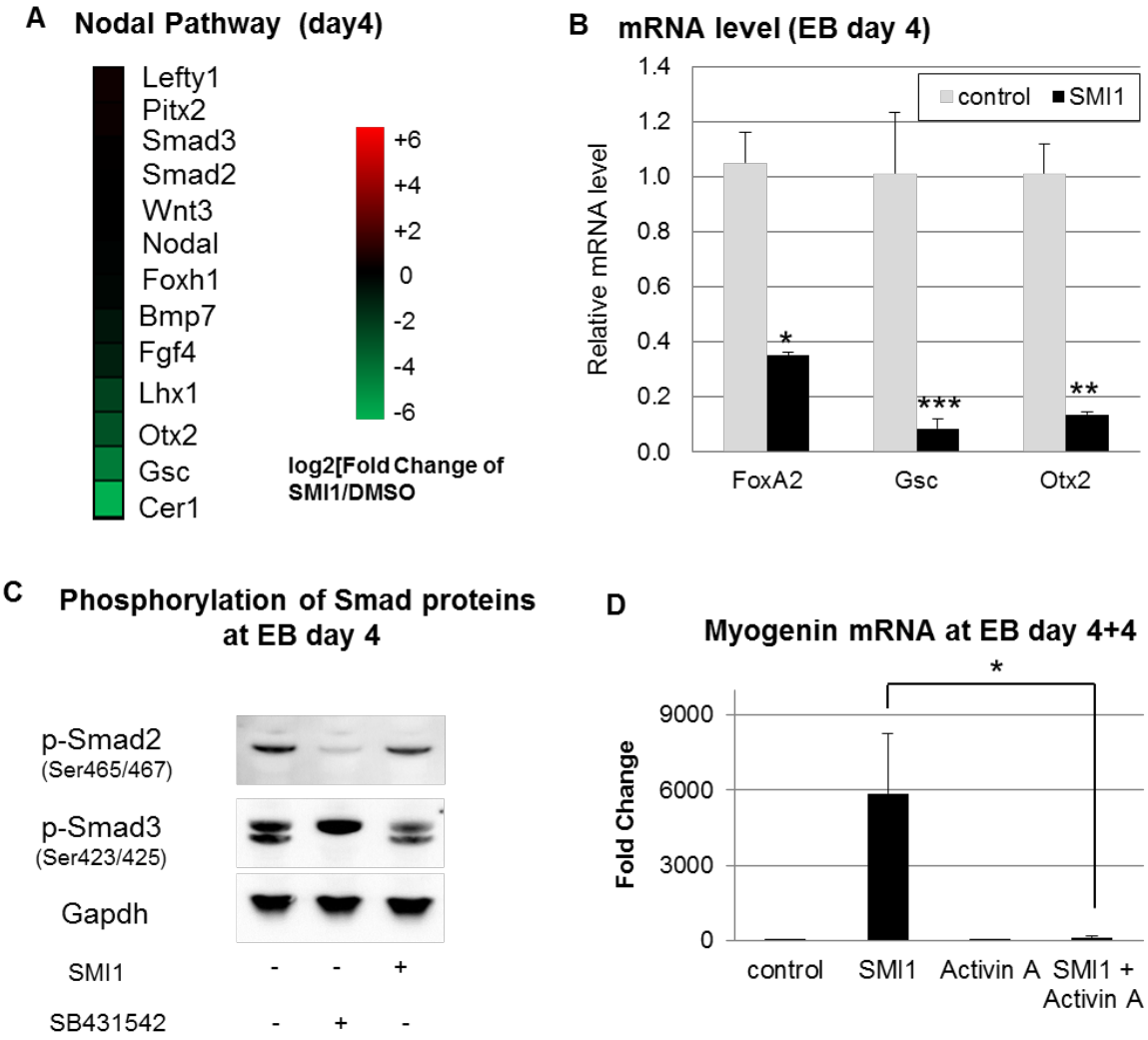
A
Nodal Pathway (day4)
Lefty1
Pitx2
Smad3
Smad2
Wnt3
Nodal
Foxh1
Bmp7
Fgf4
Lhx1
Otx2
Gsc
Cer1
+6
+4
+2
0
-2
-4
-6
log2[Fold Change of SMI1/DMSO
B
mRNA level (EB day 4)
Relative mRNA level
1.4
1.2
1.0
0.8
0.6
0.4
0.2
0.0
control
SMI1
*
***
**
FoxA2
Gsc
Otx2
C
Phosphorylation of Smad proteins at EB day 4
p-Smad2
(Ser465/467)
p-Smad3
(Ser423/425)
Gapdh
SMI1
- - +
SB431542
- + -
D
Myogenin mRNA at EB day 4+4
*
Fold Change
9000
6000
3000
0
control
SMI1
Activin A
SMI1 + Activin A

MM_Figure 5

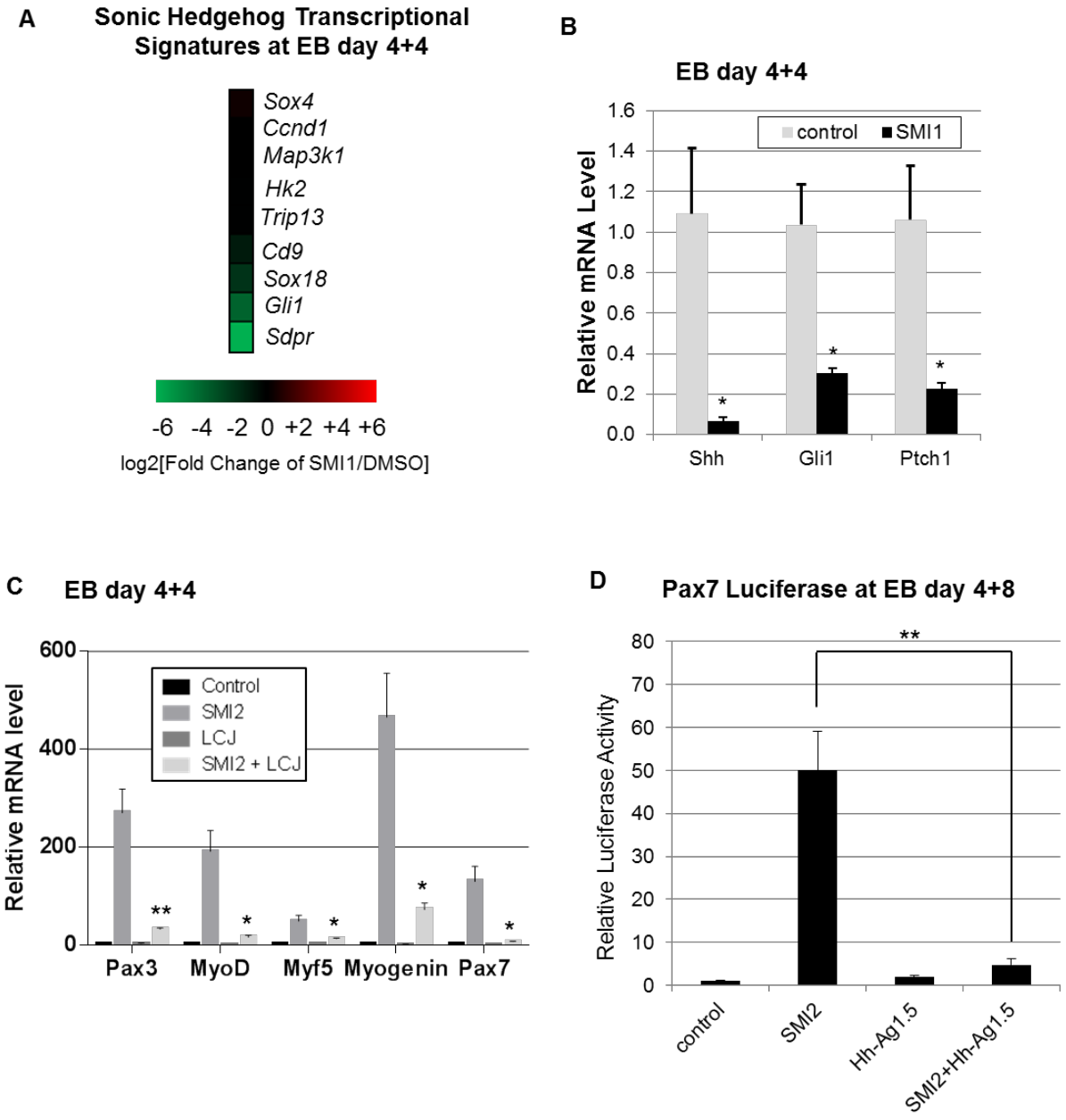
A
Sonic Hedgehog Transcriptional Signatures at EB day 4+4
Sox4
Ccnd1
Map3k1
Hk2
Trip13
Cd9
Sox18
Gli1
Sdpr
-6 -4 -2 0 +2 +4 +6
log2[Fold Change of SMI1/DMSO]
B
EB day 4+4
Relative mRNA Level
control
SMI1
Shh
Gli1
Ptch1
C
EB day 4+4
Relative mRNA level
Control
SMI2
LCJ
SMI2 + LCJ
Pax3
MyoD
Myf5
Myogenin
Pax7
D
Pax7 Luciferase at EB day 4+8
Relative Luciferase Activity
control
SMI2
Hh-Ag1.5
SMI2+Hh-Ag1.5

MM_Figure 6

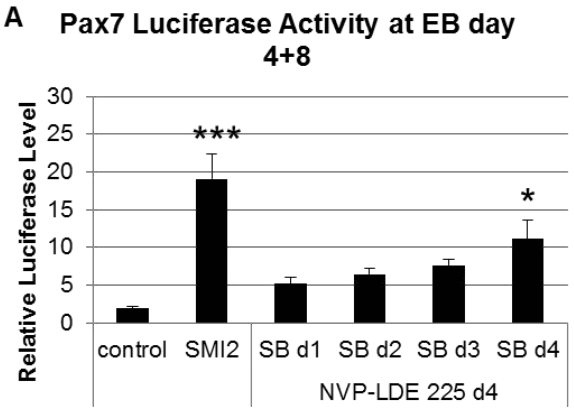
A
Pax7 Luciferase Activity at EB day 4+8
Relative Luciferase Level
30
25
20
15
10
5
0
***
*
control
SMI2
SB d1
SB d2
SB d3
SB d4
NVP-LDE 225 d4

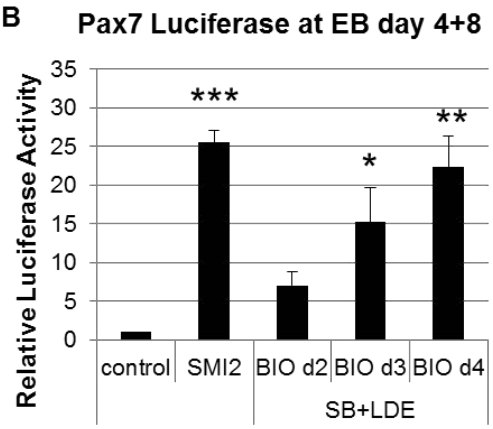
B
Pax7 Luciferase at EB day 4+8
Relative Luciferase Activity
35
30
25
20
15
10
5
0
***
*
**
control
SMI2
BIO d2
BIO d3
BIO d4
SB+LDE

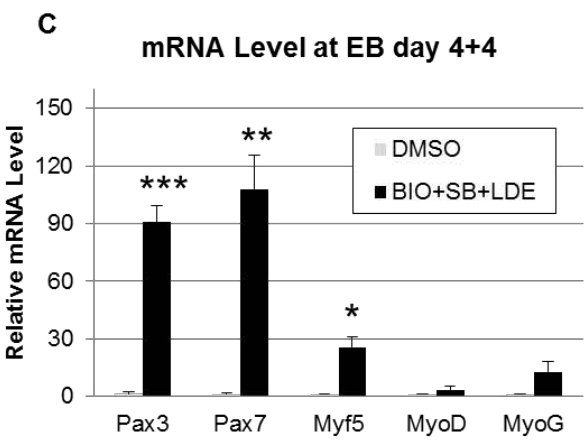
C
mRNA Level at EB day 4+4
Relative mRNA Level
150
120
90
60
30
0
***
**
*
DMSO
BIO+SB+LDE
Pax3
Pax7
Myf5
MyoD
MyoG

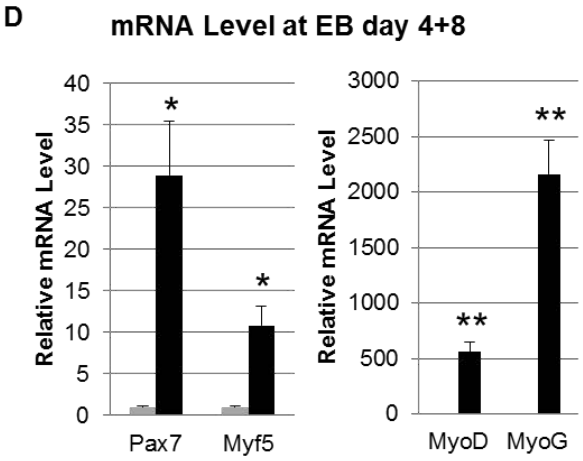
D
mRNA Level at EB day 4+8
Relative mRNA Level
40
35
30
25
20
15
10
5
0
*
*
Pax7
Myf5
Relative mRNA Level
3000
2500
2000
1500
1000
500
0
**
**
MyoD
MyoG

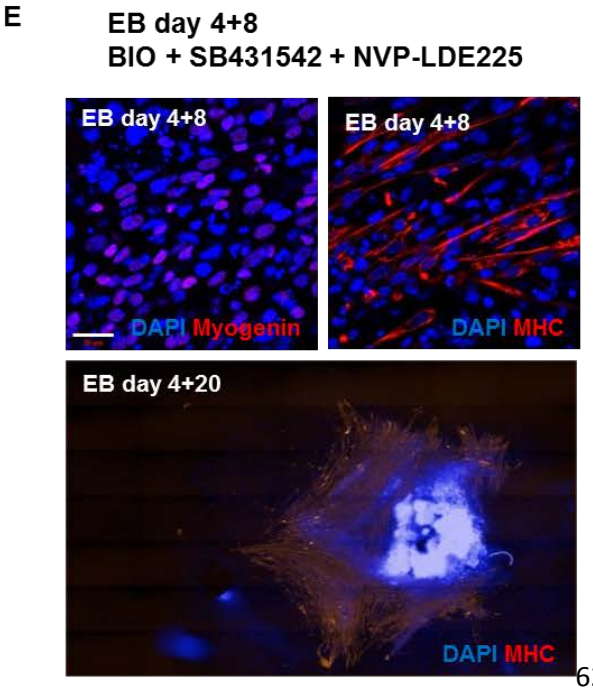
E
EB day 4+8
BIO + SB431542 + NVP-LDE225
EB day 4+8
DAPI Myogenin
EB day 4+8
DAPI MHC
EB day 4+20
DAPI MHC

MM_Figure S1

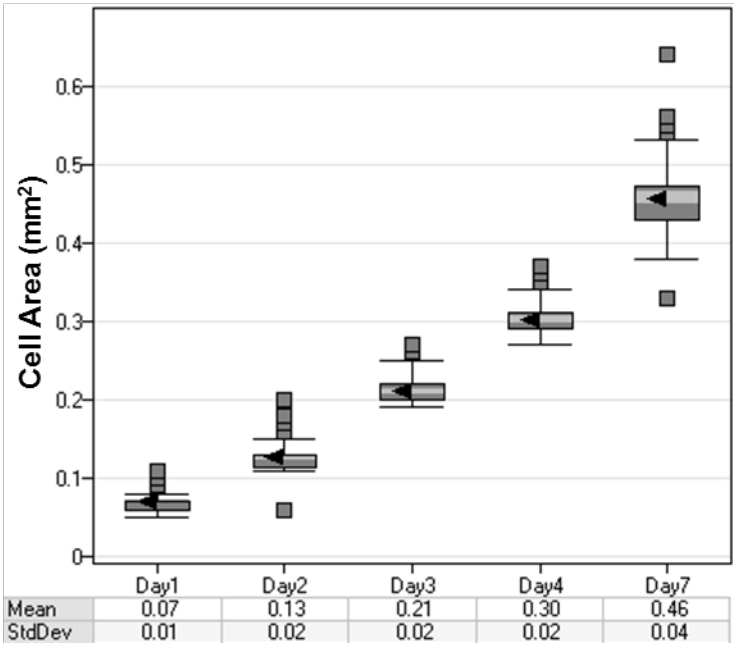

	Day1	Day2	Day3	Day4	Day7
Mean	0.07	0.13	0.21	0.30	0.46
StdDev	0.01	0.02	0.02	0.02	0.04

MM_Figure S2

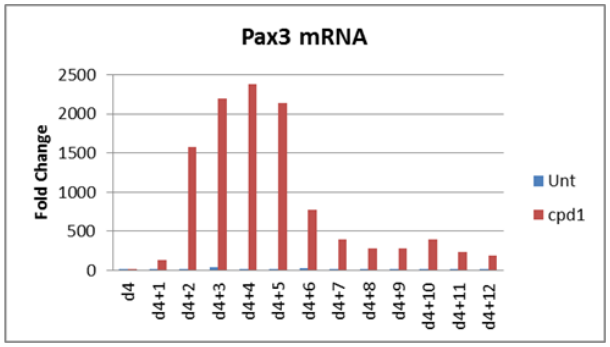
Pax3 mRNA
Fold Change
2500
2000
1500
1000
500
0
d4
d4+1
d4+2
d4+3
d4+4
d4+5
d4+6
d4+7
d4+8
d4+9
d4+10
d4+11
d4+12
Unt
cpd1

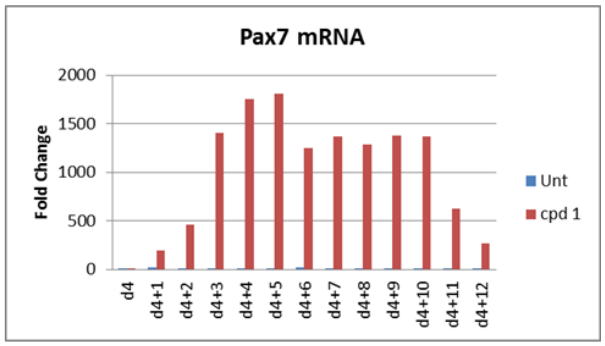
Pax7 mRNA
Fold Change
2000
1500
1000
500
0
d4
d4+1
d4+2
d4+3
d4+4
d4+5
d4+6
d4+7
d4+8
d4+9
d4+10
d4+11
d4+12
Unt
cpd 1

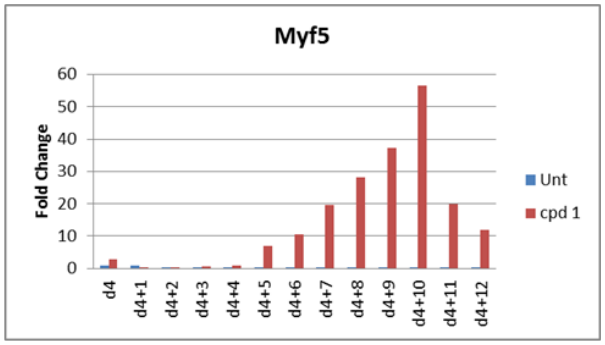
Myf5
Fold Change
60
50
40
30
20
10
0
d4
d4+1
d4+2
d4+3
d4+4
d4+5
d4+6
d4+7
d4+8
d4+9
d4+10
d4+11
d4+12
Unt
cpd 1

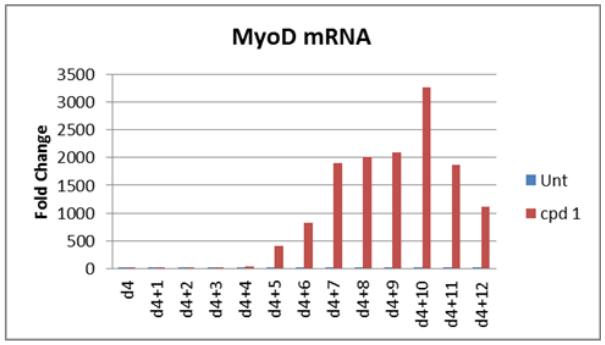
MyoD mRNA
Fold Change
3500
3000
2500
2000
1500
1000
500
0
d4
d4+1
d4+2
d4+3
d4+4
d4+5
d4+6
d4+7
d4+8
d4+9
d4+10
d4+11
d4+12
Unt
cpd 1

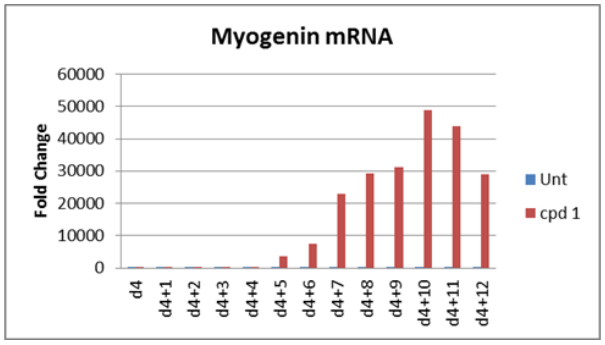
Myogenin mRNA
Fold Change
60000
50000
40000
30000
20000
10000
0
d4
d4+1
d4+2
d4+3
d4+4
d4+5
d4+6
d4+7
d4+8
d4+9
d4+10
d4+11
d4+12
Unt
cpd 1

MM_Figure S3

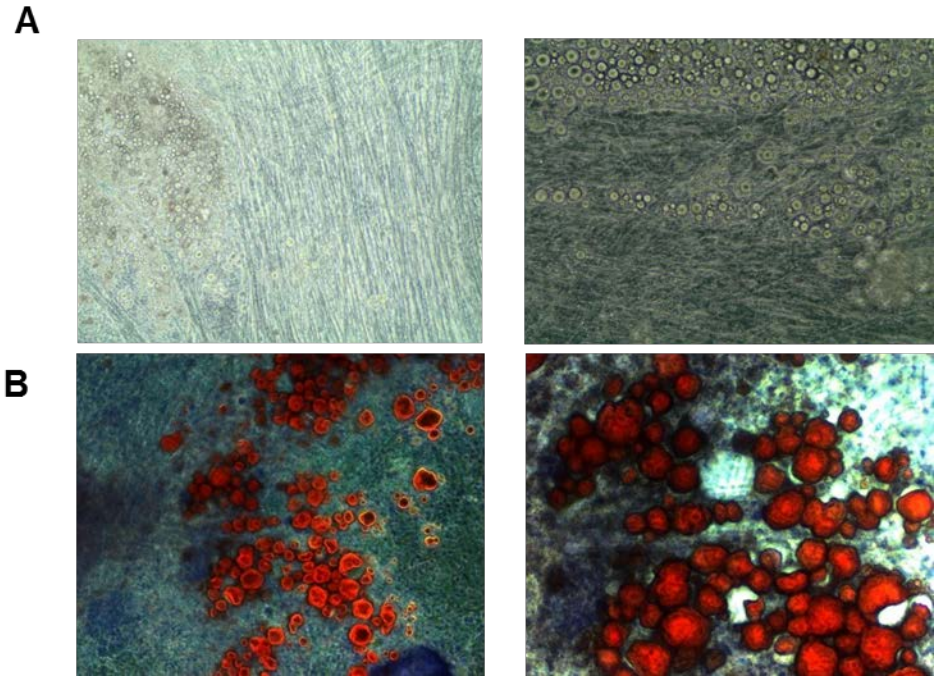

MM_Figure S4

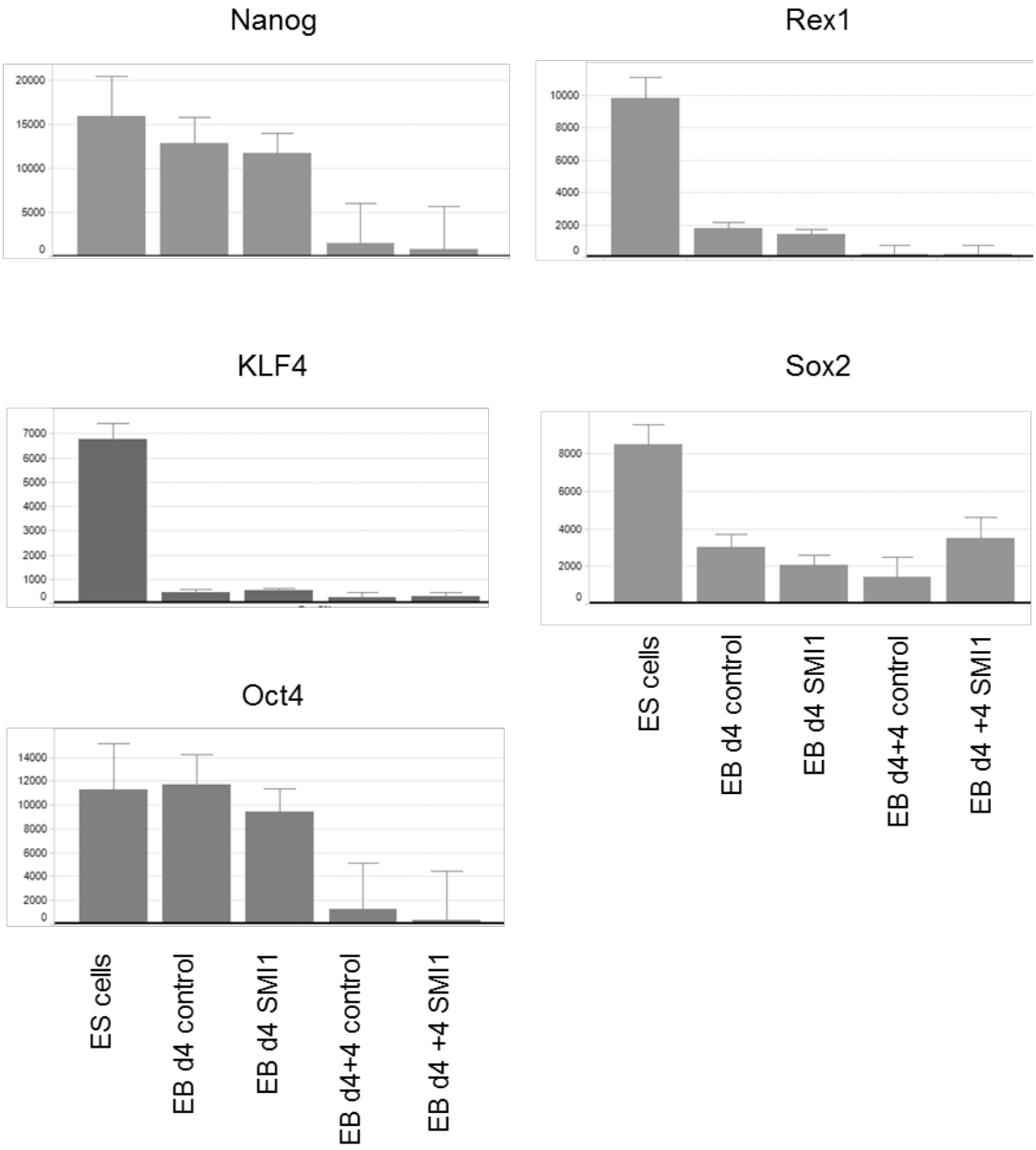
Nanog
20000
15000
10000
5000
0
Rex1
10000
8000
6000
4000
2000
0
KLF4
7000
6000
5000
4000
3000
2000
1000
0
Sox2
8000
6000
4000
2000
0
Oct4
14000
12000
10000
8000
6000
4000
2000
0
ES cells
EB d4 control
EB d4 SMI1
EB d4+4 control
EB d4 +4 SMI1

MM_Figure S5

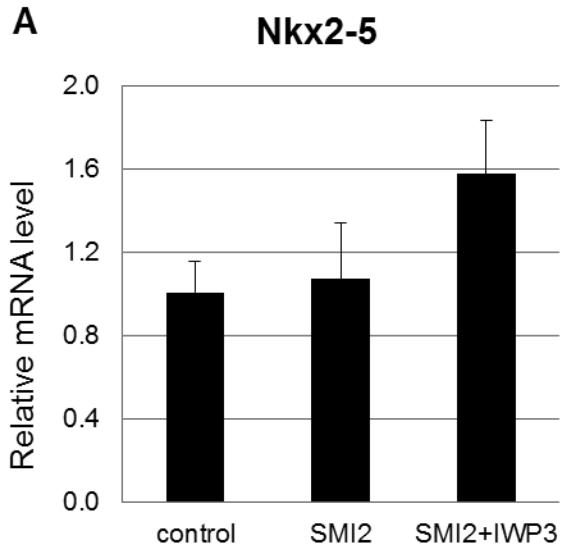
A
Nkx2-5
Relative mRNA level
2.0
1.6
1.2
0.8
0.4
0.0
control
SMI2
SMI2+IWP3

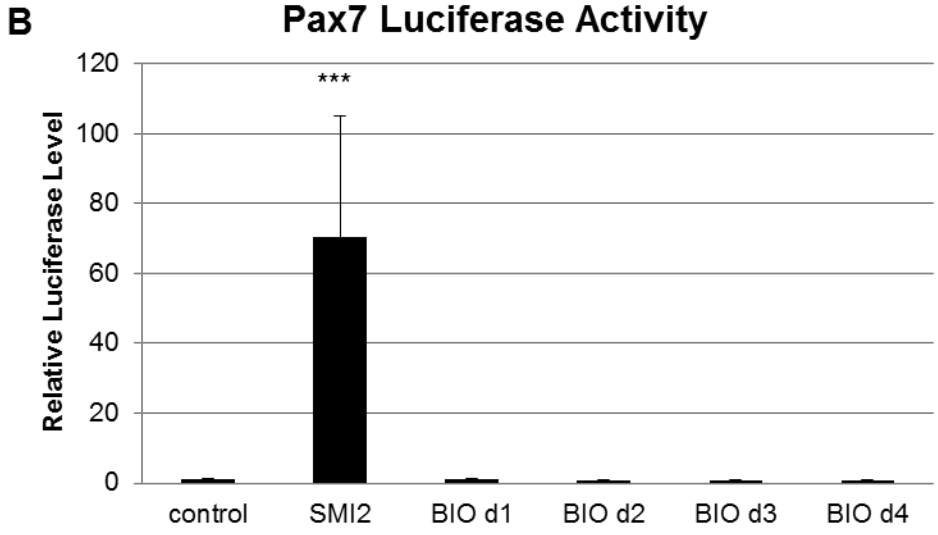
B
Pax7 Luciferase Activity
Relative Luciferase Level
120
100
80
60
40
20
0
***
control
SMI2
BIO d1
BIO d2
BIO d3
BIO d4

MM_Figure S6

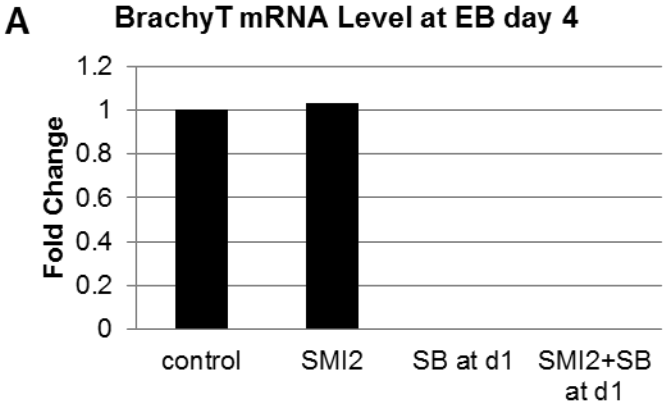
A
BrachyT mRNA Level at EB day 4
Fold Change
1.2
1
0.8
0.6
0.4
0.2
0
control
SMI2
SB at d1
SMI2+SB at d1

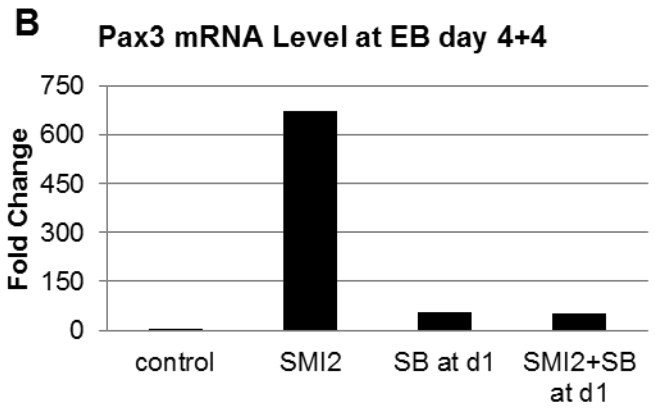
B
Pax3 mRNA Level at EB day 4+4
Fold Change
750
600
450
300
150
0
control
SMI2
SB at d1
SMI2+SB at d1

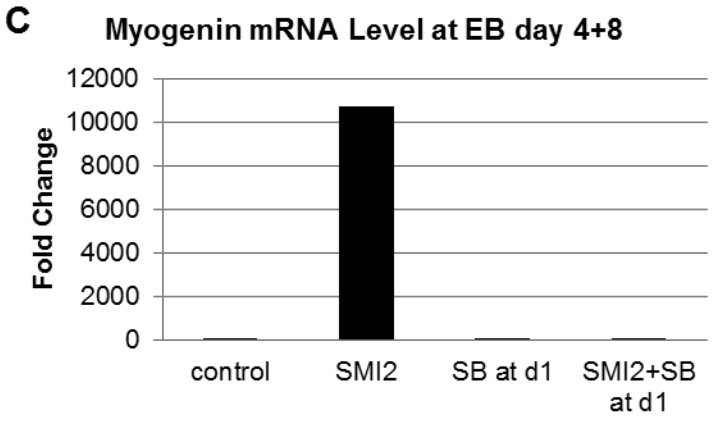
C
Myogenin mRNA Level at EB day 4+8
Fold Change
12000
10000
8000
6000
4000
2000
0
control
SMI2
SB at d1
SMI2+SB at d1

MM_Figure S7

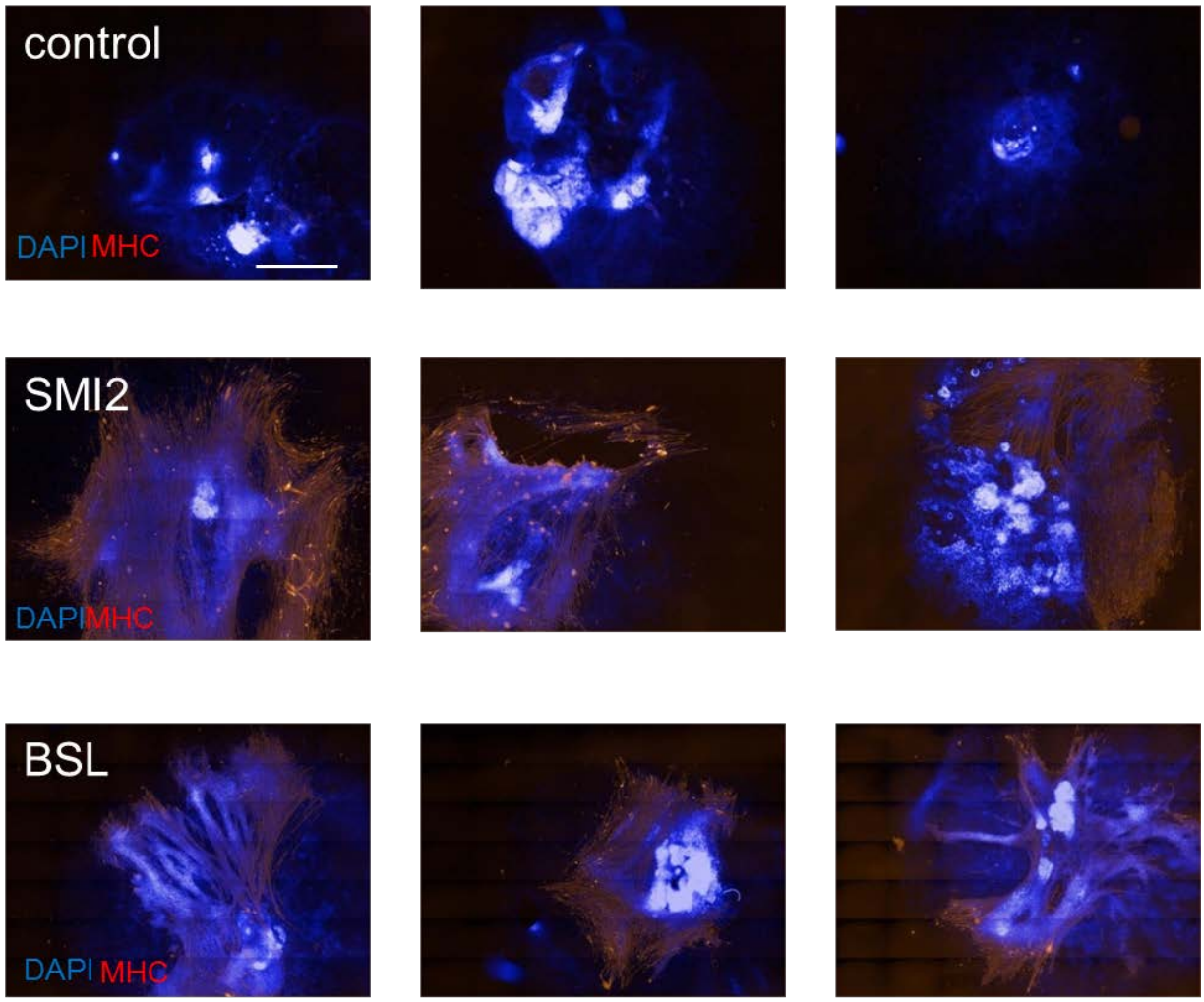

MM_Figure S8

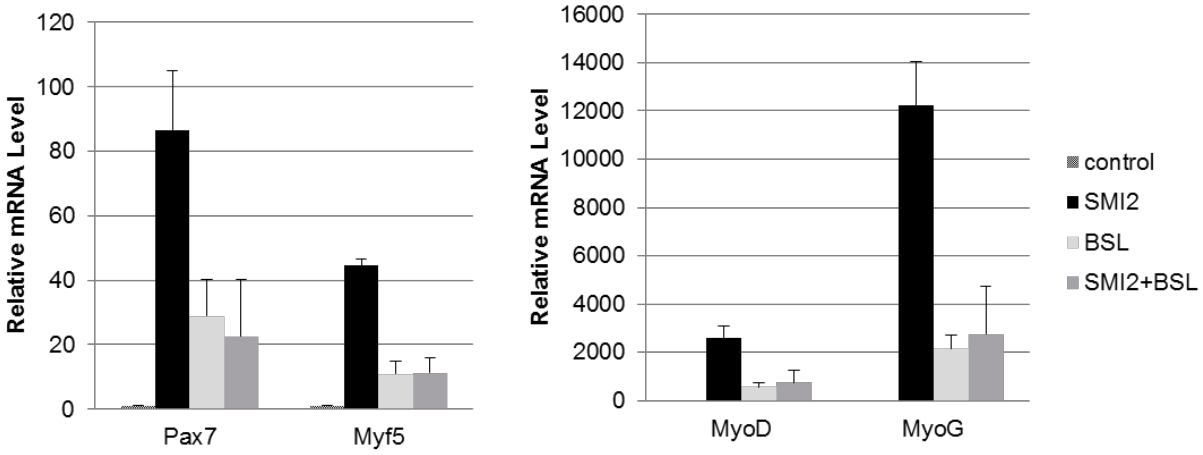

MM_Supplementary Table1. GSEA at EB day4 Applied Biosystems TaqMan Gene Expression Assays used in Real-Time RT-PCR analysis

Applied Biosystems Assay ID	Gene Symbol	Gene Name
4352339E	GAPDH	Glyceraldehyde 3-phosphate dehydrogenase
Mm00435493_m1	Pax3	Paired box gene 3
Mm00834079_m1	Pax7	Paired box gene 7
Mm0440387_m1	MyoD	MyoD1
Mm00435125_m1	Myf5	Myogenic factor 5
Mm00446194_m1	MyoG	Myogenin
Mm01318252_m1	BrachyuryT	BrachyuryT
Mm00490407_s1	Msgn1	Mesogenin1
Mm00443610_m1	Axin2	Axin2
Mm01976556_s1	FoxA2	Forkhead box A2
Mm00650681_g1	Gsc	Goosecoid homeobox
Mm00446859_m1	Otx2	Orthodenticle homolog 2
Mm00436528_m1	Shh	Sonic hedgehog
Mm00494654_m1	Gli1	GLI Family Zinc Finger 1
Mm00436026_m1	Ptch1	Patched 1
Mm00657783_m1	Nkx2-5	NK2 homeobox 5

MM_Supplementary Table2. Differentially expressed genes at day 4 and day4+4

Time point	Entrez Gene	Gene Symbol	Fold Change SMI1 vs control
day 4	101401	Adamts9	-9.26
day 4	**12622**	**Cer1**	**-6.62**
day 4	58208	Bcl11b	-6.50
day 4	66198	Them5	-5.85
day 4	15376	Foxa2	-5.21
day 4	**14836**	**Gsc**	**-4.98**
day 4	237010	Klhl4	-4.91
day 4	**13813**	**Eomes**	**-4.90**
day 4	101401	Adamts9	-4.85
day 4	58208	Bcl11b	-4.57
day 4	13813	Eomes	-4.45
day 4	17863	Myb	-4.41
day 4	101401	Adamts9	-4.30
day 4	17863	Myb	-4.30
day 4	234267	Gpm6a	4.06
day 4	27226	Pla2g7	4.08
day 4	12491	Cd36	4.08
day 4	77569	Limch1	4.09
day 4	12491	Cd36	4.10
day 4	14472	Gbx2	4.11
day 4	14468	Gbp1	4.20
day 4	237979	Sdk2	4.21
day 4	15394	Hoxa1	4.21
day 4	243931	Tshz3	4.21
day 4	23962	Oasl2	4.24
day 4	108797	Mex3b	4.27
day 4	12591	Cdx2	4.31
day 4	19224	Ptgs1	4.36
day 4	353310	Zfp703	4.43
day 4	94222	Olig3	4.44
day 4	14654	Glra1	4.53
day 4	100038882 /// 677168	Gm9706 /// Isg15	4.65
day 4	14469	Gbp2	4.66
day 4	15438	Hoxd9	4.66
day 4	15410	Hoxb3	4.68
day 4	100039796 /// 21822	Tgtp /// Tgtp2	4.71
day 4	20231	Nkx1-2	4.74
day 4	14469	Gbp2	4.76

day 4	15402	Hoxa5	4.77
day 4	13838	Epha4	4.85
day 4	13838	Epha4	5.14
day 4	229900	Gbp6	5.19
day 4	20274	Scn9a	5.24
day 4	55932	Gbp3	5.29
day 4	244867	Arhgap20	5.38
day 4	100038499	Gm10672	5.44
day 4	12903	Crabp1	5.57
day 4	54140	Avpr1a	5.59
day 4	381290	Atp2b4	5.75
day 4	208076	Pknox2	6.04
day 4	20682	Sox9	6.07
day 4	20128	Trim30	6.18
day 4	20274	Scn9a	6.20
day 4	15410	Hoxb3	6.21
day 4	11846	Arg1	6.24
day 4	15407	Hoxb1	6.73
day 4	15400	Hoxa3	6.73
day 4	218820	Zfp503	6.80
day 4	103889	Hoxb2	6.90
day 4	66640	5730446D14Rik	7.07
day 4	12591	Cdx2	7.25
day 4	68169	A930038C07Rik	7.96
day 4	15957	Ifit1	8.06
day 4	67775	Rtp4	9.16
day 4	16392	Isl1	9.19
day 4	15399	Hoxa2	9.63
day 4	100048346 /// 24110	LOC100048346 /// Usp18	9.71
day 4	20755	Sprr2a	10.83
day 4	20755	Sprr2a	11.51
day 4	15400	Hoxa3	12.36
day 4	20664	Sox1	14.18

Time point	Entrez Gene	Gene Symbol	Fold Change SMI1 vs control
day 4+4	17906	Myl2	-25.30
day 4+4	56720	Tdo2	-22.91
day 4+4	17897	Myl3	-19.49
day 4+4	71693	Colec11	-18.67
day 4+4	22139	Ttr	-17.51

day 4+4	22139	Ttr	-13.51
day 4+4	22139	Ttr	-13.50
day 4+4	17897	Myl3	-13.29
day 4+4	15375	Foxa1	-12.72
day 4+4	22044	Trh	-12.55
day 4+4	14765	Gpr50	-12.42
day 4+4	22139	Ttr	-12.04
day 4+4	**20423**	**Shh**	**-11.83**
day 4+4	20997	T	-11.52
day 4+4	17888	Myh6	-11.37
day 4+4	15227	Foxf1a	-11.12
day 4+4	19733	Rgn	-11.07
day 4+4	12404	Cbln1	-10.90
day 4+4	18511	Pax9	-10.58
day 4+4	213435	Mylk3	-10.39
day 4+4	12404	Cbln1	-10.38
day 4+4	23937	Mab21l2	-10.04
day 4+4	207683	Igsf11	-9.73
day 4+4	15110	Hand1	-9.46
day 4+4	22113	Phlda2	-9.24
day 4+4	12627	Cfc1	-9.19
day 4+4	15209	Hesx1	-8.81
day 4+4	12591	Cdx2	-8.69
day 4+4	110257 /// 15122	Hba-a1 /// Hba-a2	-8.46
day 4+4	18424	Otx2	-8.35
day 4+4	16521	Kcnj5	-8.32
day 4+4	20208	Saa1	-8.20
day 4+4	100046336 /// 268729	Gm626 /// LOC100046336	-7.81
day 4+4	15132	Hbb-bh1	-7.81
day 4+4	15132	Hbb-bh1	-7.66
day 4+4	12404	Cbln1	-7.46
day 4+4	21687	Tek	-7.44
day 4+4	68190	5330426P16Rik	-7.25
day 4+4	15110	Hand1	-7.25
day 4+4	17022	Lum	-7.19
day 4+4	17897	Myl3	-7.19
day 4+4	353283	Eras	-7.02
day 4+4	17898	Myl7	-6.94
day 4+4	21387	Tbx4	-6.94
day 4+4	76142	Ppp1r14c	-6.87
day 4+4	19662	Rbp4	-6.77
day 4+4	14261	Fmo1	-6.74

day 4+4	244954	Prss35	-6.68
day 4+4	15132	Hbb-bh1	-6.64
day 4+4	23796	Aplnr	-6.63
day 4+4	13009	Csrp3	-6.62
day 4+4	20730	Spink3	-6.59
day 4+4	57246	Tbx20	-6.54
day 4+4	12622	Cer1	-6.50
day 4+4	225583	A730017C20Rik	6.55
day 4+4	77630	Prdm8	6.55
day 4+4	70911	Phyhipl	6.55
day 4+4	72711	2810037O22Rik	6.57
day 4+4	**17927**	**Myod1**	**6.58**
day 4+4	**18509**	**Pax7**	**6.59**
day 4+4	27386	Npas3	6.70
day 4+4	271305	Phf21b	6.70
day 4+4	100039795	Ildr2	6.73
day 4+4	21826	Thbs2	6.74
day 4+4	77483	C030044C12Rik	6.75
day 4+4	100223	9630041G16Rik	6.76
day 4+4	20614	Snap25	6.84
day 4+4	108030	Lin7a	6.84
day 4+4	21826	Thbs2	6.87
day 4+4	68659	1110032E23Rik	6.89
day 4+4	208936	Adamts18	6.92
day 4+4	18124	Nr4a3	6.93
day 4+4	19283	Ptprz1	7.02
day 4+4	13388	Dll1	7.03
day 4+4	26414	Mapk10	7.09
day 4+4	15402	Hoxa5	7.11
day 4+4	13175	Dclk1	7.12
day 4+4	11468	Actg2	7.12
day 4+4	20269	Scn3a	7.18
day 4+4	20897	Stra6	7.20
day 4+4	269637	Cnpy1	7.25
day 4+4	70580	5730478J17Rik	7.26
day 4+4	12818	Col14a1	7.30
day 4+4	11899	Astn1	7.31
day 4+4	109323	C1qtnf7	7.40
day 4+4	58238	Fam181b	7.41
day 4+4	12393	Runx2	7.44
day 4+4	83671	Sytl2	7.46
day 4+4	107589	Mylk	7.46

day 4+4	16323	Inhba	7.48
day 4+4	16876	Lhx9	7.58
day 4+4	69239	2610034M16Rik	7.60
day 4+4	17313	Mgp	7.60
day 4+4	15423	Hoxc4	7.71
day 4+4	74002	Psd2	7.72
day 4+4	13175	Dclk1	7.73
day 4+4	20665	Sox10	7.79
day 4+4	13175	Dclk1	7.80
day 4+4	67828	Lce1f	7.81
day 4+4	74644	4930426D05Rik	7.83
day 4+4	18212	Ntrk2	7.97
day 4+4	26757	Dpysl4	7.97
day 4+4	101694	AI854517	8.02
day 4+4	17877	Myf5	8.06
day 4+4	21925	Tnnc2	8.06
day 4+4	20262	Stmn3	8.21
day 4+4	15950	Ifi203	8.26
day 4+4	17883	Myh3	8.26
day 4+4	16939	Lor	8.27
day 4+4	13175	Dclk1	8.32
day 4+4	15571	Elavl3	8.35
day 4+4	474332	Dnm3os	8.42
day 4+4	330096	Shisa3	8.43
day 4+4	18039	Nefl	8.46
day 4+4	225631	Onecut2	8.54
day 4+4	54003	Nell2	8.55
day 4+4	246048	Chodl	8.60
day 4+4	21367	Cntn2	8.61
day 4+4	18212	Ntrk2	8.62
day 4+4	18508	Pax6	8.64
day 4+4	18996	Pou4f1	8.74
day 4+4	17901	Myl1	8.75
day 4+4	23876	Fbln5	8.84
day 4+4	67374	Jam2	8.84
day 4+4	17756	Mtap2	8.85
day 4+4	18012	Neurod1	8.91
day 4+4	11609	Agtr2	8.98
day 4+4	15248	Hic1	9.01
day 4+4	16939	Lor	9.10
day 4+4	78286	Nav2	9.16
day 4+4	244867	Arhgap20	9.41

day 4+4	75036	4930488B01Rik	9.42
day 4+4	17907	Mylpf	9.51
day 4+4	56370	Tagln3	9.58
day 4+4	75395	0610040B09Rik	9.59
day 4+4	74694	Tbc1d30	9.63
day 4+4	70008	Ace2	9.69
day 4+4	12307	Calb1	9.82
day 4+4	18992	Pou3f2	9.90
day 4+4	16979	Lrrn1	10.00
day 4+4	67606	Fibin	10.09
day 4+4	58238	Fam181b	10.16
day 4+4	12661	Chl1	10.29
day 4+4	11438	Chrna4	11.02
day 4+4	77994	2810055G20Rik	11.27
day 4+4	15572	Elavl4	11.34
day 4+4	81799	C1qtnf3	11.66
day 4+4	100047943	LOC100047943	11.66
day 4+4	19051	Gsbs	11.80
day 4+4	75426	Igfbpl1	11.89
day 4+4	15379	Onecut1	11.97
day 4+4	110834	Chrna3	11.99
day 4+4	246104	Rhbdl3	12.08
day 4+4	15572	Elavl4	12.12
day 4+4	210293	Dock10	12.20
day 4+4	109272	Mybpc1	12.48
day 4+4	319723	9430053O09Rik	12.53
day 4+4	18197	Nsg2	12.53
day 4+4	14025	Bcl11a	12.58
day 4+4	14654	Glra1	12.71
day 4+4	75770	Brsk2	12.80
day 4+4	100047943 /// 226180	Ina /// LOC100047943	12.86
day 4+4	15424	Hoxc5	12.90
day 4+4	18214	Ddr2	12.92
day 4+4	17200	Mc2r	13.15
day 4+4	14025	Bcl11a	13.15
day 4+4	226049	Dmrt2	13.32
day 4+4	474332	Dnm3os	13.82
day 4+4	75426	Igfbpl1	13.86
day 4+4	**18505**	**Pax3**	**14.00**
day 4+4	15572	Elavl4	14.04
day 4+4	108030	Lin7a	14.06
day 4+4	20604	Sst	14.13

day 4+4	77994	2810055G20Rik	14.20
day 4+4	94090	Trim9	14.22
day 4+4	14025	Bcl11a	14.23
day 4+4	55985	Cxcl13	14.46
day 4+4	235180	Fez1	14.73
day 4+4	14025	Bcl11a	14.86
day 4+4	94090	Trim9	14.94
day 4+4	15424	Hoxc5	14.95
day 4+4	13797	Emx2	14.99
day 4+4	11921	Atoh1	15.03
day 4+4	16814	Lbx1	15.09
day 4+4	67374	Jam2	15.28
day 4+4	545474	Scrt2	15.63
day 4+4	15571	Elavl3	15.66
day 4+4	21367	Cntn2	15.72
day 4+4	268755	A930011O12Rik	15.74
day 4+4	13837	Epha3	15.91
day 4+4	545474	Scrt2	16.37
day 4+4	240690	St18	16.38
day 4+4	224419	ORF63	16.73
day 4+4	20464	Sim1	16.90
day 4+4	22408	Wnt1	17.18
day 4+4	77427	9430092D12Rik	17.24
day 4+4	68955	1500001A10Rik	17.25
day 4+4	320521	6430547I21Rik	18.58
day 4+4	12140	Fabp7	18.59
day 4+4	94090	Trim9	18.83
day 4+4	18040	Nefm	20.71
day 4+4	76161	6330527O06Rik	20.99
day 4+4	71137	Rfx4	21.43
day 4+4	545474	Scrt2	21.99
day 4+4	13176	Dcc	22.15
day 4+4	**18505**	**Pax3**	**22.36**
day 4+4	13837	Epha3	23.00
day 4+4	15208	Hes5	23.36
day 4+4	73100	2900092D14Rik	23.62
day 4+4	53626	Insm1	24.09
day 4+4	434147	D930028M14Rik	26.06
day 4+4	13193	Dcx	26.36
day 4+4	14560	Gdf10	26.42
day 4+4	100041799	Gm3515	26.96
day 4+4	21419	Tcfap2b	27.30

day 4+4	213262	Fstl5	27.41
day 4+4	232714	Mgam	27.53
day 4+4	18993	Pou3f3	27.64
day 4+4	**17928**	**Myog**	**28.92**
day 4+4	381813	Prmt8	30.57
day 4+4	94222	Olig3	31.93
day 4+4	13193	Dcx	34.06
day 4+4	**18509**	**Pax7**	**34.80**
day 4+4	17703	Msx3	36.18
day 4+4	17172	Ascl1	47.44
day 4+4	11924	Neurog2	49.74
day 4+4	18071	Nhlh1	50.45
day 4+4	20715	Serpina3g	51.10
day 4+4	66297	2610017I09Rik	54.66
day 4+4	27220	Cartpt	54.94
day 4+4	18014	Neurog1	56.27
day 4+4	21419	Tcfap2b	61.37
day 4+4	100040120	Gm2612	63.34
day 4+4	320203	C130071C03Rik	84.66
day 4+4	11923	Neurod4	85.41
day 4+4	17932	Myt1	88.40
day 4+4	13176	Dcc	93.72
day 4+4	11923	Neurod4	111.29
day 4+4	14089	Fap	139.20
day 4+4	22771	Zic1	144.00
day 4+4	320203	C130071C03Rik	149.97
day 4+4	22771	Zic1	173.37
day 4+4	18072	Nhlh2	190.03

MM_Supplementary Table3. GSEA at EB day4 and day4+4

Time Point	Pathway Name	Up/Down
day 4	Stem cells_H3K27 demethylases in differentiation of stem cells	Up
day 4	Stem cells_FGF2 signaling during embryonic stem cell differentiation	Up
day 4	Stem cells_Extraembryonic differentiation of embryonic stem cells	Up
day 4	Stem cells_Astrocyte differentiation from adult stem cells	Up
day 4	Stem cells_Scheme: FGF signaling in embryonic stem cell self-renewal and differentiation	Up
day 4	Stem cells_Embryonal epaxial myogenesis	Up
day 4	Stem cells_H3K4 demethylases in stem cell maintenance	Up

day 4	Stem cells_BMP7 in brown adipocyte differentiation	Up
day 4	Stem cells_WNT/Beta-catenin and NOTCH in induction of osteogenesis	Up
day 4	Cytoskeleton remodeling_TGF, WNT and cytoskeletal remodeling	Up
day 4	Stem cells_WNT and Notch signaling in early cardiac myogenesis	Up
day 4	Stem cells_NOTCH in inhibition of WNT/Beta-catenin-induced osteogenesis	Up
day 4	Stem cells_TNF-alpha, IL-1 alpha and WNT5A-dependent regulation of osteogenesis and adipogenesis in mesenchymal stem cells	Up
day 4	Development_WNT signaling pathway. Part 2	Up
day 4	Development_WNT5A signaling	Up
day 4	Stem cells_NODAL signaling in early mesendoderm formation	Down
day 4	Stem cells_FGF and BMP signaling in early embryonic hepatogenesis	Down
day 4	Stem cells_Histone acetylation in embryonic stem cells	Down
day 4	Stem cells_Inhibition of Hedgehog signaling in medulloblastoma stem cells	Down
day 4	Stem cells_Trophectoderm differentiation	Down
day 4	Stem cells_Role of BMP signaling in embryonic stem cell neural differentiation	Down
day 4	Stem cells_Signaling pathways in embryonic hepatocyte maturation	Down
day 4	Stem cells_FGF signaling in pancreatic and hepatic differentiation of embryonic stem cells	Down
day 4	Stem cells_Scheme: FGF signaling in embryonic stem cell self-renewal and differentiation	Down
day 4	Stem cells_TGF-beta family mediated differentiation of embryonic stem cells	Down
day 4+4	Stem cells_FGF2 signaling during embryonic stem cell differentiation	Up
day 4+4	Stem cells_H3K4 demethylases in stem cell maintenance	Up
day 4+4	Stem cells_Early embryonal hypaxial myogenesis	Up
day 4+4	Stem cells_H3K36 demethylation in stem cell maintenance	Up
day 4+4	Stem cells_Astrocyte differentiation from adult stem cells	Up
day 4+4	Stem cells_BMP7 in brown adipocyte differentiation	Up
day 4+4	Development_WNT signaling pathway. Part 1. Degradation of beta-catenin in the absence WNT signaling	Up
day 4+4	Stem cells_Embryonal epaxial myogenesis	Up

day 4+4	Signal transduction_Activin A signaling regulation	Down
day 4+4	Stem cells_NODAL signaling in early mesendoderm formation	Down
day 4+4	Stem cells_Inhibition of Hedgehog signaling in medulloblastoma stem cells	Down
day 4+4	Stem cells_Trophectoderm differentiation	Down
day 4+4	Development_VEGF-family signaling	Down
day 4+4	Development_Hedgehog and PTH signaling pathways in bone and cartilage development	Down
day 4+4	Stem cells_BMP signaling in cardiac myogenesis	Down
day 4+4	Stem cells_Scheme: FGF signaling in embryonic stem cell self-renewal and differentiation	Down
day 4+4	Stem cells_Cooperation between Hedgehog, IGF-2 and HGF signaling pathways in medulloblastoma stem cells	Down

MM_Supplementary Table4. Wnt signaling genes

Entrez Gene	Gene Symbol	Fold Change SMI1 vs control
73173	**Pcdh18**	**3.52**
22418	**Wnt5a**	**3.05**
93897	**Fzd10**	**2.90**
15401	**Hoxa4**	**2.72**
15402	**Hoxa5**	**2.61**
15413	**Hoxb5**	**2.47**
12444	**Ccnd2**	**2.41**
15412	**Hoxb4**	**2.35**
22420	**Wnt6**	**2.03**
170677	**Pcdh21**	**-2.31**
12552	**Cdh11**	**-2.88**

Chapter 3: Additional result

In this chapter I present the data of microRNA and mRNA expression levels from differentiated EBs with and without SMI1 treatment. These data were not included in the submitted manuscript. However, the data set below could give uncovered information about SMI1 and SMI2 which I did not address in the submitted manuscript.

3.1. MicroRNA Microarray during embryonic skeletal muscle differentiation by SMI1

3.1.1. Background

MicroRNAs (miRNAs) are small noncoding RNAs which are 19 to 25 nucleotides in size (Kim, 2005). They are transcribed in the nucleus, processed by the RNases Drocha/DGCR8 and Dicer (Reviewed in He and Hannon, 2004). And they are involved in controlling gene expression at post-transcriptional level by binding to complementary target mRNAs. The interaction between miRNA and mRNA in RNA induced silencing complexes results in mRNA degradation, deadenylation or translational repression at the level of the ribosome (Reviewed in He and Hannon, 2004). miRNAs have appeared as important players in controlling stem cell fate and behavior. Indeed overexpression of muscle specific microRNA, miR-1, in mouse embryonic stem cells could guide the differentiation of cells to mesoderm by suppressing differentiation to endoderm and neuroectoderm lineage (Ivey et al., 2008). Potential target of miR-1 in this system was Dll-1 which was known to promote neural differentiation and inhibit muscle differentiation in ES cells previously (Lowell et al., 2006; Nemir et al., 2006).

There are also embryonic stem cell specific miRNAs which are abundant in ES cells and keep the characteristics of pluripotency and self-renewal (Houbaviy et al., 2003; Melton et al., 2010). Most of them are encoded by the miR-290 cluster. Some of them are sharing the hexamer seed ‘AAGUGC’ including miR-290-3p, miR-291a-3p, miR-291b-3p, miR-292-3p, miR-294, miR-295. The other members of this cluster are miR-290-5p, miR-291a-5p, miR-292-5p, miR-293,

miR-293*, miR-294* and miR-295*. The miR-290 cluster is located on chromosome 7 on a DNA fragment of 2.2kb (Marson et al., 2008). Interestingly ES cells specific miRNAs like miR-291-3p, miR-294 and miR-295, which regulate cell cycle, promoted the process of induced pluripotent stem cell generation when added to the three known reprogramming factors, OSK (Oct4, Sox2 and Klf4) (Judson et al., 2009). MiR-302 family is also expressed in ES cells (Suh et al., 2004). MiR-302b plays a role in maintenance of stemness of human embryonal carcinoma (Lee et al., 2008). Overexpression of miR-302 leads to reprogramming of human hair follicle cells to induced pluripotent stem cells (Lin et al., 2011). The ES cell specific miRNAs control the unique cell cycle program of ES cells characterized by a short G1 phase and a high proportion of cells in S-phase (White and Dalton, 2005). They target the inhibitors of the G1 and S phase transition such as p21 and Rb2 (Subramanyam et al., 2011).

Besides ES cell specific miRNAs, muscle specific miRNAs also have been described. MiR-1, miR-133a and miR-206 are known as muscle specific miRNAs (Kim et al., 2006). Unlike miR-1 and miR-133a that express both in heart and skeletal muscle, miR-206 is expressed only in skeletal muscle. Skeletal muscle specific miR-206 promoted the differentiation in skeletal myoblasts by regulating many genes. For example it is reported that miR-206 targets Pax7 3'-UTR (Chen et al., 2010). By repressing Pax7, miR-206 regulates skeletal muscle satellite cell proliferation and its differentiation to myotubes.

The reports above indicate that miRNA can control the cell fate. Based on the previous findings, I asked if 1) SMI treatment is specifically inducing key miRNAs during differentiation and 2) it is possible to drive the differentiation to skeletal muscle ultimately by modifying the level of miRNAs. With the similar approach to the study of Ivey et al, I wanted to test either ectopic overexpression or inhibition of specific miRNAs during mouse ES cells differentiation.

We performed a TaqMan based miRNA Microarray with the RNA samples from EB differentiated to day 4 and day 4+4 with or without SMI1 compound using the kit named Megaplex Primer Pools and TaqMan MicroRNA from Applied Biosystems. This method was based on TaqMan analysis in the 384-well fluidic card. U6 small RNA was used for normalization of level of each miRNA. The cards were designed to detect for 591 miRNAs in total, including mouse and rat miRNAs.

3.1.2. miRNAs changes at EB day 4

Table 3.1: Differentially regulated miRNAs by SMI1 at EB day 4

microRNA ID -Part Number	Fold Change EBs at d4 Unt VS. SMI1	p-value EBs at d4 Unt VS. SMI1	Reference
mmu-miR-133a -4395357	-8.206	9.67E-03	Specifically expressed in muscles (Yu et al., 2014a)
mmu-miR-193* -4395707	-6.941	7.17E-03	Suppress the metastasis of human lung cancer (Yu et al., 2014b)
mmu-miR-741 -4395587	-3.859	1.78E-02	
mmu-miR-302b* -4381043	-3.823	3.40E-02	Highly expressed in ES cells (Suh et al., 2004)
mmu-miR-302c* -4395687	-2.991	6.28E-03	Highly expressed in ES cells (Suh et al., 2004)
mmu-miR-339-3p -4395663	-2.858	3.36E-02	
mmu-miR-292-5p -4373324	-2.480	4.06E-02	Highly expressed in ES cells (Zheng et al., 2011)
mmu-miR-143 -4395360	21.499	7.61E-06	Control the proliferation of smooth muscle (Cordes et al., 2009)
mmu-miR-491 -4381053	20.661	2.72E-02	Induce apoptosis in colorectal cancer cells (Nakano et al., 2010)
mmu-miR-196b -4395326	13.900	6.50E-03	Regulate translation of mouse insulin2 (Panda et al., 2014)
mmu-miR-377 -4373025	9.791	3.43E-02	Inhibit proliferation of human glioblastoma cells (Zhang et al., 2014)
mmu-miR-154 -4373270	9.769	9.64E-03	Inhibit prostate cancer cell proliferation (Zhu et al., 2014)
mmu-miR-674 -4395193	6.779	5.10E-05	
mmu-miR-375 -4373027	6.494	3.01E-02	Regulate insulin secretion (Poy et al., 2004)
mmu-miR-132 -4373143	5.942	1.46E-06	Suppress migration of lung cancer cells (You et al., 2014)
mmu-miR-467e -4395698	5.347	1.97E-02	

mmu-miR-181c -4373115	2.986	2.39E-02	Regulate myeloid differentiation and acute myeloid leukemia (Su et al., 2014)
mmu-miR-500 -4395736	2.791	6.18E-03	Potential diagnostic marker for hepatocellular carcinoma (Yamamoto et al., 2009)
mmu-miR-590-5p -4395176	2.708	2.70E-02	Inhibition of human cardiosphere-derived stem cells differentiation (Tousi et al., 2014)
mmu-miR-351 -4373345	2.527	3.01E-02	Promote muscle progenitor cell proliferation (Chen et al., 2012)
mmu-miR-135b -4395372	2.405	1.10E-02	Promote cancer progression in colon cancer (Valeri et al., 2014)
mmu-miR-652 -4395463	2.087	1.41E-02	Control heart function and hypertrophy (Bernardo et al., 2014)
rno-miR-351 -4395764	2.012	2.44E-03	Promote muscle progenitor cell proliferation (Chen et al., 2012)

At day 4 of EB formation, 3 days after SMI1 treatment, 7 miRNAs were decreased and 16 miRNAs were increased more than 2 fold with a p-value of 0.05 (Table 3.1). Although there were few miRNAs that were changed, one of the pronounced differences in SMI1 treated EBs compared to negative control group was the ES cell specific expressed miRNAs' level. MiR-302b*, miR-302c* and miR-292-5p were significantly down-regulated by SMI1. The SMI1 treated EBs seemed more differentiated already at day4 compared to the negative control group. Muscle specific miRNA-133a was the most downregulated one by SMI1 incubation. MiR-133a is expressed in both heart and skeletal muscle (Kim et al., 2006). Decreased miR-133a can be because of inhibition of cardiac muscle differentiation by SMI1. In the control group without SMI1 incubation, beating cardiomyocytes appear but not in EB with SMI1. Compared to the control group, reduced differentiation to cardiac muscle lineage could be reflected as decreased level of miR-133a.

MiR-143 has been repeatedly reported to be downregulated in human colorectal adenocarcinoma together with miR-145 (Michael et al., 2003). In other study miR-143 was reported as the most enriched miRNA during differentiation of mouse ES cells into multipotent cardiac progenitors before localized to smooth muscle cells and vascular smooth muscle cells (Ivey et al., 2008). In

our study, the level of miR-143 was also peaked at EB day4 with SMI1 treatment. Continued study of the other group revealed that miR-143 and miR-145 regulates the proliferation of smooth muscle cells *via* modulating the complex of SRF (serum response factor) (Cordes et al., 2009).

MiR-375 was expressed about 6 times more in EB treated by SMI1. Knockdown of miR-375 using morpholino oligonucleotides in zebrafish demonstrated that miR-375 is essential for embryonic development and function of endocrine pancreas (Kloosterman et al., 2007). Inhibition of miR-375 causes defects in the morphology of the pancreatic islet. The known target of miR-375 is myotropin, one of the regulators in insulin secretion (Poy et al., 2004). Interestingly, overexpression of miR-375 in human ES cells showed the pancreatic islet differentiation expressing endodermal and endocrine-specific markers such as HNF4alpha, Pdx1, Pax6 and releasing insulin upon glucose stimulation (Lahmy et al., 2013).

MiR-351 was expressed around 2.5 times more in SMI1 treated EB group. The level of miR-351 was increased transiently in muscle regeneration model by CTX injection. It promotes skeletal muscle progenitor cell proliferation and survival upon differentiation (Chen et al., 2012). Inhibition of miR-351 in muscle progenitor cell differentiation showed more apoptosis. And overexpression of miR-351 did the opposite action suggesting miR-351 inhibits apoptosis. However the effect of miR-351 in EB differentiation was not revealed yet.

3.1.3. Increased miRNAs at EB day 4+4

Table 3.2: Top 20 increased miRNAs by SMI1 at EB day 4+4

microRNA ID -Part Number	Fold Change EBs at d4+4 Unt VS. Cpd1	p-value EBs at d4+4 Unt VS. Cpd1	Reference
rno-miR-219-3p -4395501	688.875	5.64E-16	Tumor suppressor in gastric cancer (Lei et al., 2013)
mmu-miR-219-5p -4373080	372.828	7.39E-06	Regulate neural precursor differentiation (Hudish et al., 2013)
mmu-miR-206 -4373092	306.243	6.79E-07	Specifically expressed in skeletal muscles (McCarthy, 2008)
mmu-miR-615-5p -4395464	283.479	2.20E-07	
mmu-miR-124 -4373295	231.537	7.24E-05	Control neural differentiation (Neo et al., 2014)
mmu-miR-9 -4373285	160.056	3.71E-08	Control neural differentiation (Krichevsky et al., 2006)
mmu-miR-137 -4373301	136.510	1.32E-14	Tumor suppressor in neuroblastoma (Althoff et al., 2013)
mmu-miR-216b -4395437	94.683	9.53E-05	Biomarker for acute pancreatic injury (Endo et al., 2013)
mmu-let-7b -4373168	93.918	1.20E-04	
mmu-miR-125b* -4395638	80.061	7.67E-08	
mmu-miR-217 -4395686	80.035	3.14E-10	
mmu-miR-9* -4395342	75.807	6.28E-08	
mmu-miR-486 -4378096	32.938	3.08E-04	Skeletal muscle enriched microRNA (Small et al., 2010)
mmu-let-7c -4373167	31.459	3.97E-07	
rno-miR-99a* -4395774	30.510	2.06E-04	
mmu-miR-383 -4381093	26.981	5.52E-04	Regulate testicular embryonal carcinoma cell proliferation (Lian et al., 2010)
mmu-miR-214 -4395417	24.279	1.94E-04	Regulate skeletal myoblast differentiation

			(Juan et al., 2009)
mmu-miR-99a -4373008	23.563	2.12E-03	
mmu-let-7f -4373164	23.287	2.37E-04	
mmu-miR-199a-5p -4373272	23.062	2.13E-02	Affect Wnt signaling and myogenic differentiation in dystrophic muscle (Alexander et al., 2013)

In comparison with the time point at day 4, more miRNAs were differentially expressed at EB day 4+4. 50 miRNAs in total were increased by SMI1 at day 4+4. As expected, the skeletal muscle specific miRNA miR-206, was upregulated in SMI1 treated EB. Interestingly expression pattern of miRNAs suggests that SMI1 drives EBs into not only skeletal muscle but also the neuronal lineages. Some neuron specific miRNAs were also highly induced by SMI.

MiR-124a and miR-9 which are annotated as brain specific microRNAs were dramatically up-regulated by SMI1. This upregulation was also found in ES cell derived neurogenesis *in vitro* (Krichevsky et al., 2006). The function of miR-124a and miR-9 was tested during neuron differentiation by overexpression. They carried out a quantitative analysis to determine the proportion of neuronal and astroglial-like cell populations. Transient overexpression of miR-124a and miR-9 in neural precursors resulted in reduction of GFAP positive cells (astrocytes) and slight increase on the number of Tuj1 positive cells (neurons). As a result the ratio between GFAP positive cells and Tuj1 positive cells was shifted in more Tuj1 positive cells. It shows that these miRNAs play a functional role in the determination of neural fates during ES cell differentiation.

MiR-214 was also significantly upregulated by SMI1 treatment. Previously it was reported that miR-214 targets the polycomb protein Ezh2 by binding to 3'-UTR of Ezh2 (Juan et al., 2009). In the study, miR-214 transduction in myoblasts reduced the level of Ezh2 and initiated premature expressions of myogenin and myosin heavy chain. It resulted in higher percentage of MHC positive cells. In ES cells overexpression of miR-214 did repress the pluripotent marker Oct4 and influence many developmental regulators for example increased Nestin, Dkk1, Sox17 and Pax7.

But it did not activate the transcription of MyoD. It suggests that miR-214 controls the differentiation at distinct developmental steps by regulating Ezh2 protein levels.

Based on the observation that skeletal muscle specific miR-206 was upregulated by SMI1, I tested overexpression of miR-206 during EB differentiation. The pre-miR-206 was amplified from genomic DNA. The level of miR-206 was induced over 120 times in comparison with control group. However, there was no dramatic increase on Myogenin which is a marker for skeletal muscle. At EB day4+8, there was a tendency of increased Myogenin and decreased Pax6 and Myh6, marker for neuronal and cardiomyocyte lineage, respectively. Overexpression of miR-206 was not sufficient to push drive EB differentiation to skeletal muscle.

For further study, modification of multiple miRNAs, for example decreased embryonic stem cell specific miRNAs and increased skeletal muscle specific miRNA at the same time could improve the direct differentiation process to skeletal muscle from ES cells.

(A) miR-206 level in EB at day 4+8

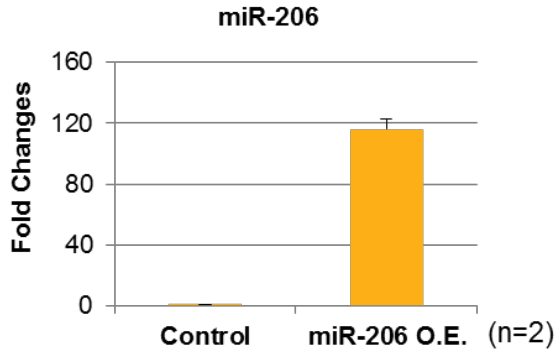

(B) Level of lineage markers in EB at day 4+8

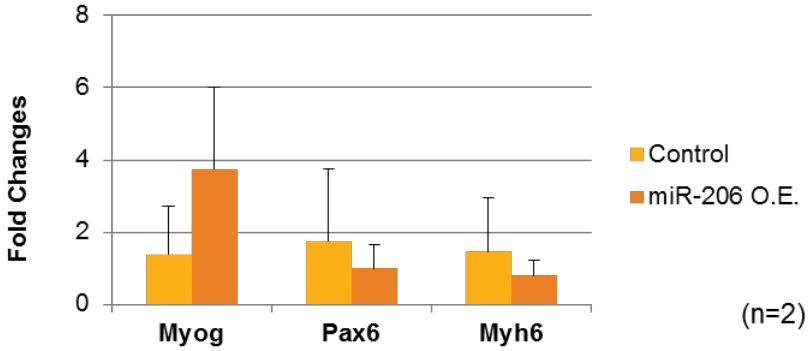

Figure 3.1: RNA levels in EB (A) Level of miR-206 measured by real-time RT-qPCR. (B) mRNA levels measured by real-time RT-PCR. Bars indicate the standard deviation in 2 samples from 10 EBs.

3.1.4. Decreased miRNAs at EB day 4+4

38 miRNAs were downregulated significantly at EB day 4+4 in total. ES cell specific miRNAs were still downregulated at day 4+4. Compared to day 4, more ES cell specific miRNAs' were reduced, including miR-290-3p, -5p, miR-291a-3p, 291b-5p and miR-302 family. Interestingly, expression of miR-1, one of the muscle specific miRNAs, was reduced in SMI1 treated group. MiR-1 expression was found in both cardiac and skeletal muscle. It is probable that decreased cardiac muscle differentiation in SMI1 treated group could be reflected to the decreased level of miR-1.

MiR-483*, known as miR-483-3p, was significantly down-regulated. In adipocyte differentiation system, knocking down of this miRNA leads to more differentiation of adipose tissues (Ferland-McCollough et al., 2012). Indeed SMI treatment not only results in skeletal muscle but also in adipocyte formation. The decrease of miR-483-3p might support this observation.

By taking advantage of bioinformatics tools, further analysis can give potential key microRNAs which can program the differentiation of EBs to skeletal muscle. For example, target prediction algorithm expected that six miRNAs, miR-182, miR-186, miR-135, miR-491, miR-329 and miR-96 had the seed sequence to bind the myogenin 3'-UTR (Antoniou et al., 2014). The potential miRNAs which target myogenic regulatory factors should be decreased. At the same time, miRNAs which target proteins enhancing differentiation of other cell lineages should be upregulated.

Table 3.3: Top 20 decreased miRNAs by SMI1 at EB day 4+4

microRNA ID -Part Number	Fold Change EBs at d4+4 Unt VS. Cpd1	p-value EBs at d4+4 Unt VS. Cpd1	Reference
mmu-miR-291b-5p -4395667	-81.119	4.36E-06	Highly expressed in ES cells (Zheng et al., 2011)
mmu-miR-302c* -4395687	-48.969	6.17E-08	Highly expressed in ES cells (Suh et al., 2004)
mmu-miR-294* -4395725	-44.742	2.86E-04	Highly expressed in ES cells (Zheng et al., 2011)
mmu-miR-302c -4395688	-41.016	2.87E-07	Highly expressed in ES cells (Suh et al., 2004)
mmu-miR-297c -4395610	-35.533	1.69E-06	Modulate multidrug resistance in human colorectal carcinoma (Xu et al., 2012)
mmu-miR-302a* -4395745	-27.018	1.38E-04	Highly expressed in ES cells (Suh et al., 2004)
mmu-miR-367 -4373034	-26.751	3.50E-08	Highly expressed in ES cells (Suh et al., 2004)
mmu-miR-96 -4373372	-23.760	8.49E-03	Repress neural induction in human ES cells (Du et al., 2013)
mmu-miR-302b -4378071	-20.249	1.13E-07	Highly expressed in ES cells (Suh et al., 2004)
mmu-miR-302a -4378070	-18.547	7.13E-04	Highly expressed in ES cells (Suh et al., 2004)
mmu-miR-292-5p -4373324	-13.865	2.39E-05	Highly expressed in ES cells (Zheng et al., 2011)
mmu-miR-302d -4373063	-12.609	1.30E-08	Highly expressed in ES cells (Suh et al., 2004)
mmu-miR-200a* -4373273	-12.465	1.42E-02	Repress neural induction in human ES cells (Du et al., 2013)
mmu-miR-721 -4381073	-9.216	7.44E-04	
mmu-miR-200b* -4395385	-8.978	3.77E-03	Repress neural induction in human ES cells (Du et al., 2013)
mmu-miR-375 -4373027	-8.810	1.44E-02	Promote beta pancreatic differentiation in human iPS cells (Lahmy et al., 2014)
mmu-miR-200a -4378069	-8.304	3.01E-05	Repress neural induction in human ES cells (Du et al., 2013)

mmu-miR-326 -4373335	-7.233	7.30E-03	Regulate human dopamine D2 receptor expression (Shi et al., 2014)
mmu-miR-293 -4386754	-6.613	2.35E-07	Highly expressed in ES cells (Zheng et al., 2011)
mmu-miR-290-3p -4395721	-5.923	5.78E-07	Highly expressed in ES cells (Zheng et al., 2011)

Follow-up study with ES cells which express a combination of miRNAs upregulated by SMI1 can be applied in order to see the functional impacts of miRNAs in the directed differentiation to skeletal muscle. Cross analysis between decreased mRNA and increased miRNA level or increased mRNA and decreased miRNA will be useful to identify networks which are involved in the mechanism of SMI1. Further, analyzing the common seed sequences and targets of miRNAs affected by SMI can give ideas for further mechanism identification studies of SMI1.

3.2 mRNA Microarray during early embryonic skeletal muscle differentiation by SMI1

To identify the direct events of SMI, comprehensive mRNA level analysis was carried out with RNAs which were prepared from untreated EBs and EBs incubated with SMI1 and its higher efficient analogue SMI2 for 2, 6 and 24 hours. Microarray analysis was carried out with Affymetrix Mouse430 2.0 GeneChip.

3.2.1 mRNA levels at 2 hours incubation

After 2 hours of incubation, there is no change by SMIs (Fig. 3.1A and B) (Criteria to screen the probes were fold changes more than 2 and relative expression level more than 50).

3.2.2 mRNA levels at 6 hours incubation

Furthermore, 6 hours incubation did not give dramatic changes in terms of gene expression level. Only a few genes were significantly changed with more than 2 fold changes. By SMI1, Bhlha15 (also known as Mist1) and Krtdap were decreased (Fig. 3.2A). Interestingly alsoBhlha15 and a not annotated cDNA were downregulated by SMI2 (Fig. 3.2B). Not any single gene was upregulated by each compound by 6 hours incubation with more than 2 fold change. However, expression levels of the 3 genes which were downregulated were very low over all the time points. Nevertheless it is interesting that two independent compounds showed one identical gene expression change, Mist1. Mist1 was reported as a transcriptional repressor of MyoD in myoblasts differentiation (Lemercier et al., 1998). Mist1 is also a basic helix-loop-helix protein (bHLH) and its expression pattern is overlapped partially with the MyoD protein family in proliferating myoblasts. Mist1 forms homodimers and heterodimers with MyoD and E-proteins in order to inhibit MyoD activity. Although there is a time gap between embryonic skeletal muscle differentiation and myoblasts differentiation, studying the role of Mist1 during embryonic skeletal muscle differentiation will be worth. Mist1 appears in skeletal muscle-forming regions during embryonic days E12.5 and E16.5.

(A)

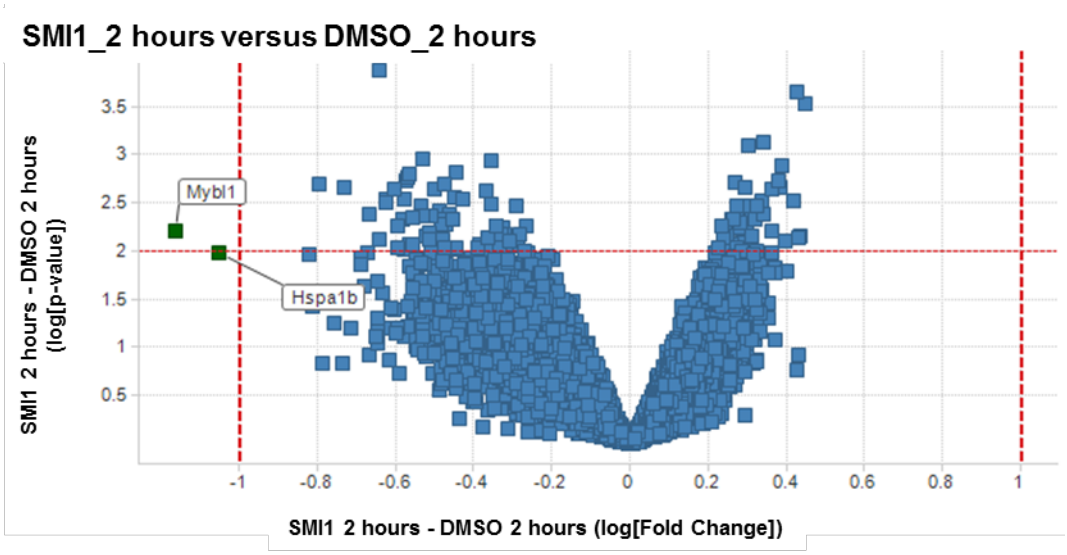

(B)

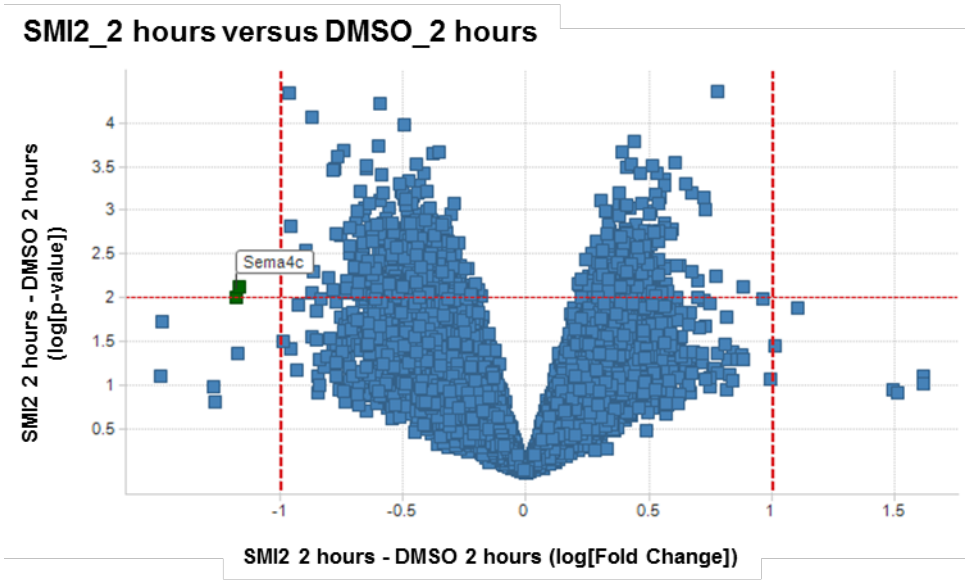

Figure 3.2: mRNA levels from EBs incubated with SMIs for 2 hours

(A)

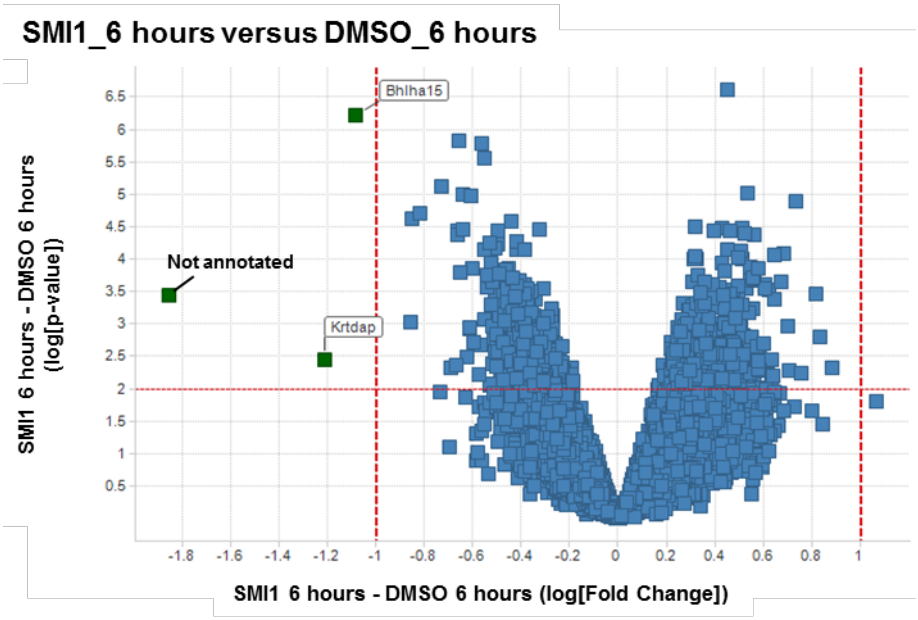

(B)

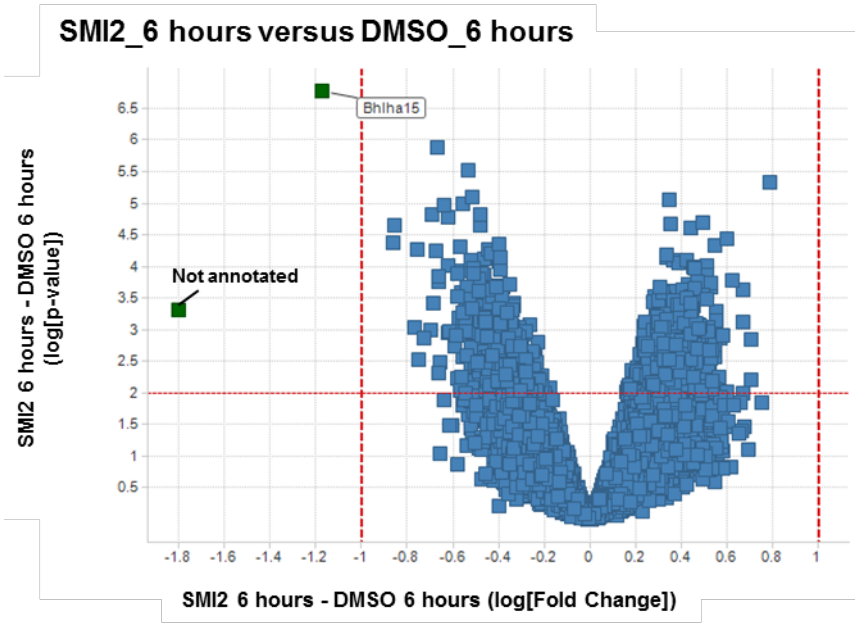

Figure 3.3: mRNA levels from EBs incubated with SMIs for 6 hours

3.2.3 mRNA levels at 24 hours incubation

After 24 hours incubation, more changes of gene expression were observed compared to 2 and 6 hours incubation. SMI1 induced more gene expression changes than SMI2.

From downregulated genes by SMI1 after filtering genes whose expressions are low (intensity less than 50), 5 genes were identified, which are Lifr, Lrrc2, Mreg, Mtap7 and TET2 (Fig. 3.3A). LIF (Leukemia Inhibitory Factor) is a member of the interleukin-6 family of cytokines. It binds to a receptor complex consisting of a LIF specific receptor (LIFR) and the signal transducer gp130 (Gearing et al., 1992). In mouse ES cells and adipocytes culture, LIF also acts as an inhibitor of differentiation. In embryoid bodies differentiation, LIF modulates cardiogenesis in two different ways depending on the stage of differentiation (Bader et al., 2000). At the period when mesodermal precursors of cardiomyocyte form in EBs, presence of LIF delayed the commitment to cardiomyocyte significantly.

Furthermore, Eif4g3, Gpb1, Gbp2, Gpm6a, Id2, Psmb8, Sox1, Tspan6 and Zbp1 are the set of genes which were upregulated by 24 hours incubation with SMI1. By SMI2, Bcl11a, Bcll11b, Dusp9, Enpp2, Etv4, Lrrc2, Mtap7, Tnnt1 and Zfp827 were identified as downregulated genes after 24 hours incubation. Only Hoxa3 was upregulated significantly by SMI2 at that time point.

The signature in common from the two compounds was the downregulation of Lrrc2 and Mtap7.

(A)

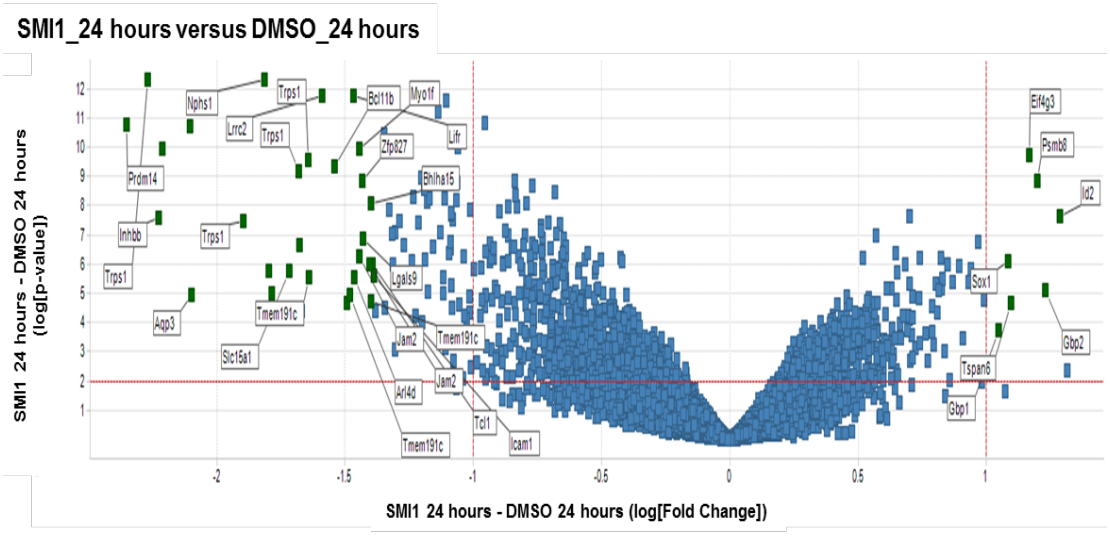

(B)

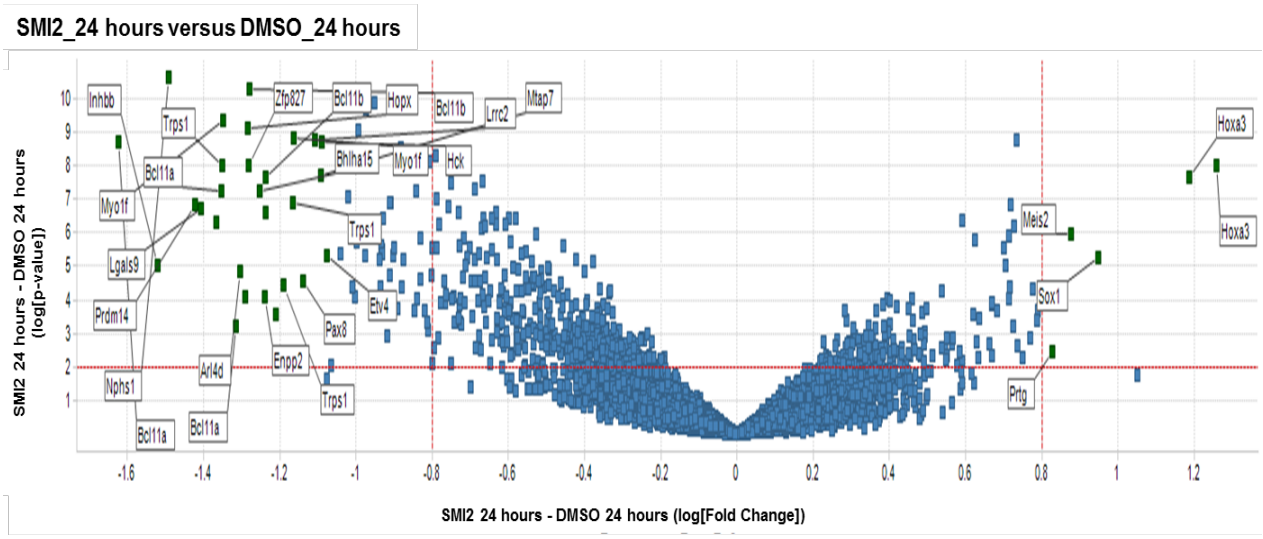

Figure 3.4: mRNA levels from EBs incubated with SMIs for 24 hours

Lrrc2 and Mtap7 are in the list of genes which are downregulated by both SMI1 and SMI2 with 24 hours incubation. Lrrc2 is Leucine Rich Repeat Containing Protein 2. In human LRRC2 transcript was detected only in heart, skeletal muscle and kidney (Kiss et al., 2002). Its exact function is not elucidated yet. Lrrc2 may be related to tumorigenesis because RSP-1 (Ras Suppressor Protein 1), the closest relative of Lrrc2 with seven leucine-rich repeats, is capable of suppressing v-ras transformation *in vitro* (Cutler et al., 1992). Mtap7 is a microtubule-associated protein and is involved in microtubule dynamics. One identified function of Mtap7 in mouse is an essential role in microtubule function for spermatogenesis (Magnan et al., 2009).

To find out the significance of these two downregulated genes in regard of skeletal muscle differentiation, I have applied siRNA (small interfering RNA) approach to modify the level of Lrrc2 and Mtap7 during ES cell differentiation. Reverse transfection of siRNAs was carried out upon ES cell culture. EBs were made after 48 hours from transfection. It showed reduced Mtap7 mRNA level to less than 60%. Reduced Mtap7 level by siRNA increased Pax3 at EB day 4+4. At EB day 4+8 there is a tendency that Myogenin mRNA level was increased. However, the skeletal muscle phenotype was not seen by visual examination under microscope. Stable knockdown or knockout could improve this effect of Mtap7 since the duration of siRNA is generally short and transient. Also the decreased level of Mtap7 by siRNA could be also improved by using stable knockdown. In contrast to Mtap7 siRNA against Lrrc2 showed no effect on the level of Pax3 and Myogenin (data not shown).

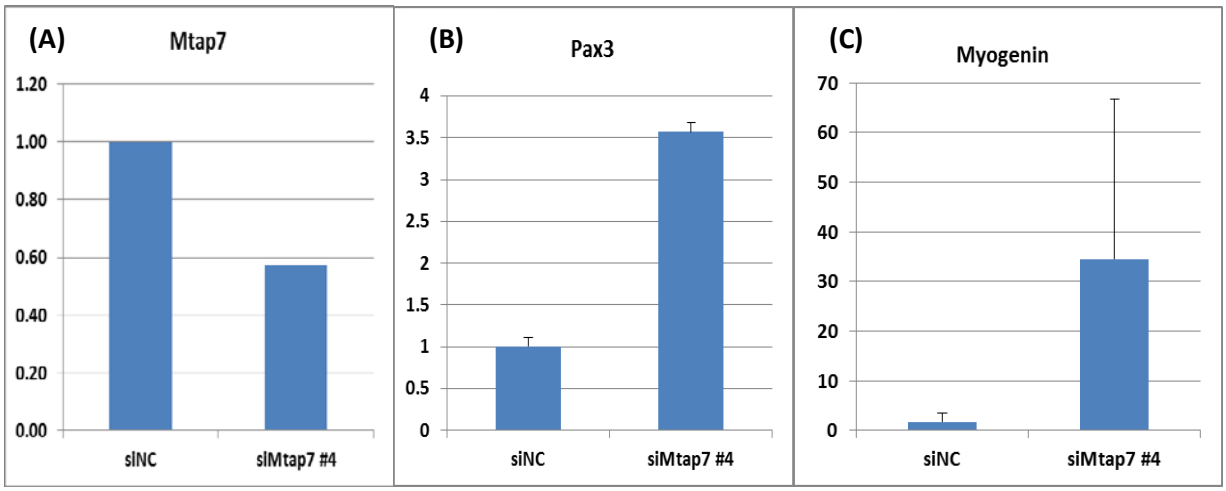

Figure 3.5: mRNA levels measured by real-time RT-PCR. (A) Mtap7 mRNA in ES cells after 48 hours from siRNA transfection. (B) Pax3 mRNA level at EB day 4+4. Error bars indicate the standard deviation of 3 samples of 10 individual EBs. (C) Myogenin mRNA level at EB day4+10. Error bars indicate the standard deviation of 3 samples of 10 individual EBs.

Chapter 4: Concluding remarks and future prospects

In this thesis, I have investigated two small molecules (SMA1 and SMA2) driving mouse EBs to skeletal muscle. In order to elucidate the mechanism of action of SMAs, we analyzed the level of mRNA from EBs in either presence or absence of SMA1. Based on mRNA Microarray data, we applied the pathway analysis and gene set enrichment analysis. From our work, we can draw the major conclusion that the concerted modulation of Wnt pathway, Smad2/3 signaling and Shh pathway is important in skeletal muscle differentiation from mouse ES cells. And I confirmed this hypothesis that the modulation of these three pathways by known small molecules was sufficient to differentiate skeletal muscle from mouse embryonic stem cells.

The role of Wnt pathway activation in the myogenic program during development has been well documented (Rios et al., 2011). Wnt1 and Wnt3 are secreted from the dorsal neural tube and are positively involved in somite patterning. During ES cell differentiation, Wnt pathway activation is critical for skeletal muscle differentiation (Borchin et al., 2013; Shelton et al., 2014; Xu et al., 2013), while inhibition of Wnt pathway is necessary for cardiac muscle differentiation (Wang et al., 2011).

Smad2/3 signaling activation by Nodal/Activin A is important for endoderm specification during development (Schier and Shen, 2000). I speculate that SMI may guide the EB to the mesoderm formation by inhibiting endoderm formation which is a very prominent pathway in early EB differentiation. The role of Shh in skeletal muscle differentiation is less clear. Previous reports explained that Shh regulates skeletal muscle precursor cell survival, proliferation and differentiation during vertebrate's development (Reviewed in Bentzinger et al., 2012). However, presence of skeletal muscle in Shh knockout mice suggests that skeletal muscle can be formed without Shh (Chiang et al., 1996). It is important to note that our *in vitro* EB differentiation system does not produce the structures resembling somites which appear during embryo development *in vivo*. Therefore the effect of these pathways could act in different ways compared to the *in vivo* situation where a somite is formed.

Future prospects

With the findings about skeletal muscle differentiation from mouse ES cells in this thesis, there are still open questions. The future directions described below will improve the mouse embryonic stem cells as a discovery tool in skeletal muscle biology.

1. Further characterization of skeletal muscle induced by SMI

Skeletal muscle derived from mouse ES cells by SMI showed dynamic and dramatic twitching movement on the culture plate, starting around 2 weeks of differentiation. However, it was not tested if these skeletal muscles could integrate and recover the phenotype of animal models of skeletal muscle disease. In the report of Darabi and colleague, the skeletal muscle from mouse ES cells could restore the functional properties in mdx disease model mice (Darabi et al., 2008). It will be of great interest to test injection of ES cell derived skeletal muscle to see if they can ameliorate the pathology *in vivo*. To inject these cells in mdx mice, a model for Duchenne muscluar dystrophy, and look for their integration for the possible improvement of the muscular function would be a great chance to show the potential of our cells. Also the presence of neuromuscular junction in our culture system is needed to be tested. If there are motor neurons innervated to skeletal muscle, the protocol we established can be applied to the research of motor-neuron disease area as a cellular model.

2. Protocol transfer to human pluripotent stem cells

The protocol we established in this thesis was not optimized in human pluripotent stem cells differentiation system. The SMI could not generate skeletal muscle from human pluripotent stem cells so far (data not shown). Interestingly BSL protocol modifying Wnt, Smad and Shh pathway could induces early markers from the preliminary experiments. However, the differentiation could not lead to the mature phenotype of skeletal muscle. The reason could be because the protocol that we tested was not optimal. In mouse EB differentiation, SMI1 and BSL protocol showed different efficiency of skeletal muscle differentiation depending on the time points and concentrations of treatment. Testing different protocols combining different time points and

concentrations during the differentiation of human ES or iPS cells will give an answer to this question. It is important to consider that normally differentiation protocols in human ES or iPS cells are more than approximately 3 times slower compared to mouse cells. The culture condition for example EB formation, attached culture and serum in the medium could affect the whole process of skeletal muscle differentiation.

Originally SMI1 was identified from a GPCR (G-protein coupled receptor) modulating compounds set. The molecules were collected based on the observation of GPCR modulating activity from elsewhere. It was confirmed that SMI1 works as a Gi receptor agonist in SW982 cells. Unfortunately the relevant receptor could not be identified by co-incubation of SMI with known GPCR agonist/antagonist. The activity modulation on the specific receptors remains to be tested. New strategy can be to knockout a GPCR in SW982 *via* Crispr gene editing technique to identify the functional receptor that inhibits SMI's action in knockout cell lines (Cho et al., 2013). Previously knockout or knockdown approach was difficult due to the low transfection efficiency in SW982 cells. By identifying the GPCR which SMI1 interacts with, we will understand the direct mechanism of action of SMI. Once the receptor is revealed, the modulation of that receptor activity could be also used for a protocol transfer to human pluripotent stem cells.

3. Pull down assay for direct target identification

One of the first approaches to understand small molecule's mechanisms is the identification of the binding proteins which interact with the molecule. Extensive structure activity relationship (SAR) studies of SMI1 guided us to understand essential functional groups in the structure for its activity. This knowledge allows us to add a linker to either urea or nitrate group, resulting in linker analogues with similar activity to the original SMI1 compound. Protein lysate of EB day 1 was taken to perform pull-down assay using active SMI linker analogue (Methods described in Huang et al., 2009). Unfortunately we could not identify any probable binding target from EB lysate (data not shown). Most reliable interpretation of this result is that the target is either membrane bound, low abundance or very small size protein. Or, if the interaction between analogue and target is weak, it could not be identified by this method either.

As an alternative tool of labeling and detecting the SMI1 linker molecule, we took advantage of click chemistry in cell culture situation (Koo et al., 2012). However the effort for tracing the

localization of SMI1 with fluorophore with click chemistry did not work out (data not shown). It can be due to the absence of target inside of the cells or the weak binding affinity between SMI1 and target. Probably without cross linking step, compound could be washed away while cells are processed for click chemistry. For the strategy to include the cross linking step before labeling, I also found an analogue containing a part that is compatible to photo affinity labeling (PAL) with UV crosslinking. It would be of interest to test this analogue if this binds to the components in cells with competing manner with the parental compound.

Reference

Alexander, M.S., Kawahara, G., Motohashi, N., Casar, J.C., Eisenberg, I., Myers, J.A., Gasperini, M.J., Estrella, E.A., Kho, A.T., Mitsuhashi, S., et al. (2013). MicroRNA-199a is induced in dystrophic muscle and affects WNT signaling, cell proliferation, and myogenic differentiation. Cell death and differentiation 20, 1194-1208.

Althoff, K., Beckers, A., Odersky, A., Mestdagh, P., Koster, J., Bray, I.M., Bryan, K., Vandesompele, J., Speleman, F., Stallings, R.L., et al. (2013). MiR-137 functions as a tumor suppressor in neuroblastoma by downregulating KDM1A. International journal of cancer Journal international du cancer 133, 1064-1073.

Antoniou, A., Mastroyiannopoulos, N.P., Uney, J.B., and Phylactou, L.A. (2014). miR-186 inhibits muscle cell differentiation through myogenin regulation. The Journal of biological chemistry 289, 3923-3935.

Aoki, K., and Taketo, M.M. (2007). Adenomatous polyposis coli (APC): a multi-functional tumor suppressor gene. Journal of cell science 120, 3327-3335.

Aulehla, A., and Pourquie, O. (2006). On periodicity and directionality of somitogenesis. Anatomy and embryology 211 Suppl 1, 3-8.

Aulehla, A., and Pourquie, O. (2010). Signaling gradients during paraxial mesoderm development. Cold Spring Harbor perspectives in biology 2, a000869.

Bader, A., Al-Dubai, H., and Weitzer, G. (2000). Leukemia inhibitory factor modulates cardiogenesis in embryoid bodies in opposite fashions. Circulation research 86, 787-794.

Bailey, P., Holowacz, T., and Lassar, A.B. (2001). The origin of skeletal muscle stem cells in the embryo and the adult. Current opinion in cell biology 13, 679-689.

Bajard, L., Relaix, F., Lagha, M., Rocancourt, D., Daubas, P., and Buckingham, M.E. (2006). A novel genetic hierarchy functions during hypaxial myogenesis: Pax3 directly activates Myf5 in muscle progenitor cells in the limb. Genes & development 20, 2450-2464.

Bentzinger, C.F., Wang, Y.X., and Rudnicki, M.A. (2012). Building muscle: molecular regulation of myogenesis. Cold Spring Harbor perspectives in biology 4.

Bernardo, B.C., Nguyen, S.S., Winbanks, C.E., Gao, X.M., Boey, E.J., Tham, Y.K., Kiriazis, H., Ooi, J.Y., Porrello, E.R., Igoor, S., et al. (2014). Therapeutic silencing of miR-652 restores heart function and attenuates adverse remodeling in a setting of established

pathological hypertrophy. FASEB journal : official publication of the Federation of American Societies for Experimental Biology.

Bessarabova, M., Ishkin, A., JeBailey, L., Nikolskaya, T., and Nikolsky, Y. (2012). Knowledge-based analysis of proteomics data. BMC bioinformatics 13 Suppl 16, S13.

Bismuth, K., and Relaix, F. (2010). Genetic regulation of skeletal muscle development. Experimental cell research 316, 3081-3086.

Boheler, K.R., Czyz, J., Tweedie, D., Yang, H.T., Anisimov, S.V., and Wobus, A.M. (2002). Differentiation of pluripotent embryonic stem cells into cardiomyocytes. Circulation research 91, 189-201.

Borchin, B., Chen, J., and Barberi, T. (2013). Derivation and FACS-Mediated Purification of PAX3+/PAX7+ Skeletal Muscle Precursors from Human Pluripotent Stem Cells. Stem cell reports 1, 620-631.

Borycki, A.G., Brunk, B., Tajbakhsh, S., Buckingham, M., Chiang, C., and Emerson, C.P., Jr. (1999). Sonic hedgehog controls epaxial muscle determination through Myf5 activation. Development 126, 4053-4063.

Borycki, A.G., Mendham, L., and Emerson, C.P., Jr. (1998). Control of somite patterning by Sonic hedgehog and its downstream signal response genes. Development 125, 777-790.

Bradley, A., Evans, M., Kaufman, M.H., and Robertson, E. (1984). Formation of germ-line chimaeras from embryo-derived teratocarcinoma cell lines. Nature 309, 255-256.

Braun, T., Bober, E., Winter, B., Rosenthal, N., and Arnold, H.H. (1990). Myf-6, a new member of the human gene family of myogenic determination factors: evidence for a gene cluster on chromosome 12. The EMBO journal 9, 821-831.

Braun, T., Rudnicki, M.A., Arnold, H.H., and Jaenisch, R. (1992). Targeted inactivation of the muscle regulatory gene Myf-5 results in abnormal rib development and perinatal death. Cell 71, 369-382.

Brook, J.D., McCurrach, M.E., Harley, H.G., Buckler, A.J., Church, D., Aburatani, H., Hunter, K., Stanton, V.P., Thirion, J.P., Hudson, T., et al. (1992). Molecular basis of myotonic dystrophy: expansion of a trinucleotide (CTG) repeat at the 3' end of a transcript encoding a protein kinase family member. Cell 68, 799-808.

Bryson-Richardson, R.J., and Currie, P.D. (2008). The genetics of vertebrate myogenesis. Nature reviews Genetics 9, 632-646.

Burdon, T., Stracey, C., Chambers, I., Nichols, J., and Smith, A. (1999). Suppression of SHP-2 and ERK signalling promotes self-renewal of mouse embryonic stem cells. Developmental biology 210, 30-43.

Burghes, A.H., Logan, C., Hu, X., Belfall, B., Worton, R.G., and Ray, P.N. (1987). A cDNA clone from the Duchenne/Becker muscular dystrophy gene. Nature 328, 434-437.

Campbell, K.P., and Kahl, S.D. (1989). Association of dystrophin and an integral membrane glycoprotein. Nature 338, 259-262.

Chambers, S.M., Fasano, C.A., Papapetrou, E.P., Tomishima, M., Sadelain, M., and Studer, L. (2009). Highly efficient neural conversion of human ES and iPS cells by dual inhibition of SMAD signaling. Nature biotechnology 27, 275-280.

Chang, H., Yoshimoto, M., Umeda, K., Iwasa, T., Mizuno, Y., Fukada, S., Yamamoto, H., Motohashi, N., Miyagoe-Suzuki, Y., Takeda, S., et al. (2009). Generation of transplantable, functional satellite-like cells from mouse embryonic stem cells. FASEB journal : official publication of the Federation of American Societies for Experimental Biology 23, 1907-1919.

Chaturvedi, L.S., Mukherjee, M., Srivastava, S., Mittal, R.D., and Mittal, B. (2001). Point mutation and polymorphism in Duchenne/Becker muscular dystrophy (D/BMD) patients. Experimental & molecular medicine 33, 251-256.

Chen, B., Dodge, M.E., Tang, W., Lu, J., Ma, Z., Fan, C.W., Wei, S., Hao, W., Kilgore, J., Williams, N.S., et al. (2009a). Small molecule-mediated disruption of Wnt-dependent signaling in tissue regeneration and cancer. Nature chemical biology 5, 100-107.

Chen, J.F., Tao, Y., Li, J., Deng, Z., Yan, Z., Xiao, X., and Wang, D.Z. (2010). microRNA-1 and microRNA-206 regulate skeletal muscle satellite cell proliferation and differentiation by repressing Pax7. The Journal of cell biology 190, 867-879.

Chen, S., Borowiak, M., Fox, J.L., Maehr, R., Osafune, K., Davidow, L., Lam, K., Peng, L.F., Schreiber, S.L., Rubin, L.L., et al. (2009b). A small molecule that directs differentiation of human ESCs into the pancreatic lineage. Nature chemical biology 5, 258-265.

Chen, X., Xu, H., Yuan, P., Fang, F., Huss, M., Vega, V.B., Wong, E., Orlov, Y.L., Zhang, W., Jiang, J., et al. (2008). Integration of external signaling pathways with the core transcriptional network in embryonic stem cells. Cell 133, 1106-1117.

Chen, Y., Melton, D.W., Gelfond, J.A., McManus, L.M., and Shireman, P.K. (2012). MiR-351 transiently increases during muscle regeneration and promotes progenitor cell proliferation and survival upon differentiation. Physiological genomics 44, 1042-1051.

Chiang, C., Litingtung, Y., Lee, E., Young, K.E., Corden, J.L., Westphal, H., and Beachy, P.A. (1996). Cyclopia and defective axial patterning in mice lacking Sonic hedgehog gene function. Nature 383, 407-413.

Cho, S.W., Kim, S., Kim, J.M., and Kim, J.S. (2013). Targeted genome engineering in human cells with the Cas9 RNA-guided endonuclease. Nature biotechnology 31, 230-232.

Ciemerych, M.A., Archacka, K., Grabowska, I., and Przewozniak, M. (2011). Cell cycle regulation during proliferation and differentiation of mammalian muscle precursor cells. Results and problems in cell differentiation 53, 473-527.

Clark, A.M., Garland, K.K., and Russell, L.D. (2000). Desert hedgehog (Dhh) gene is required in the mouse testis for formation of adult-type Leydig cells and normal development of peritubular cells and seminiferous tubules. Biology of reproduction 63, 1825-1838.

Conlon, F.L., Lyons, K.M., Takaesu, N., Barth, K.S., Kispert, A., Herrmann, B., and Robertson, E.J. (1994). A primary requirement for nodal in the formation and maintenance of the primitive streak in the mouse. Development 120, 1919-1928.

Cordes, K.R., Sheehy, N.T., White, M.P., Berry, E.C., Morton, S.U., Muth, A.N., Lee, T.H., Miano, J.M., Ivey, K.N., and Srivastava, D. (2009). miR-145 and miR-143 regulate smooth muscle cell fate and plasticity. Nature 460, 705-710.

Cutler, M.L., Bassin, R.H., Zanoni, L., and Talbot, N. (1992). Isolation of rsp-1, a novel cDNA capable of suppressing v-Ras transformation. Molecular and cellular biology 12, 3750-3756.

Darabi, R., and Perlingeiro, R.C. (2008). Lineage-specific reprogramming as a strategy for cell therapy. Cell cycle 7, 1732-1737.

Darabi, R., Arpke, R.W., Irion, S., Dimos, J.T., Grskovic, M., Kyba, M., and Perlingeiro, R.C. (2012). Human ES- and iPS-derived myogenic progenitors restore DYSTROPHIN and improve contractility upon transplantation in dystrophic mice. Cell stem cell 10, 610-619.

Darabi, R., Gehlbach, K., Bachoo, R.M., Kamath, S., Osawa, M., Kamm, K.E., Kyba, M., and Perlingeiro, R.C. (2008). Functional skeletal muscle regeneration from differentiating embryonic stem cells. Nature medicine 14, 134-143.

Davila, J.C., Cezar, G.G., Thiede, M., Strom, S., Miki, T., and Trosko, J. (2004). Use and application of stem cells in toxicology. Toxicological sciences : an official journal of the Society of Toxicology 79, 214-223.

Davis, R.L., Weintraub, H., and Lassar, A.B. (1987). Expression of a single transfected cDNA converts fibroblasts to myoblasts. Cell 51, 987-1000.

Dodge, J.E., Kang, Y.K., Beppu, H., Lei, H., and Li, E. (2004). Histone H3-K9 methyltransferase ESET is essential for early development. Molecular and cellular biology 24, 2478-2486.

Du, Z.W., Ma, L.X., Phillips, C., and Zhang, S.C. (2013). miR-200 and miR-96 families repress neural induction from human embryonic stem cells. Development 140, 2611-2618.

Echelard, Y., Epstein, D.J., St-Jacques, B., Shen, L., Mohler, J., McMahon, J.A., and McMahon, A.P. (1993). Sonic hedgehog, a member of a family of putative signaling molecules, is implicated in the regulation of CNS polarity. Cell 75, 1417-1430.

Endo, K., Weng, H., Kito, N., Fukushima, Y., and Iwai, N. (2013). MiR-216a and miR-216b as markers for acute phased pancreatic injury. Biomedical research 34, 179-188.

Ervasti, J.M., and Campbell, K.P. (1991). Membrane organization of the dystrophin-glycoprotein complex. Cell 66, 1121-1131.

Evans, M.J., and Kaufman, M.H. (1981). Establishment in culture of pluripotential cells from mouse embryos. Nature 292, 154-156.

Feng, X., Adiarte, E.G., and Devoto, S.H. (2006). Hedgehog acts directly on the zebrafish dermomyotome to promote myogenic differentiation. Developmental biology 300, 736-746.

Ferland-McCollough, D., Fernandez-Twinn, D.S., Cannell, I.G., David, H., Warner, M., Vaag, A.A., Bork-Jensen, J., Brons, C., Gant, T.W., Willis, A.E., et al. (2012). Programming of adipose tissue miR-483-3p and GDF-3 expression by maternal diet in type 2 diabetes. Cell death and differentiation 19, 1003-1012.

Fior, R., Maxwell, A.A., Ma, T.P., Vezzaro, A., Moens, C.B., Amacher, S.L., Lewis, J., and Saude, L. (2012). The differentiation and movement of presomitic mesoderm progenitor cells are controlled by Mesogenin 1. Development 139, 4656-4665.

Frank-Kamenetsky, M., Zhang, X.M., Bottega, S., Guicherit, O., Wichterle, H., Dudek, H., Bumcrot, D., Wang, F.Y., Jones, S., Shulok, J., et al. (2002). Small-molecule modulators of Hedgehog signaling: identification and characterization of Smoothened agonists and antagonists. Journal of biology 1, 10.

Gearing, D.P., Comeau, M.R., Friend, D.J., Gimpel, S.D., Thut, C.J., McGourty, J., Brasher, K.K., King, J.A., Gillis, S., Mosley, B., et al. (1992). The IL-6 signal transducer, gp130:

an oncostatin M receptor and affinity converter for the LIF receptor. Science 255, 1434-1437.

Gesta, S., Tseng, Y.H., and Kahn, C.R. (2007). Developmental origin of fat: tracking obesity to its source. Cell 131, 242-256.

Goldring, K., Partridge, T., and Watt, D. (2002). Muscle stem cells. The Journal of pathology 197, 457-467.

Goulding, M.D., Chalepakis, G., Deutsch, U., Erselius, J.R., and Gruss, P. (1991). Pax-3, a novel murine DNA binding protein expressed during early neurogenesis. The EMBO journal 10, 1135-1147.

Grumolato, L., Liu, G., Mong, P., Mudbhary, R., Biswas, R., Arroyave, R., Vijayakumar, S., Economides, A.N., and Aaronson, S.A. (2010). Canonical and noncanonical Wnts use a common mechanism to activate completely unrelated coreceptors. Genes & development 24, 2517-2530.

Gurdon, J.B., Dyson, S., and St Johnston, D. (1998). Cells' perception of position in a concentration gradient. Cell 95, 159-162.

Hao, J., Daleo, M.A., Murphy, C.K., Yu, P.B., Ho, J.N., Hu, J., Peterson, R.T., Hatzopoulos, A.K., and Hong, C.C. (2008). Dorsomorphin, a selective small molecule inhibitor of BMP signaling, promotes cardiomyogenesis in embryonic stem cells. PloS one 3, e2904.

Hasty, P., Bradley, A., Morris, J.H., Edmondson, D.G., Venuti, J.M., Olson, E.N., and Klein, W.H. (1993). Muscle deficiency and neonatal death in mice with a targeted mutation in the myogenin gene. Nature 364, 501-506.

He, L., and Hannon, G.J. (2004). MicroRNAs: small RNAs with a big role in gene regulation. Nature reviews Genetics 5, 522-531.

Hogan, B.L. (1996). Bone morphogenetic proteins in development. Current opinion in genetics & development 6, 432-438.

Houbaviy, H.B., Murray, M.F., and Sharp, P.A. (2003). Embryonic stem cell-specific MicroRNAs. Developmental cell 5, 351-358.

Huang, S.M., Mishina, Y.M., Liu, S., Cheung, A., Stegmeier, F., Michaud, G.A., Charlat, O., Wiellette, E., Zhang, Y., Wiessner, S., et al. (2009). Tankyrase inhibition stabilizes axin and antagonizes Wnt signalling. Nature 461, 614-620.

Hudish, L.I., Blasky, A.J., and Appel, B. (2013). miR-219 regulates neural precursor differentiation by direct inhibition of apical par polarity proteins. Developmental cell 27, 387-398.

Iacovino, M., Bosnakovski, D., Fey, H., Rux, D., Bajwa, G., Mahen, E., Mitanoska, A., Xu, Z., and Kyba, M. (2011). Inducible cassette exchange: a rapid and efficient system enabling conditional gene expression in embryonic stem and primary cells. Stem cells 29, 1580-1588.

Ikeya, M., and Takada, S. (2001). Wnt-3a is required for somite specification along the anteroposterior axis of the mouse embryo and for regulation of cdx-1 expression. Mechanisms of development 103, 27-33.

Ingham, P.W., Nakano, Y., and Seger, C. (2011). Mechanisms and functions of Hedgehog signalling across the metazoa. Nature reviews Genetics 12, 393-406.

Inman, G.J., Nicolas, F.J., Callahan, J.F., Harling, J.D., Gaster, L.M., Reith, A.D., Laping, N.J., and Hill, C.S. (2002). SB-431542 is a potent and specific inhibitor of transforming growth factor-beta superfamily type I activin receptor-like kinase (ALK) receptors ALK4, ALK5, and ALK7. Molecular pharmacology 62, 65-74.

Ivey, K.N., Muth, A., Arnold, J., King, F.W., Yeh, R.F., Fish, J.E., Hsiao, E.C., Schwartz, R.J., Conklin, B.R., Bernstein, H.S., et al. (2008). MicroRNA regulation of cell lineages in mouse and human embryonic stem cells. Cell stem cell 2, 219-229.

Johnson, R.L., Laufer, E., Riddle, R.D., and Tabin, C. (1994). Ectopic expression of Sonic hedgehog alters dorsal-ventral patterning of somites. Cell 79, 1165-1173.

Jostes, B., Walther, C., and Gruss, P. (1990). The murine paired box gene, Pax7, is expressed specifically during the development of the nervous and muscular system. Mechanisms of development 33, 27-37.

Juan, A.H., Kumar, R.M., Marx, J.G., Young, R.A., and Sartorelli, V. (2009). Mir-214-dependent regulation of the polycomb protein Ezh2 in skeletal muscle and embryonic stem cells. Molecular cell 36, 61-74.

Judson, R.L., Babiarz, J.E., Venere, M., and Blelloch, R. (2009). Embryonic stem cell-specific microRNAs promote induced pluripotency. Nature biotechnology 27, 459-461.

Jung, D.W., and Williams, D.R. (2012). Reawakening atlas: chemical approaches to repair or replace dysfunctional musculature. ACS chemical biology 7, 1773-1790.

Kattman, S.J., Witty, A.D., Gagliardi, M., Dubois, N.C., Niapour, M., Hotta, A., Ellis, J., and Keller, G. (2011). Stage-specific optimization of activin/nodal and BMP signaling

promotes cardiac differentiation of mouse and human pluripotent stem cell lines. Cell stem cell 8, 228-240.

Kennedy, K.A., Porter, T., Mehta, V., Ryan, S.D., Price, F., Peshdary, V., Karamboulas, C., Savage, J., Drysdale, T.A., Li, S.C., et al. (2009). Retinoic acid enhances skeletal muscle progenitor formation and bypasses inhibition by bone morphogenetic protein 4 but not dominant negative beta-catenin. BMC biology 7, 67.

Kiefer, J.C., and Hauschka, S.D. (2001). Myf-5 is transiently expressed in nonmuscle mesoderm and exhibits dynamic regional changes within the presegmented mesoderm and somites I-IV. Developmental biology 232, 77-90.

Kim, H.K., Lee, Y.S., Sivaprasad, U., Malhotra, A., and Dutta, A. (2006). Muscle-specific microRNA miR-206 promotes muscle differentiation. The Journal of cell biology 174, 677-687.

Kim, V.N. (2005). MicroRNA biogenesis: coordinated cropping and dicing. Nature reviews Molecular cell biology 6, 376-385.

Kiss, H., Yang, Y., Kiss, C., Andersson, K., Klein, G., Imreh, S., and Dumanski, J.P. (2002). The transcriptional map of the common eliminated region 1 (C3CER1) in 3p21.3. European journal of human genetics : EJHG 10, 52-61.

Kloosterman, W.P., Lagendijk, A.K., Ketting, R.F., Moulton, J.D., and Plasterk, R.H. (2007). Targeted inhibition of miRNA maturation with morpholinos reveals a role for miR-375 in pancreatic islet development. PLoS biology 5, e203.

Koo, H., Lee, S., Na, J.H., Kim, S.H., Hahn, S.K., Choi, K., Kwon, I.C., Jeong, S.Y., and Kim, K. (2012). Bioorthogonal copper-free click chemistry in vivo for tumor-targeted delivery of nanoparticles. Angewandte Chemie 51, 11836-11840.

Krichevsky, A.M., Sonntag, K.C., Isacson, O., and Kosik, K.S. (2006). Specific microRNAs modulate embryonic stem cell-derived neurogenesis. Stem cells 24, 857-864.

Lahmy, R., Soleimani, M., Sanati, M.H., Behmanesh, M., Kouhkan, F., and Mobarra, N. (2013). Pancreatic islet differentiation of human embryonic stem cells by microRNA overexpression. Journal of tissue engineering and regenerative medicine.

Lahmy, R., Soleimani, M., Sanati, M.H., Behmanesh, M., Kouhkan, F., and Mobarra, N. (2014). MiRNA-375 promotes beta pancreatic differentiation in human induced pluripotent stem (hiPS) cells. Molecular biology reports 41, 2055-2066.

Lang, T., Streeper, T., Cawthon, P., Baldwin, K., Taaffe, D.R., and Harris, T.B. (2010). Sarcopenia: etiology, clinical consequences, intervention, and assessment. Osteoporosis

international : a journal established as result of cooperation between the European Foundation for Osteoporosis and the National Osteoporosis Foundation of the USA 21, 543-559.

Leahy, A., Xiong, J.W., Kuhnert, F., and Stuhlmann, H. (1999). Use of developmental marker genes to define temporal and spatial patterns of differentiation during embryoid body formation. The Journal of experimental zoology 284, 67-81.

Lee, K.L., Lim, S.K., Orlov, Y.L., Yit le, Y., Yang, H., Ang, L.T., Poellinger, L., and Lim, B. (2011). Graded Nodal/Activin signaling titrates conversion of quantitative phospho-Smad2 levels into qualitative embryonic stem cell fate decisions. PLoS genetics 7, e1002130.

Lee, N.S., Kim, J.S., Cho, W.J., Lee, M.R., Steiner, R., Gompers, A., Ling, D., Zhang, J., Strom, P., Behlke, M., et al. (2008). miR-302b maintains "stemness" of human embryonal carcinoma cells by post-transcriptional regulation of Cyclin D2 expression. Biochemical and biophysical research communications 377, 434-440.

Lei, H., Zou, D., Li, Z., Luo, M., Dong, L., Wang, B., Yin, H., Ma, Y., Liu, C., Wang, F., et al. (2013). MicroRNA-219-2-3p functions as a tumor suppressor in gastric cancer and is regulated by DNA methylation. PloS one 8, e60369.

Lemercier, C., To, R.Q., Carrasco, R.A., and Konieczny, S.F. (1998). The basic helix-loop-helix transcription factor Mist1 functions as a transcriptional repressor of myoD. The EMBO journal 17, 1412-1422.

Li, W., Li, K., Wei, W., and Ding, S. (2013). Chemical approaches to stem cell biology and therapeutics. Cell stem cell 13, 270-283.

Lian, J., Tian, H., Liu, L., Zhang, X.S., Li, W.Q., Deng, Y.M., Yao, G.D., Yin, M.M., and Sun, F. (2010). Downregulation of microRNA-383 is associated with male infertility and promotes testicular embryonal carcinoma cell proliferation by targeting IRF1. Cell death & disease 1, e94.

Lin, S.L., Chang, D.C., Lin, C.H., Ying, S.Y., Leu, D., and Wu, D.T. (2011). Regulation of somatic cell reprogramming through inducible mir-302 expression. Nucleic acids research 39, 1054-1065.

Liu, Z., Scannell, D.R., Eisen, M.B., and Tjian, R. (2011). Control of embryonic stem cell lineage commitment by core promoter factor, TAF3. Cell 146, 720-731.

Lo, K.W., Jiang, T., Gagnon, K.A., Nelson, C., and Laurencin, C.T. (2014). Small-molecule based musculoskeletal regenerative engineering. Trends in biotechnology 32, 74-81.

Lohmann, F., Loureiro, J., Su, H., Fang, Q., Lei, H., Lewis, T., Yang, Y., Labow, M., Li, E., Chen, T., et al. (2010). KMT1E mediated H3K9 methylation is required for the maintenance of embryonic stem cells by repressing trophectoderm differentiation. Stem cells 28, 201-212.

Lowell, S., Benchoua, A., Heavey, B., and Smith, A.G. (2006). Notch promotes neural lineage entry by pluripotent embryonic stem cells. PLoS biology 4, e121.

MacDonald, B.T., Tamai, K., and He, X. (2009). Wnt/beta-catenin signaling: components, mechanisms, and diseases. Developmental cell 17, 9-26.

Maeda, M., Harris, A.W., Kingham, B.F., Lumpkin, C.J., Opdenaker, L.M., McCahan, S.M., Wang, W., and Butchbach, M.E. (2014). Transcriptome profiling of spinal muscular atrophy motor neurons derived from mouse embryonic stem cells. PloS one 9, e106818.

Magli, A., Schnettler, E., Rinaldi, F., Bremer, P., and Perlingeiro, R.C. (2013). Functional dissection of Pax3 in paraxial mesoderm development and myogenesis. Stem cells 31, 59-70.

Magnan, D.R., Spacek, D.V., Ye, N., Lu, Y.C., and King, T.R. (2009). The male sterility and histoincompatibility (mshi) mutation in mice is a natural variant of microtubule-associated protein 7 (Mtap7). Molecular genetics and metabolism 97, 155-162.

Marcelle, C., Stark, M.R., and Bronner-Fraser, M. (1997). Coordinate actions of BMPs, Wnts, Shh and noggin mediate patterning of the dorsal somite. Development 124, 3955-3963.

Marson, A., Levine, S.S., Cole, M.F., Frampton, G.M., Brambrink, T., Johnstone, S., Guenther, M.G., Johnston, W.K., Wernig, M., Newman, J., et al. (2008). Connecting microRNA genes to the core transcriptional regulatory circuitry of embryonic stem cells. Cell 134, 521-533.

Martin, G.R. (1981). Isolation of a pluripotent cell line from early mouse embryos cultured in medium conditioned by teratocarcinoma stem cells. Proceedings of the National Academy of Sciences of the United States of America 78, 7634-7638.

Marvin, M.J., Di Rocco, G., Gardiner, A., Bush, S.M., and Lassar, A.B. (2001). Inhibition of Wnt activity induces heart formation from posterior mesoderm. Genes & development 15, 316-327.

Massague, J. (1998). TGF-beta signal transduction. Annual review of biochemistry 67, 753-791.

Massague, J., Seoane, J., and Wotton, D. (2005). Smad transcription factors. Genes & development 19, 2783-2810.

Massari, M.E., and Murre, C. (2000). Helix-loop-helix proteins: regulators of transcription in eucaryotic organisms. Molecular and cellular biology 20, 429-440.

Mauro, A. (1961). Satellite cell of skeletal muscle fibers. The Journal of biophysical and biochemical cytology 9, 493-495.

McCarthy, J.J. (2008). MicroRNA-206: the skeletal muscle-specific myomiR. Biochimica et biophysica acta 1779, 682-691.

McPherron, A.C., and Lee, S.J. (1997). Double muscling in cattle due to mutations in the myostatin gene. Proceedings of the National Academy of Sciences of the United States of America 94, 12457-12461.

Melton, C., Judson, R.L., and Blelloch, R. (2010). Opposing microRNA families regulate self-renewal in mouse embryonic stem cells. Nature 463, 621-626.

Merico, D., Isserlin, R., Stueker, O., Emili, A., and Bader, G.D. (2010). Enrichment map: a network-based method for gene-set enrichment visualization and interpretation. PloS one 5, e13984.

Michael, M.Z., SM, O.C., van Holst Pellekaan, N.G., Young, G.P., and James, R.J. (2003). Reduced accumulation of specific microRNAs in colorectal neoplasia. Molecular cancer research : MCR 1, 882-891.

Miller, R.G., Sharma, K.R., Pavlath, G.K., Gussoni, E., Mynhier, M., Lanctot, A.M., Greco, C.M., Steinman, L., and Blau, H.M. (1997). Myoblast implantation in Duchenne muscular dystrophy: the San Francisco study. Muscle & nerve 20, 469-478.

Muir, L.A., and Chamberlain, J.S. (2009). Emerging strategies for cell and gene therapy of the muscular dystrophies. Expert reviews in molecular medicine 11, e18.

Nakano, H., Miyazawa, T., Kinoshita, K., Yamada, Y., and Yoshida, T. (2010). Functional screening identifies a microRNA, miR-491 that induces apoptosis by targeting Bcl-X(L) in colorectal cancer cells. International journal of cancer Journal international du cancer 127, 1072-1080.

Nemir, M., Croquelois, A., Pedrazzini, T., and Radtke, F. (2006). Induction of cardiogenesis in embryonic stem cells via downregulation of Notch1 signaling. Circulation research 98, 1471-1478.

Neo, W.H., Yap, K., Lee, S.H., Looi, L.S., Khandelia, P., Neo, S.X., Makeyev, E.V., and Su, I.H. (2014). MicroRNA miR-124 Controls the Choice between Neuronal and Astrocyte Differentiation by Fine-tuning Ezh2 Expression. The Journal of biological chemistry 289, 20788-20801.

Ogawa, K., Saito, A., Matsui, H., Suzuki, H., Ohtsuka, S., Shimosato, D., Morishita, Y., Watabe, T., Niwa, H., and Miyazono, K. (2007). Activin-Nodal signaling is involved in propagation of mouse embryonic stem cells. Journal of cell science 120, 55-65.

Pan, S., Wu, X., Jiang, J., Gao, W., Wan, Y., Cheng, D., Han, D., Liu, J., Englund, N.P., Wang, Y., et al. (2010). Discovery of NVP-LDE225, a Potent and Selective Smoothened Antagonist. ACS medicinal chemistry letters 1, 130-134.

Panda, A.C., Sahu, I., Kulkarni, S.D., Martindale, J.L., Abdelmohsen, K., Vindu, A., Joseph, J., Gorospe, M., and Seshadri, V. (2014). miR-196b-mediated translation regulation of mouse insulin2 via the 5'UTR. PloS one 9, e101084.

Partridge, T.A. (2011). Impending therapies for Duchenne muscular dystrophy. Current opinion in neurology 24, 415-422.

Popperl, H., Schmidt, C., Wilson, V., Hume, C.R., Dodd, J., Krumlauf, R., and Beddington, R.S. (1997). Misexpression of Cwnt8C in the mouse induces an ectopic embryonic axis and causes a truncation of the anterior neuroectoderm. Development 124, 2997-3005.

Pourquie, O., Fan, C.M., Coltey, M., Hirsinger, E., Watanabe, Y., Breant, C., Francis-West, P., Brickell, P., Tessier-Lavigne, M., and Le Douarin, N.M. (1996). Lateral and axial signals involved in avian somite patterning: a role for BMP4. Cell 84, 461-471.

Pownall, M.E., Gustafsson, M.K., and Emerson, C.P., Jr. (2002). Myogenic regulatory factors and the specification of muscle progenitors in vertebrate embryos. Annual review of cell and developmental biology 18, 747-783.

Poy, M.N., Eliasson, L., Krutzfeldt, J., Kuwajima, S., Ma, X., Macdonald, P.E., Pfeffer, S., Tuschl, T., Rajewsky, N., Rorsman, P., et al. (2004). A pancreatic islet-specific microRNA regulates insulin secretion. Nature 432, 226-230.

Qu, X.B., Pan, J., Zhang, C., and Huang, S.Y. (2008). Sox17 facilitates the differentiation of mouse embryonic stem cells into primitive and definitive endoderm in vitro. Development, growth & differentiation 50, 585-593.

Relaix, F., and Zammit, P.S. (2012). Satellite cells are essential for skeletal muscle regeneration: the cell on the edge returns centre stage. Development 139, 2845-2856.

Relaix, F., Rocancourt, D., Mansouri, A., and Buckingham, M. (2005). A Pax3/Pax7-dependent population of skeletal muscle progenitor cells. Nature 435, 948-953.

Rhodes, S.J., and Konieczny, S.F. (1989). Identification of MRF4: a new member of the muscle regulatory factor gene family. Genes & development 3, 2050-2061.

Rios, A.C., Serralbo, O., Salgado, D., and Marcelle, C. (2011). Neural crest regulates myogenesis through the transient activation of NOTCH. Nature 473, 532-535.

Rohwedel, J., Maltsev, V., Bober, E., Arnold, H.H., Hescheler, J., and Wobus, A.M. (1994). Muscle cell differentiation of embryonic stem cells reflects myogenesis in vivo: developmentally regulated expression of myogenic determination genes and functional expression of ionic currents. Developmental biology 164, 87-101.

Rudnicki, M.A., Braun, T., Hinuma, S., and Jaenisch, R. (1992). Inactivation of MyoD in mice leads to up-regulation of the myogenic HLH gene Myf-5 and results in apparently normal muscle development. Cell 71, 383-390.

Rudnicki, M.A., Schnegelsberg, P.N., Stead, R.H., Braun, T., Arnold, H.H., and Jaenisch, R. (1993). MyoD or Myf-5 is required for the formation of skeletal muscle. Cell 75, 1351-1359.

Ruiz i Altaba, A., Palma, V., and Dahmane, N. (2002). Hedgehog-Gli signalling and the growth of the brain. Nature reviews Neuroscience 3, 24-33.

Ryan, T., Liu, J., Chu, A., Wang, L., Blais, A., and Skerjanc, I.S. (2012). Retinoic acid enhances skeletal myogenesis in human embryonic stem cells by expanding the premyogenic progenitor population. Stem cell reviews 8, 482-493.

Sakurai, H., Okawa, Y., Inami, Y., Nishio, N., and Isobe, K. (2008). Paraxial mesodermal progenitors derived from mouse embryonic stem cells contribute to muscle regeneration via differentiation into muscle satellite cells. Stem cells 26, 1865-1873.

Sandri, M., Sandri, C., Gilbert, A., Skurk, C., Calabria, E., Picard, A., Walsh, K., Schiaffino, S., Lecker, S.H., and Goldberg, A.L. (2004). Foxo transcription factors induce the atrophy-related ubiquitin ligase atrogin-1 and cause skeletal muscle atrophy. Cell 117, 399-412.

Sanes, J.R. (2003). The basement membrane/basal lamina of skeletal muscle. The Journal of biological chemistry 278, 12601-12604.

Sartori, R., Gregorevic, P., and Sandri, M. (2014). TGFbeta and BMP signaling in skeletal muscle: potential significance for muscle-related disease. Trends in endocrinology and metabolism: TEM.

Sato, N., Meijer, L., Skaltsounis, L., Greengard, P., and Brivanlou, A.H. (2004). Maintenance of pluripotency in human and mouse embryonic stem cells through activation of Wnt signaling by a pharmacological GSK-3-specific inhibitor. Nature medicine 10, 55-63.

Schiaffino, S., Dyar, K.A., Ciciliot, S., Blaauw, B., and Sandri, M. (2013). Mechanisms regulating skeletal muscle growth and atrophy. The FEBS journal 280, 4294-4314.

Schier, A.F., and Shen, M.M. (2000). Nodal signalling in vertebrate development. Nature 403, 385-389.

Seale, P., Sabourin, L.A., Girgis-Gabardo, A., Mansouri, A., Gruss, P., and Rudnicki, M.A. (2000). Pax7 is required for the specification of myogenic satellite cells. Cell 102, 777-786.

Seifert, J.R., and Mlodzik, M. (2007). Frizzled/PCP signalling: a conserved mechanism regulating cell polarity and directed motility. Nature reviews Genetics 8, 126-138.

Shan, J., Schwartz, R.E., Ross, N.T., Logan, D.J., Thomas, D., Duncan, S.A., North, T.E., Goessling, W., Carpenter, A.E., and Bhatia, S.N. (2013). Identification of small molecules for human hepatocyte expansion and iPS differentiation. Nature chemical biology 9, 514-520.

Shelton, M., Metz, J., Liu, J., Carpenedo, R.L., Demers, S.P., Stanford, W.L., and Skerjanc, I.S. (2014). Derivation and Expansion of PAX7-Positive Muscle Progenitors from Human and Mouse Embryonic Stem Cells. Stem cell reports 3, 516-529.

Shi, S., Leites, C., He, D., Schwartz, D., Moy, W., Shi, J., and Duan, J. (2014). MicroRNA-9 and microRNA-326 regulate human dopamine D2 receptor expression, and the microRNA-mediated expression regulation is altered by a genetic variant. The Journal of biological chemistry 289, 13434-13444.

Small, E.M., O'Rourke, J.R., Moresi, V., Sutherland, L.B., McAnally, J., Gerard, R.D., Richardson, J.A., and Olson, E.N. (2010). Regulation of PI3-kinase/Akt signaling by muscle-enriched microRNA-486. Proceedings of the National Academy of Sciences of the United States of America 107, 4218-4223.

Straub, V., Bittner, R.E., Leger, J.J., and Voit, T. (1992). Direct visualization of the dystrophin network on skeletal muscle fiber membrane. The Journal of cell biology 119, 1183-1191.

Su, R., Lin, H.S., Zhang, X.H., Yin, X.L., Ning, H.M., Liu, B., Zhai, P.F., Gong, J.N., Shen, C., Song, L., et al. (2014). MiR-181 family: regulators of myeloid differentiation and acute myeloid leukemia as well as potential therapeutic targets. Oncogene 0.

Subramanian, A., Tamayo, P., Mootha, V.K., Mukherjee, S., Ebert, B.L., Gillette, M.A., Paulovich, A., Pomeroy, S.L., Golub, T.R., Lander, E.S., et al. (2005). Gene set enrichment analysis: a knowledge-based approach for interpreting genome-wide expression profiles. Proceedings of the National Academy of Sciences of the United States of America 102, 15545-15550.

Subramanyam, D., Lamouille, S., Judson, R.L., Liu, J.Y., Bucay, N., Derynck, R., and Blelloch, R. (2011). Multiple targets of miR-302 and miR-372 promote reprogramming of human fibroblasts to induced pluripotent stem cells. Nature biotechnology 29, 443-448.

Suh, M.R., Lee, Y., Kim, J.Y., Kim, S.K., Moon, S.H., Lee, J.Y., Cha, K.Y., Chung, H.M., Yoon, H.S., Moon, S.Y., et al. (2004). Human embryonic stem cells express a unique set of microRNAs. Developmental biology 270, 488-498.

Tabar, V., and Studer, L. (2014). Pluripotent stem cells in regenerative medicine: challenges and recent progress. Nature reviews Genetics 15, 82-92.

Takada, S., Stark, K.L., Shea, M.J., Vassileva, G., McMahon, J.A., and McMahon, A.P. (1994). Wnt-3a regulates somite and tailbud formation in the mouse embryo. Genes & development 8, 174-189.

Takahashi, K., and Yamanaka, S. (2006). Induction of pluripotent stem cells from mouse embryonic and adult fibroblast cultures by defined factors. Cell 126, 663-676.

Tam, P.P., and Behringer, R.R. (1997). Mouse gastrulation: the formation of a mammalian body plan. Mechanisms of development 68, 3-25.

Tam, P.P., and Loebel, D.A. (2007). Gene function in mouse embryogenesis: get set for gastrulation. Nature reviews Genetics 8, 368-381.

Thomas, E.D., Lochte, H.L., Jr., Lu, W.C., and Ferrebee, J.W. (1957). Intravenous infusion of bone marrow in patients receiving radiation and chemotherapy. The New England journal of medicine 257, 491-496.

Thomas, P.D., Campbell, M.J., Kejariwal, A., Mi, H., Karlak, B., Daverman, R., Diemer, K., Muruganujan, A., and Narechania, A. (2003). PANTHER: a library of protein families and subfamilies indexed by function. Genome research 13, 2129-2141.

Tousi, S.E., Soltani, B.M., Sadeghizadeh, M., Mowla, S.J., Parsi, S., and Soleimani, M. (2014). Inhibitory effect of hsa-miR-590-5p on cardiosphere-derived stem cells differentiation through downregulation of TGFB signaling. Journal of cellular biochemistry.

Trendelenburg, A.U., Meyer, A., Rohner, D., Boyle, J., Hatakeyama, S., and Glass, D.J. (2009). Myostatin reduces Akt/TORC1/p70S6K signaling, inhibiting myoblast differentiation and myotube size. American journal of physiology Cell physiology 296, C1258-1270.

Valeri, N., Braconi, C., Gasparini, P., Murgia, C., Lampis, A., Paulus-Hock, V., Hart, J.R., Ueno, L., Grivennikov, S.I., Lovat, F., et al. (2014). MicroRNA-135b promotes cancer progression by acting as a downstream effector of oncogenic pathways in colon cancer. Cancer cell 25, 469-483.

Wang, H., Hao, J., and Hong, C.C. (2011). Cardiac induction of embryonic stem cells by a small molecule inhibitor of Wnt/beta-catenin signaling. ACS chemical biology 6, 192-197.

White, J., and Dalton, S. (2005). Cell cycle control of embryonic stem cells. Stem cell reviews 1, 131-138.

Willems, E., Spiering, S., Davidovics, H., Lanier, M., Xia, Z., Dawson, M., Cashman, J., and Mercola, M. (2011). Small-molecule inhibitors of the Wnt pathway potently promote cardiomyocytes from human embryonic stem cell-derived mesoderm. Circulation research 109, 360-364.

Williams, R.L., Hilton, D.J., Pease, S., Willson, T.A., Stewart, C.L., Gearing, D.P., Wagner, E.F., Metcalf, D., Nicola, N.A., and Gough, N.M. (1988). Myeloid leukaemia inhibitory factor maintains the developmental potential of embryonic stem cells. Nature 336, 684-687.

Wobus, A.M., and Boheler, K.R. (2005). Embryonic stem cells: prospects for developmental biology and cell therapy. Physiological reviews 85, 635-678.

Wu, Z., Woodring, P.J., Bhakta, K.S., Tamura, K., Wen, F., Feramisco, J.R., Karin, M., Wang, J.Y., and Puri, P.L. (2000). p38 and extracellular signal-regulated kinases regulate the myogenic program at multiple steps. Molecular and cellular biology 20, 3951-3964.

Xu, C., Tabebordbar, M., Iovino, S., Ciarlo, C., Liu, J., Castiglioni, A., Price, E., Liu, M., Barton, E.R., Kahn, C.R., et al. (2013). A zebrafish embryo culture system defines factors that promote vertebrate myogenesis across species. Cell 155, 909-921.

Xu, K., Liang, X., Shen, K., Cui, D., Zheng, Y., Xu, J., Fan, Z., Qiu, Y., Li, Q., Ni, L., et al. (2012). miR-297 modulates multidrug resistance in human colorectal carcinoma by down-regulating MRP-2. The Biochemical journal 446, 291-300.

Yamaguchi, T.P. (2001). Heads or tails: Wnts and anterior-posterior patterning. Current biology : CB 11, R713-724.

Yamamoto, Y., Kosaka, N., Tanaka, M., Koizumi, F., Kanai, Y., Mizutani, T., Murakami, Y., Kuroda, M., Miyajima, A., Kato, T., et al. (2009). MicroRNA-500 as a potential diagnostic marker for hepatocellular carcinoma. Biomarkers : biochemical indicators of exposure, response, and susceptibility to chemicals 14, 529-538.

Ying, Q.L., Wray, J., Nichols, J., Batlle-Morera, L., Doble, B., Woodgett, J., Cohen, P., and Smith, A. (2008). The ground state of embryonic stem cell self-renewal. Nature 453, 519-523.

You, J., Li, Y., Fang, N., Liu, B., Zu, L., Chang, R., Li, X., and Zhou, Q. (2014). MiR-132 suppresses the migration and invasion of lung cancer cells via targeting the EMT regulator ZEB2. PloS one 9, e91827.

Yu, H., Lu, Y., Li, Z., and Wang, Q. (2014a). microRNA-133: expression, function and therapeutic potential in muscle diseases and cancer. Current drug targets 15, 817-828.

Yu, T., Li, J., Yan, M., Liu, L., Lin, H., Zhao, F., Sun, L., Zhang, Y., Cui, Y., Zhang, F., et al. (2014b). MicroRNA-193a-3p and -5p suppress the metastasis of human non-small-cell lung cancer by downregulating the ERBB4/PIK3R3/mTOR/S6K2 signaling pathway. Oncogene.

Zhang, R., Luo, H., Wang, S., Chen, W., Chen, Z., Wang, H.W., Chen, Y., Yang, J., Zhang, X., Wu, W., et al. (2014). MicroRNA-377 inhibited proliferation and invasion of human glioblastoma cells by directly targeting specificity protein 1. Neuro-oncology 16, 1510-1522.

Zheng, G.X., Ravi, A., Calabrese, J.M., Medeiros, L.A., Kirak, O., Dennis, L.M., Jaenisch, R., Burge, C.B., and Sharp, P.A. (2011). A latent pro-survival function for the mir-290-295 cluster in mouse embryonic stem cells. PLoS genetics 7, e1002054.

Zhu, C., Shao, P., Bao, M., Li, P., Zhou, H., Cai, H., Cao, Q., Tao, L., Meng, X., Ju, X., et al. (2014). miR-154 inhibits prostate cancer cell proliferation by targeting CCND2. Urologic oncology 32, 31 e39-16.

Zhu, S., Wurdak, H., Wang, J., Lyssiotis, C.A., Peters, E.C., Cho, C.Y., Wu, X., and Schultz, P.G. (2009). A small molecule primes embryonic stem cells for differentiation. Cell stem cell 4, 416-426.

Abbreviation List

Alk	Activin Receptor-like Kinase
APC	Adenomatous Polyposis Coli
BMP	Bone Morphogenic Protein
DGC	Dystrophin Glycoprotein Complex
DMD	Duchenne Muscular Dystrophy
DMPK	Dystrophia Myotonica Protein Kinase
EB	Embryoid Body
ESC	Embryonic Stem Cells
GPCR	G-protein coupled receptor
GSK	Glycogen Synthase Kinase
Hh	Hedgehog
IP	Immunoprecipitation
iPS	Induced Pluripotent Stem
LIF	Leukemia Inhibitory Factor
MHC	Myosin Heavy Chain
MRF	Myogenic regulatory factor
MyoG	Myogenin
NFAT	Nuclear Factor of Activated T-cells
PKC	Protein Kinase C
PSM	Presomitic Mesoderm
RA	Retinoic Acid

RAR	Retinoic Acid Receptor
R-Smad	Receptor-regulated Smad
SAR	Structure Activity Relationship
sFRP	Secreted Frizzled-related protein
Shh	Sonic Hedgehog
siRNA	Small Interfering RNA
Smo	Smoothened
SRF	Serum Response Factor
TGF	Transforming Growth Factor

Acknowledgements

The research work for this Ph.D. thesis was conducted at the Novartis Institutes for Biomedical Research in Basel under supervision of Dr. Matthias Mueller. I would like to thank Dr. Matthias Mueller sincerely for giving me the opportunity to do my Ph.D. in his lab. I appreciate his enthusiastic support, the daily fruitful discussions and the great time in the lab.

I thank Prof. Susan Gasser and Prof. Patrick Matthias for being members of my Ph.D. thesis committee and supporting the project with helpful advices. The meetings with them were very constructive and encouraging.

I want to express my special thanks to Dr. Bernd Kinzel and Dr. Tewis Bouwmeester for their permission and encouragement to do my Ph.D. in Developmental and Molecular Pathways platform.

I would like to thank all the past and present members of Dr. Mueller's lab as well as mouse model group. I felt very welcomed from the beginning and learned a lot from them in a creative and enjoyable working atmosphere.

I am thankful to Dr. Laure Bouchez Lab for chemistry support, Dr. Caroline Gubser-Keller Lab for bioinformatics analysis, Mrs. Angelika Meyer Lab for experimental technique and materials, Dr. Fred Bassilana Lab for GPCR expertise, Dr. Iwona Ksiazek Lab for histology, Dr. Hans Voshol for pull-down analysis and Dr. Jan Weiler Lab for small RNA analysis.

I am grateful to Samson Jacca and Claudia Klinter for proof-reading the dissertation manuscript.

Special thanks to Andrea, Rossa, Yujeong and Carole for supporting me and sharing the great and unforgettable time in Basel.

I do thank Munkyung, my family and friends for supporting me during these four years.

Curriculum Vitae

Hyunwoo, LEE

Address: St.Johanns-Ring 83, Basel, Switzerland.
Mobile: +41 78 637 02 75
E-mail: gusn85@gmail.com

Date of Birth: 14 Nov 1985
Gender: Male
Nationality: Republic of Korea
Marital Status: Single

Professional Experience

01/2011 – present **Doctoral Candidate**
NIBR (Novartis Institutes for BioMedical Research), Basel, Switzerland
Cellular Engeering Lab of Dr. Matthias Mueller

03/2010 – 12/2010 **Internship Student**
NIBR (Novartis Institutes for BioMedical Research), Basel, Switzerland
Mouse Model Generation Lab of Dr. Matthias Mueller

03/2008 – 02/2010 **Master Student**
Sungkyunkwan University, Republic of Korea
Biochemistry and Molecular Biology Lab of Prof. Dr. Jeung-Whan Han

03/2008 – 07/2008 **Teaching Assistant**
Sungkyunkwan University, Republic of Korea

05/2008 – 05/2009 **Weekend Duty Pharmacist**

Cha University Hospital, Republic of Korea

01/2007 **Internship Training for Clinical Pharmacy**

Educations

01/2011 – present **Ph.D. Candidate (Major in Cellular Biology), Basel University, Switzerland**

Dissertation: Studying Molecular Mechanism of Embryonic Skeletal Muscle Differentiation with Small Molecules

Dissertation Committee: Dr. Matthias Mueller, Prof. Dr. Susan Gasser, Prof. Dr. Patrick Matthias

03/2008 – 02/2010 **M.Sc., Graduate School of Pharmacy, Sungkyunkwan University, Korea**

Dissertation: Role of Protein L-Isoaspartyl Methyltransferase during Skeletal Muscle Differentiation

Dissertation Committee: Prof. Dr. Jeung-Whan Han, Prof. Dr. Hyang Woo Lee, Prof. Dr. Eun-Jung Cho

03/2004 – 02/2008 **B.S., College of Pharmacy, Sungkyunkwan University, Korea**

Obtained Korean Pharmacist License

Personal Skill

Molecular and cellular biological laboratory skill

Completed Ph.D. and Master Thesis with excellent laboratory technical skills

Broad experiences of human iPS, mouse ES and primary cell culture, High throughput screening design, Cellular genetic engineering for establishing stable cell lines, qPCR, ELISA, Flow cytometry analysis, Confocal microscopy imaging

Analytical and writing skill

Analyzed massive genomic expression profiling and visualized it with softwares (SpotFire, Prism) during Ph.D. study

Wrote master thesis summarizing 2 years' work and well-trained for keeping laboratory notebook with good quality

Project management

Managing the Ph.D. project collaborating with chemists and bioinformaticians in NIBR

Organizing project meetings and discussions for scientists involved

Communication skill

Updated the result of experiment weekly basis and discussed it with team members in lab meeting

Presented posters at scientific meetings

- FMI(Friedrich Miescher Institute) Annual Meetings (2012 and 2013)
- NIBR(Novartis Institutes for BioMedical Research) DMP(Developmental and Molecular Pathways) Retreats (2011 and 2013)

Taught bachelor students in pharmaceutical biochemical laboratory lecture (2008)

Team work

Dedicated team player, highly adaptable and flexible to new environment

Successfully collaborated with chemists and bioinformaticians across departments during Ph.D. project

Computer skill

Good knowledge of MS Word, Excel and PowerPoint to make summary and presentation during Ph.D. study

Language Korean (Mother tongue), English (Fluent), German (Intermediate), French (Basic)

Personal Development

05/2014 Molecular biology of muscle development and regeneration (Lecce, Italy)

11/2012 Stem Cells, Development and Regulation Conference (Amsterdam, Netherlands)

05/2011 The Molecular and Cellular Mechanisms, Regulating Skeletal Muscle, Development and Regeneration Conference (Wiesbaden, Germany)

Award

Scholarship

2004 - 2005 Academic Excellence Scholarhip from Sungkyunkwan University, Republic of Korea

2006 - 2007 Yuhan Fund Scholarship from Yuhan Pharmaceutical Corporation, Republic of Korea

2008 - 2009 Brain Korea 21 Scholarship from Korea Research Foundation, Republic of Korea

Prize

2008 Graduation with distinction from Sungkyungkwan University, Republic of Korea

Publication

H. Lee, C. Haller, T. Doll, I. Fruh, C. Guber-Keller, S. Richards, Y. Ibig, M. Patoor, M. Goette, L. Bouchez, M. Mueller, A Small Molecule Drives Skeletal Muscle Differentiation in Embryonic Stem Cells via Reciprocal Activation of the Wnt Pathway and Inhibition of Smad2/3 and Sonic Hedgehog Pathways. (Manuscript Preparation)

M. Kim, S.A. Yi, **H. Lee**, S.Y. Bang, E.K. Park, M.G. Lee, K.H. Nam, J.H. Yoo, D.H. Lee, H-W. Ryu, S.H. Kwon, J-W. Han, Reversine Induces Multipotency of Lineage-Committed Cells through Epigenetic Silencing of miR-133a, Biochemical and Biophysical Research Communications (2014)